UNIVERSIDADE DE LISBOA
INSTITUTO SUPERIOR TÉCNICO

THREE-DIMENSIONAL CULTURE SYSTEMS FOR THE STUDY OF HUMAN PLURIPOTENT STEM CELLS: MICROARRAYS AND SPHEROIDS

Jorge Filipe da Conceição Pascoal

Supervisor: Doctor Joaquim Manuel Sampaio Cabral
Co-Supervisors: Doctor Jonathan Seth Dordick
Doctor Maria Margarida Fonseca Rodrigues Diogo

Thesis approved in public session to obtain a Ph.D. Degree in

Bioengineering

Jury final classification: Pass with Distinction

2020

TÉCNICO LISBOA

UNIVERSIDADE DE LISBOA

INSTITUTO SUPERIOR TÉCNICO

THREE-DIMENSIONAL CULTURE SYSTEMS FOR THE STUDY OF HUMAN PLURIPOTENT STEM CELLS: MICROARRAYS AND SPHEROIDS

Jorge Filipe da Conceição Pascoal

Supervisor: Doctor Joaquim Manuel Sampaio Cabral
Co-Supervisors: Doctor Jonathan Seth Dordick
Doctor Maria Margarida Fonseca Rodrigues Diogo

Thesis approved in public session to obtain a Ph.D. Degree in
Bioengineering

Jury final classification: Pass with Distinction

Jury

Chairperson: Doctor Duarte Miguel de França Teixeira dos Prazeres, Instituto Superior Técnico, Universidade de Lisboa

Members of the Committee:

Doctor Jonathan Seth Dordick, School of Engineering, Rensselaer Polytechnic Institute, USA

Doctor Lino da Silva Ferreira, Faculdade de Medicina, Universidade de Coimbra

Doctor Gabriel António Amaro Monteiro, Instituto Superior Técnico, Universidade de Lisboa

Doctor José Eduardo Marque Bragança, Departamento de Ciências Biomédicas e Medicina, Universidade do Algarve

Doctor Tiago Paulo Gonçalves Fernandes, Instituto Superior Técnico, Universidade de Lisboa

Doctor Maria Margarida de Carvalho Negrão Serra, Instituto de Biologia Experimental e Tecnológica

Funding Institution

Fundação para a Ciência e Tecnologia

2020

RESUMO

As células estaminais pluripotentes humanas têm a capacidade de se autorrenovar e de gerar derivados das três camadas germinativas. Por esse motivo, representam um potencial significativo para estudos em embriogénese, *screening* de fármacos e, em particular, para o desenvolvimento de aplicações terapêuticas para medicina regenerativa e de precisão. Este potencial motivou muita da investigação feita durante os últimos vinte anos em biologia de células estaminais, mas a sua concretização tem sido retardada devido a uma incompleta compreensão dos complexos e intrincados mecanismos moleculares e dos sinais do microambiente que controlam a autorrenovação e diferenciação celulares. Para mais, o desenvolvimento de sistemas de cultura tridimensionais de células estaminais pluripotentes, além de potenciar estratégias de *scale-up*, providenciou modelos celulares *in vitro* que mimetizam mais fidedignamente as condições *in vivo*, ao emular interações célula-célula, gradientes químicos e sinais biomecânicos que nos tradicionais sistemas bidimensionais são residuais ou inexistentes. A utilização de plataformas de *high-throughput screening* para estudar os efeitos de sinais do microambiente, tais como fatores solúveis, pode contribuir significativamente para a criação de modelos mecanísticos que descrevam as interações moleculares que definem as decisões celulares.

O objetivo geral da presente tese foi desenvolver, caracterizar e comparar sistemas de cultura tridimensional de células estaminais pluripotentes humanas, especificamente: 1) desenvolver uma plataforma de *microarray* celular tridimensional para estudos *high-throughput*, incluindo ferramentas quantitativas e de análise de imagens para avaliar viabilidade e proliferação celulares, bem como a expressão de marcadores, e testar o efeito de diferentes compostos diluídos no meio de cultura na autorrenovação e diferenciação; e 2) caracterizar a cultura em suspensão estática de células estaminais pluripotentes humanas como esferoides, em termos de crescimento, tamanho, morfologia e expressão de marcadores de pluripotência e diferenciação, e investigar se os resultados obtidos na plataforma de *microarray* são replicáveis neste sistema de cultura.

Espera-se que os resultados apresentados contribuam para o desenvolvimento de novas metodologias e plataformas de estudo, e para a compreensão geral de como as condições de cultura tridimensional influenciam as células estaminais pluripotentes humanas.

Palavras-chave: Células estaminais pluripotentes humanas; *microarray* celular; *high-throughput screening*; esferoides celulares; cultura em suspensão estática.

ABSTRACT

Human pluripotent stem cells have the ability to self-renew and to generate derivates of the three germ layers. For this reason, they hold significant potential for the study of embryogenesis, drug screening and, particularly, the development of therapeutic applications for regenerative and precision medicine. This potential fueled much of the research and advances made in stem cell biology during the last twenty years, but its translation to practice has been hindered by an incomplete understanding of the complex and intricate molecular mechanisms and microenvironmental cues that control self-renewal and differentiation. Furthermore, the development of three-dimensional culture systems for human pluripotent stem cells enhanced the potential of scale-up approaches and provided *in vitro* cellular models that better resemble in vivo conditions, by emulating cell-cell interactions, chemical gradients and biomechanical signals that are reduced or absent in traditional two-dimensional cultures. The use of high-throughput screening platforms to study the effects of microenvironmental cues, such as soluble factors, can greatly contribute to the establishment of mechanistic models to describe the molecular interactions that drive stem cell fate.

The general aim of this thesis was to develop, characterize and compare three-dimensional culture systems for human pluripotent stem cells, specifically: 1) to develop a three-dimensional cellular microarray platform for high-throughput studies on human pluripotent stem cells, including quantitative image analysis tools to assess cellular viability, growth, and marker expression, and test how different media-diluted compounds affect cell proliferation and pluripotency maintenance; and 2) to characterize human pluripotent stem cell spheroids cultured in static suspension in terms of growth, size, morphology, and marker expression for pluripotency maintenance and differentiation, and study how the results obtained in the microarray platform translate to this culture system.

The results presented will hopefully contribute to the development of new methodologies and study platforms, and to the overall understanding of how human pluripotent stem cells are affected by three-dimensional culture conditions *in vitro*.

Keywords: Human pluripotent stem cells; cellular microarray; high-throughput screening; cellular spheroids; static suspension culture.

ACKNOWLEDGMENTS

When I first decided to pursue a doctoral degree, I had no idea of the tremendous experience that it would become, or how all of it would change me on several levels. The successful conclusion of this process would not have been possible if it weren't for the many people with whom I was fortunate to work, discuss, learn, share hardships, or simply unwind.

Firstly, I must acknowledge my supervisor, Professor Joaquim Cabral. I thank him for the trust and availability since the very first time I contacted him, and particularly for all the patience during these last stages. I am deeply grateful for the opportunity that I have been given, for the chance to learn from him, and for how this work shaped me as a scientist and as an individual.

A considerable part of this work, and the one that strikes me as the greatest challenge I've faced, was developed at Rensselaer Polytechnic Institute, in the US. I thank Professor Jonathan Dordick, one of my co-supervisors, for making this possible and for accepting me in his laboratory as one of his students, even before meeting me. I thank him for all the thoughtful advice and for pushing me to be pragmatic and focus on the essential.

I thank Professor Margarida Diogo, also my co-supervisor, for all the conversations and all her kind words of encouragement and recognition; for her sincerity, patience, and, above all, for having and readily sharing the optimism that I often lacked.

I thank all my colleagues from IBB-SCERG and RPI that in some way or another helped me through this adventure, either by sharing knowledge, discussing work and other stuff or just by making the daily routine a little better. Specifically, I am extremely grateful for all the help that Greg Nierode has given, both with the many challenges posed by the microarray platform as well as for being a great friend through the great challenge of being away from home – and, of course, for teaching how to properly cut a round cake [G F (1906) Cutting a Round Cake on Scientific Principles. *Nature*, 75, p. 173. **DOI**: 10.1038/075173c0]. I must also acknowledge the invaluable contributions of Sean McFarland and Brian Perea from the University of California Berkeley, for sharing their work and results, thus contributing to the development of the microarray platform. I also thank Sandra Pinto from IBB, for her availability and assistance with the confocal microscope. Although all the labmates that somehow contributed to this work are too many to name individually, I'd like to acknowledge the ones with whom I've worked more closely. From RPI, Luciana Meli, Hélder Barbosa, Sandrine Lavenus, Maurício Mora Pale, Anne Marie Hickey, Seok-Joon Kwon, and Israel Lidsky; and from IBB-SCERG: Carlos Rodrigues, Tiago Fernandes, Teresa Silva, Cláudia Miranda, Tiago Dias, Mariana Branco, Ana Rita Gomes, Cátia Bandeiras, Gonçalo Rodrigues, and João Silva.

Outside the lab, I thank the MIT-Portugal gang, Daniel Simão, Marisa Santos, Ricardo Costa, and Sérgio Gonçalves, for sharing a significant part of this adventure and for all the relaxed moments and words of encouragement.

I acknowledge Fundação para a Ciência e Tecnologia, National Institutes of Health and Instituto Superior Técnico for funding this work and/or supporting me financially.

Finally, I acknowledge those closest to me. I thank my parents for making all of this possible, for supporting, trusting, and believing in me, regardless of all the time that had went by since I set this goal for myself. I also thank my sister for being the person I always looked up to and for inspiring me to reach higher.

And I thank Janine. I thank her for all her endless patience and for always standing by my side, even when far apart, sharing the good and bearing with me through the toughest of times.

TABLE OF CONTENTS

TABLE OF FIGURES

ABBREVIATIONS

2-D – two-dimensional.

3-D – three-dimensional.

BMP – bone morphogenetic protein.

BSA – bovine serum albumin.

C_T – threshold cycle [in qPCR].

CDC – cell division cycle.

CDK – cyclin-dependent kinase.

DAPI – 4',6-diamidino-2-phenylindole.

DMEM | **DMEM/F-12** – Dulbecco's modified Eagle medium | DMEM with nutrient mixture F12 (1:1).

DMSO – dimethyl sulfoxide.

DNA | **cDNA** – deoxyribonucleic acid | complementary DNA.

E8 – Essential 8 medium.

ECM – extracellular matrix.

EDTA – ethylenediaminetetraacetic acid.

EGF – epidermal growth factor.

EMEM – Eagle's minimum essential medium.

EMT – epithelial-to-mesenchymal transition.

ERK – extracellular signal-related kinases.

EpiSC – epiblast-derived stem cells.

ESC | **hESC** – embryonic stem cell | human ESC.

EtHD – Ethidium homodimer-1.

FBS – fetal bovine serum.

FCS – fetal calf serum.

FGF – fibroblast growth factor.

GMP – good manufacturing practices.

GSK – glycogen synthase kinase.

GUI – graphical user interface.

HLA – human leukocyte antigen.

ICM – inner cell mass [of the blastocyst].

IGF – insulin-like growth factor.

iPSC | **hiPSC** – induced pluripotent stem cells | human iPSC.

LIF – leukemia inhibitory factor.

MEF – mouse embryonic fibroblasts.

MG – growth factor-reduced Matrigel®.

MPMW – MicroPillar/MicroWell [chip system].

MSC – mesenchymal stem cells.

NGS – normal goat serum.

NT-ESC – nuclear transfer embryonic stem cells.

PBS | **PBS-Ca/Mg** – phosphate-buffered saline | PBS with calcium and magnesium.

PCR | **qPCR** – polymerase chain reaction | quantitative PCR.

Pen/Strep – 50 U/mL penicillin and 50 µg/mL streptomycin (final concentrations).

PI3K – phosphatidylinositol 3-kinase.

PLL – poly-L-lysine.

PSC | **hPSC** – pluripotent stem cells | human PSC.

PS-MA – poly(styrene-*co*-maleic-anhydride).

PS-TC – tissue culture-treated polystyrene.

RNA | mRNA | miRNA – ribonucleic acid | messenger RNA | micro RNA.

rpm – rotations per minute.

ROCK | **ROCKi** – Rho-associated coiled-coil containing protein kinase | ROCK inhibitor Y-27632.

SCNT – somatic cell nuclear transfer.

SDS – sodium dodecyl sulfate.

SSEA – stage-specific embryonic antigen.

TBS | **TBS-T** – tris-buffered saline | TBS with 0.05% Tween-20.

TGF – transforming growth factor.

TF – transcription factor.

I. Introduction

I.1. Research subject and aim

Ever since their discovery, human pluripotent stem cells (hPSC) have been regarded as holding significant potential for the study of embryogenesis, drug screening and, particularly, the development of therapeutic applications for regenerative and precision medicine. This potential fueled much of the research and advances made in stem cell biology during the last 20 years, but its translation to practice has been hindered by an incomplete understanding of the complex and intricate molecular mechanisms and microenvironmental cues that control self-renewal and differentiation. Furthermore, it is necessary to develop robust protocols that not only allow an efficient production of cellular products, but that comply with strict clinical-grade requirements. The development of three-dimensional culture systems enhanced the potential of scale-up approaches and provided *in vitro* cellular models that better resemble in vivo conditions, by emulating cell-cell interactions, chemical gradients and biomechanical signals that are reduced or absent in traditional two-dimensional cultures. The addition of these variables requires new characterization and quantitative methods to understand their role and significance in the molecular processes that direct stem cell fate. Comprehensive knowledge and tight control over such processes are required to maximize the potential benefit and reliability of new applications and therapies while reducing uncertainties and inherent risks to an acceptable minimum.

Novel tools emerged with the scientific and technological progress over the last decades, which enabled new ways of doing deeper and broader research. The development of microfabrication technologies, along with an increasingly accessible and enhanced computer power, allowed the miniaturization of experimental conditions in cell biology and the generation and efficient analysis of big data sets. These tools can potentially provide useful information on cellular and microenvironmental interactions, and enable high-throughput screening studies of efficiency and toxicity of candidate molecules, thus accelerating drug development and the overall creation of knowledge.

The general aim of this thesis is to explore and characterize three-dimensional culture systems of human pluripotent stem cells, specifically: 1) to develop a three-dimensional cellular microarray platform for high-throughput studies on human pluripotent stem cells, and 2) to characterize human pluripotent stem cell spheroids cultured in suspension and study the translation of the results obtained in the microarray platform. The results presented

will hopefully contribute to the development of new methods and study platforms, and to the overall understanding of how human pluripotent stem cells are affected by three-dimensional conditions *in vitro*.

I.2. Stem cells and regenerative medicine

Regeneration is generally defined as the biological ability of an organism to autonomously renew or recover lost or damaged tissues. Though it has been recognized since Ancient Greece, it was only first described systematically by René-Antoine Ferchault de Réaumur in 1712, after his observations on the regrowth of lost limbs in crayfish [(Carlson BM, 2007a; Réaumur R-AF de, 1712)]. Today, processes of regeneration are considered ubiquitous in virtually all kingdoms of life although they are highly differentiated among species. While some plant cuttings can generate entire functional specimens, for example, vertebrate animals are generally only capable of regenerating certain tissues [(Stocum DL & Zupanc GKH, 2008)]. In humans, for instance, there is an almost constant renewal (or turnover) of body tissues such as hair, nails, epidermis, and blood. This regenerative process is known as physiological or homeostatic regeneration since, unlike reparative regeneration, it is not triggered by wounding to the tissues. Upon damage, other organs such as the liver can regenerate to some extent but this ability is very limited when it comes to cardiac muscle or nervous tissue [(Stocum DL & Zupanc GKH, 2008; Carlson BM, 2007a)]. The source of the cells that contribute to regeneration processes may be varied – processes of cell dedifferentiation (mature cells revert to a progenitor state) occur in some cases. However, varying levels of regeneration capability are typically related to the existence of progenitor or stem cell niches for the different tissues that compose the organisms [(Singh SR, 2012; Morrison SJ & Spradling AC, 2008; Robey PG, 2000)].

After the initial enthusiasm surrounding regeneration processes in the late 18th and 19th centuries, there was a significant decrease in interest during most of the 20th century, mainly due to the perception of a limited regeneration capability in humans [(Carlson BM, 2007a)]. It was only by the end of the century that emerging studies on stem cells gave new impetus to the field of regenerative biology. The studies of Till and McCulloch in 1961 provided the first experimental evidence supporting the existence of multipotent hematopoietic progenitor cells [(Bianco P, 2015; Till JE & McCulloch EA, 1961)] and led to the implementation of bone marrow

transplants. In 1981, after several decade-spanning unsuccessful efforts, Evans and Kaufman (Evans MJ & Kaufman MH, 1981) and Martin (Martin GR, 1981) independently described, for the first time, the derivation of pluripotent stem (PS) cells from mouse embryos. It would take close to twenty years for the equivalent accomplishment to be achieved with human cells – in 1998, James Thomson and coworkers isolated and derived the first human pluripotent stem cell lines (Thomson JA et al., 1998). The ensuing burst of new knowledge and technical advancement, along with the exciting potential attributed to stem cells for therapeutic applications, revived the interest in regeneration research and prompted the rise of new scientific fields, such as regenerative medicine and tissue engineering (Simkin J & Seifert AW, 2018; Carlson BM, 2007a).

Current research is focused not only on the study of underlying molecular signaling pathways involved in the proliferation and differentiation processes of stem cells but also on the development and optimization of clinical-grade production conditions. It is expected that further progress will enable the use of highly specific cellular products to relieve the symptoms or treat acute and chronic debilitating conditions, such as cardiovascular and neurodegenerative diseases, spinal cord injuries, diabetes, and cancer.

I.2.1. Stem cells

The concept of stemness in cell biology may be traced back to the formulation of classical Cell Theory. When in 1839 Theodor Schwann proposed the general theory that cells are the basic units of life and the building blocks of all organisms, and that the different structures or tissues that compose an organism arise from distinct types of cells (Schwann T, 1847), he did not provide a definite resolution as to where the cells come from. Research on cell cleavage was scarce then, and the origin of animal cells was believed to be extracellular (Wolpert L, 1995). However, in 1855 a third tenet for the cell theory was proposed by Robert Remak and Rudolf Virchow, eventually establishing that all cells arise from pre-existing cells (*Omnis cellula e cellula*) (Wolpert L, 1995; Remak R, 1855). This notion, while very basic and not fully defining stemness by today's understanding, laid the foundation for that concept and eventually steered research towards modern cell and developmental biology.

Stem cells are broadly defined as being unspecialized and able to self-replicate or differentiate, generating different lineages or specialized cells. Nevertheless, the term refers

to very distinct cell types, generated from diverse sources and at different developmental stages. The most common classification system for stem cells is based on their potential to produce progeny of different lineages. This variability in potency is naturally illustrated during embryonic development, as will be explained in the following sections.

I.2.1.1. Embryonic stem cells

The human embryogenic process, as in other vertebrates, entails a highly complex sequence of programmed cellular events, such as divisions, differentiations, and migrations. It all starts with one cell – the zygote – generated after fecundation. The zygote has the potential do develop into a complete functioning organism, as well as into the extra-embryonic tissues needed for embryonic support, such as the placenta (Mitalipov SM & Wolf D, 2009; Jaenisch R & Young R, 2008). It is thus classified as a totipotent stem cell. If transplanted into an appropriate recipient, a totipotent stem cell is able to generate an embryo and to support a term birth. In animal models, this potential was shown to be retained throughout the first divisions until initial cell commitment (Mitalipov SM et al., 2002; Johnson W et al., 1995). By the time the blastocyst phase is reached, there is a clear phenotypic difference between the cells composing the outer layer – the trophoblast – which will give rise to extra-embryonic structures, and the cells in the inner cell mass (ICM), which will generate the actual embryo (De Paepe C et al., 2014). Although they don't have the full potential to generate an embryo as totipotent cells, the cells in the ICM have the potential to differentiate into any of the main three germ layers – ectoderm, endoderm, and mesoderm – for which they are classified as pluripotent (Mitalipov SM & Wolf D, 2009). The ectoderm produces the progenitors that will eventually generate the epidermis, the nervous system, hair, mammary glands, and other surface tissues. The endoderm gives rise to the digestive tube and organs such as the liver, the stomach, and the pancreas, along with the lungs and the urinary bladder, among others. The mesoderm produces all the muscle tissues and circulatory system, the bones, most cartilage, the adipose tissues and the lymphatic system (Arey LB et al., 2017).

Human pluripotent stem cells (hPSC) were first isolated and derived *in vitro* from the ICM of blastocysts in 1998 (Thomson JA et al., 1998). Given their embryonic origin, these cells are typically designated as embryonic stem cells (ESC). However, the term "pluripotent stem

cells" may also refer to somatic cells reprogrammed to a pluripotent state, which will be described further on. hPSCs are standardly characterized by 1) the expression of specific markers, such as OCT4, NANOG, SOX2, stage-specific embryonic antigen (SSEA)-3, SSEA-4 and alkaline phosphatase, among others; 2) the capacity to generate embryoid bodies *in vitro*, containing differentiated cells derived from the three germ layers; 3) and the *in vivo* generation of teratomas, also containing differentiated cells of the three germ layers (Martí M et al., 2013). Their self-replication and differentiation capabilities, while being valuable for *in vitro* studies and conferring them a greater potential for therapeutic applications, also pose significant limitations. The risk of teratoma formation, in particular, has limited the use of these cells in regenerative medicine (reviewed in Ben-David U & Benvenisty N, 2011). Additionally, the lack of highly specific and defined protocols for expansion and directed differentiation, along with the inefficient purification of cellular products, were major hurdles that only recently started to be overcome (reviewed in Martin U, 2017).

Pluripotency is a rather transient state *in vivo*. After uterine implantation, as further differentiation ensues, the potency of the cells composing the embryo decreases gradually while the proportion of fully committed specialized cells increases (Zhou X et al., 2015). This process carries on for several years after birth, until the organism reaches full maturity and relatively limited pools of somatic stem cells are confined to specific tissues.

I.2.1.2. Adult stem cells

One very common dichotomy in stem cell-related literature is that between embryonic stem cells – those isolated from the ICM of the blastocyst – and adult or somatic stem cells, which are located within niches in differentiated tissues after birth (Carlson BM, 2007b). In adult organisms, these cells usually have a role in the maintenance of homeostasis within the tissues where they are integrated, replacing old or damaged cells, and participating in tissue repair upon injury. Although being more specialized than PSCs, they still retain a high capacity for self-renewal through symmetric division (Wabik A & Jones PH, 2015; Alison M & Islam S, 2009).

In terms of differentiation potential, adult stem cells are generally considered either multipotent when they can produce several different lineages, or unipotent when the progeny is confined to a single lineage. The term "oligopotent" is also sometimes attributed

to cells that differentiate into two or three lineages. For example, hematopoietic stem cells, which are found in the bone marrow, are multipotent, as they can generate the varied types of blood cells, contributing to maintain the cellular turnover or recover from blood loss (Lee Y et al., 2017). Similarly, neural stem cells, found in the brain within the subventricular zone and the dentate gyrus can produce new neurons, astrocytes, and oligodendrocytes (Ruddy RM & Morshead CM, 2018). Mesenchymal stem cells (MSC) are another common example of multipotent cells. The designation includes cells found in several tissues with certain common properties such as the presence and absence of specific surface markers and the ability to differentiate into bone, cartilage and adipose tissue (Samsonraj RM et al., 2015; Dominici M et al., 2006). Nevertheless, despite their probable mesodermal origin and generally accepted multipotency, some MSCs have been shown to transdifferentiate and produce cells from other lineages, such as neural cells (neuroectoderm) (Anghileri E et al., 2008; Sanchez-Ramos J et al., 2000) and hepatocytes (endoderm) (Lee K-D et al., 2004; Schwartz RE et al., 2002).

Comparatively to other adult stem cells, unipotent stem cells are much less studied, despite their recognized potential for medical applications (Chen Z et al., 2014; Ko K et al., 2009). Some examples are lineage-restricted mammary stem cells (Van Keymeulen A et al., 2011, 2017), spermatogonial stem cells (Kubota H et al., 2004) and skeletal muscle satellite cells (Costamagna D et al., 2015; Kuang S et al., 2007).

The described nomenclature and definitions of stem cells, though useful in terms of systematization, are generally oversimplified as they rely mostly on limited specific functional or phenotypical aspects that may not be sufficient to accurately distinguish between different cells with similar traits. This is particularly evident in the case of MSCs (Bianco P et al., 2013). Furthermore, when cultured in vitro, the differing biological sources and/or methods by which the cells are collected, derived or expanded may lead to varying endpoint cellular characteristics, such as culture heterogeneity, proliferation rate, and differentiation potential. It is, therefore, necessary to establish comprehensive definitions and standardizations, robust and reproducible methodologies for cellular culture, and stringent, extensive characterization protocols.

I.2.1.3. Stem cell applications and safety considerations

As mentioned before, stem cells hold great potential for the development of new therapies that may alleviate or cure currently untreatable and debilitating conditions. Notwithstanding the difficulty in materializing much of this potential, stem cell research has already enabled significant progress in fields spanning from developmental biology to disease modeling and drug discovery. There is now a much clearer understanding of the possible applications and limitations of stem cells and of the steps needed to achieve successful translation from bench to clinic, as well as the safety and ethical constraints that must be considered and overcome.

Among adult stem cells, MSCs are possibly the most promising in terms of clinical applications given their accessibility and availability in several tissues, such as the umbilical cord, bone marrow, and adipose tissue. Aside from their ability to produce different cellular lineages that could potentially be used to regenerate damaged tissues, MSCs have also been shown to have trophic and immunomodulatory properties that could be applied in the treatment of inflammatory conditions (Ankrum JA et al., 2014). Some examples of conditions with therapies already being tested include graft-versus-host disease (Le Blanc K et al., 2008), Crohn's disease (Zhang J et al., 2018; García-Arranz M et al., 2016) and myocardial infarction (Gao LR et al., 2015). Despite encouraging progress in the use of MSCs, some safety concerns must be considered, particularly the uncontrolled differentiation of transplanted cells (Breitbach M et al., 2007), or the promotion of tumor growth and metastasis (Ljujic B et al., 2013).

Because of the potential of hPSCs to produce virtually any of the many cell types in the human body, they may be perceived as sort of a "holy grail" in regenerative medicine. However, unlike human MSCs that can be retrieved from the patients or other consenting donors without significant risks, the isolation of hESCs involves the destruction of human embryos. All the ethical constraints associated with that circumstance (reviewed in Bobbert M, 2006) considerably hindered the initial work with these cells, along with the prospects of using them for medical purposes. Some countries still have strict regulations related to hESCs, limiting their production, or outright forbidding their use in research (Wikipedia, 2017). In 2006, Takahashi and Yamanaka generated mouse PSCs from adult fibroblasts by induced expression of defined factors (Takahashi K & Yamanaka S, 2006), and named them induced pluripotent stem cells (iPSC). The following year, the same feat was achieved using human cells (Takahashi K et al., 2007; Yu J et al., 2007),

thus enabling the opportunity to further explore human pluripotency without the destruction of embryos and circumventing most of the ethical concerns related to work with hESCs.

hPSCs (including both ESC and iPSCs) are currently being used in a wide range of applications. The most straightforward is the study of stem cell biology, which aims at understanding the basic mechanisms behind the control of pluripotency and differentiation. The possibility of generating iPSCs from patient-derived somatic cells and then producing high quantities of otherwise inaccessible cells, such as cardiomyocytes and neurons, enabled the development of new disease models. These models can be used to study the etiology of specific pathologies, providing new clues and/or complementing existing *in vivo* models (Hino K et al., 2017). Some of the most common diseases being studied with iPSC-derived models include Alzheimer's disease (Hossini AM et al., 2015; Israel MA et al., 2012) and Parkinson's disease (Schöndorf DC et al., 2014; Jiang H et al., 2012). Coupled with high-throughput technologies, hPSC-derived cells can also be used to run toxicity tests (Tang L et al., 2017) and assess the safety and efficacy of a multitude of candidate compounds in the search for new treatments (Sharma A et al., 2017).

hPSCs differentiated *in vitro* and transplanted into animal models have produced promising results for the treatment of several conditions, such as retinal degeneration (Ben M'Barek K et al., 2017), myocardial infarction (Rojas S V et al., 2017), Parkinson's disease (Kikuchi T et al., 2017) and Alzheimer's disease (Cha M-Y et al., 2017), among others. The first clinical trial involving hPSCs was launched in 2010, by Geron Corporation. It was a phase I trial designed to assess the safety of using hESC-derived oligodendrocytes to treat spinal cord injury. After Geron discontinued all stem cell-related research due to funding difficulties, the trial was picked up by Asterias Biotherapeutics, who continued patient follow-up and, following favorable results, launched a dose-escalation study (Hayden EC, 2014). ClinicalTrials.gov currently lists several active clinical trials testing the safety and efficacy of transplanted hESC-derived cells to treat different conditions, including age-related macular degeneration, Stargardt's macular dystrophy, ischemic heart disease, type I Diabetes Mellitus and Parkinson's disease. Some have already been completed, with overall favorable results (Schwartz SD et al., 2015; Song WK et al., 2015). The first study using patient-derived iPSCs was sponsored by RIKEN Institute in Japan and was meant to assess the safety of using these cells to treat age-related macular degeneration. Started in 2013, it was halted due to regulatory changes two years later, after only one transplant, and was unable to provide conclusive results despite the absence of any major protocol-related complications (Mandai M et al., 2017). In 2017, a new study was initiated in Japan to test the safety

and efficacy of allogeneic iPSC-derived retinal epithelium, again to treat macular degeneration [Cyranoski D, 2017].

One of the most significant safety concerns in the transplantation of hPSCs into the human body is the possibility of teratoma formation. It is therefore of critical importance to remove undifferentiated cells from the samples transplanted into the patients, to reduce the risk of tumor formation. This can be achieved by separation processes, such as cell sorting [Li Y et al., 2017; Rodrigues GMC et al., 2014], or by causing the selective death of undifferentiated cells [Lee M-O et al., 2013]. While any therapy using ESCs would necessarily be allogeneic, the development of induced pluripotency enables the possibility of treating the patients with their own reprogrammed cells, which would, in theory, avoid immune rejections. Although several studies provide evidence of safe transplants, recent research suggests that autologous iPSC-derived cells could be immunogenic depending on the differentiated cell type and transplantation site, possibly due to epigenetic abnormalities, somatic coding mutations and/or genomic translocation caused by genetic instability [reviewed in Liu X et al., 2017]. Furthermore, given the high costs associated with cellular reprogramming and good manufacturing practices (GMP) compliance, a discussion on the economic viability of wide-spread autologous iPSC transplants is still ongoing. Banking of iPSCs and HLA-matching has been proposed as a solution for off-the-shelf cell therapies, but the answer to which approach is best is still a matter of debate [Bravery CA, 2015; Solomon S et al., 2015]. Aside from immunogenicity, genetic instability in the form of genetic mutations or chromosomal aberrations is a source of concern related to transplantation of iPSCs in humans, as it may lead to carcinogenesis. Therefore, understanding why that instability occurs, monitoring it and assessing its actual risks, together with developing safer and more stable reprogramming methods, is necessary for further advances in the use of hiPSCs [Yoshihara M et al., 2017]. Overall, further research will be required to determine the optimal cell type and delivery strategy for each specific application, maximizing the effectiveness with minimal associated risk.

I.2.2. Pluripotency

Pluripotency is commonly defined as the capacity of cells to differentiate along any of the three germ layers, therefore representing a functional property rather than a

developmental stage. This is evidenced by the fact that somatic cells can be reverted to a pluripotent state, as well as by the notion that PSCs can be derived from different tissues and at varying development time points. For example, in some of the first studies involving PSCs, tissue samples were taken from testicular teratomas in mice and engrafted in other mice to analyze the production of teratomas containing different lineages (Stevens LC, 1958). Furthermore, it is now well established that mouse ESC lines can be derived from pre-implantation embryos or a slightly later epiblast phase, generating cells with very different characteristics but in both cases retaining pluripotency (Brons IGM et al., 2007; Tesar PJ et al., 2007). While the complexity of the mechanisms that govern pluripotency has been partly deciphered over the last decades, the extension of the variables that play a role in its regulation or outcomes is still far from clarified.

I.2.2.1. Pluripotency in the human embryo

Understanding pluripotency, its biological significance, and that of the molecular mechanisms governing the differentiation of hPSCs requires a comprehensive grasp of the phenomena that characterize early human embryonic development. Although a detailed explanation would require a long and complex exposition, it is possible to summarize the main events that take place during the initial stages of differentiation, to provide context and introduce specific terminology.

One of the first most clear phenotypical changes during human (and mammalian, in general) embryogenesis occurs upon blastocyst formation (blastulation), at which point two cellular structures are defined: 1) the trophectoderm, an outer cell layer that generates the trophoblast and, later on, extraembryonic tissues including parts of the placenta; and 2) a compact ICM, which contains PSCs and develops into the embryo itself, as well as some extra-embryonic tissues. Starting at around week 2 of development, as implantation occurs, the ICM undergoes a series of transformations, eventually leading to gastrulation and the generation of the three germ layers. First, it forms a disc composed of two distinct layers: the epiblast, adjacent to the trophoblast and, beneath, the hypoblast or primitive endoderm. This constitutes the first definition of the dorsal-ventral axis of the embryo. As fluid collects between the epiblast and the overlying trophoblast, epiblast cells proliferate along the trophoblast towards the embryonic pole and line the newly formed amniotic cavity. At the

same time, hypoblast cells proliferate down into the blastocyst cavity creating a layer of extraembryonic endoderm that forms the primary yolk sac. A consecutive wave of proliferating extraembryonic endoderm then replaces it with the definitive yolk sac, as the remaining blastocyst cavity is gradually populated by extraembryonic mesoderm cells (Schoenwolf GC et al., 2009a).

Surrounded by early supporting structures and already fully implanted in the maternal uterus, the embryo develops within the embryonic disc at the interface of the epiblast and the hypoblast. By the start of week 3, a thickening containing a midline groove forms in the epiblast along with the disc and elongating to about half its length. This thickening (primitive streak) and a structure adjacent to it called the primitive node, define the cranial-caudal and medial-lateral axes of the embryo and represent the start of gastrulation. At this stage, epiblast cells migrate towards and into the primitive streak and ingress between the epiblast and hypoblast, undergoing epithelial-to-mesenchymal transition (EMT). The first cells to migrate into the primitive streak displace the hypoblast cells replacing them as definitive endoderm. As more epiblast cells migrate and occupy the space between epiblast and nascent definitive endoderm, the mesoderm is formed. By the time the definitive endoderm and mesoderm are established, and cells stop migrating towards the primitive streak, the remaining epiblast constitutes the ectoderm, which rapidly undergoes further differentiation. Gastrulation is then followed by a sequence of events leading to organogenesis. The mesoderm forms the notochord along with the primitive streak that, together with the primitive node, induces overlying ectodermal cells to differentiate into a neuroepithelium called neuroectoderm, thus initiating the formation of the neural tube (Schoenwolf GC et al., 2009b).

The progressive differentiation of structures and restriction of fate is a hallmark of embryonic development. Further specification naturally implies less plasticity and differentiation potential. But, as we now know, it can be reversed.

I.2.2.2. Reverting the potential of cells

While sharing the same genetic content, the identity of a cell within an adult organism is defined by its specific epigenomic profile which, by influencing its transcriptome and proteome, modulates fundamental properties such as the cell's capacity to divide and

differentiate. This means that what determines the phenotype of a cell it's not so much the genome, but rather the way by which that genome is expressed. Typically, the differentiation potential of cells tends to decrease along with the development of the organism, owing to progressive changes in genome expression, with some genes being silenced or restricted while others are activated. However, by having the same genetic information as a stem cell, a fully committed cell would, in theory, still retain the potential to have its state reverted upon the appropriate stimuli. It would then be able to generate any other cell type, or even to clone an entire organism, producing a fully functional new individual, genetically identical to the original donor. This concept was initially tested in the 1950s and '60s, by experiments of nuclear transfer in amphibian models (reviewed in Gurdon JB & Byrne JA, 2003). The work of John Gurdon is of particular relevance since he was the first to demonstrate that the nuclei of terminally differentiated cells, specifically from the intestinal epithelium of *Xenopus laevis* tadpoles, when transferred into enucleated eggs, were able to develop into normal feeding tadpoles (Gurdon JB, 1962). It was further evidenced when the same approach was used to clone several mammal species, starting in the late 1990s with "Dolly" the sheep (Wilmut I et al., 1997), and when cell fusion experiments combining human fibroblasts and ESCs reprogrammed the somatic genome to an embryonic-like state (Cowan CA, 2005). Taken together, those achievements showed that the nuclei of somatic cells contained all the information required to generate an entire organism, and that specific factors present in the cytoplasm of oocytes or ESCs enabled the expression of the genes necessary to trigger an early development stage. The uncovering or identification of such factors would be the focus of several following studies.

In 2006, Takahashi and Yamanaka published a paper describing the generation of ESC-like cells from mouse embryonic and adult fibroblasts, after the induced expression of specific transcription factors (TF) by retroviral transduction (Takahashi K & Yamanaka S, 2006). Starting from a pool of 24 genes that had been previously associated with either the maintenance of pluripotency or the proliferation of ESCs, they were able to identify four essential TF's – OCT4, SOX2, KLF4, and c-MYC – that, when combined, reprogrammed somatic cells to a pluripotent state. The generated cells, named iPSCs, had a genetic expression similar to those of ESCs and were able to differentiate into the three germ layers *in vitro* and *in vivo* (Takahashi K & Yamanaka S, 2006). Using improved selection protocols in later studies, iPSCs were shown to have DNA methylation more resembling of that of ESCs, and to produce chimeras when introduced into developing blastocysts, with a contribution to the germline (Okita K et al., 2007; Wernig M et al., 2007). In

the following year, the same approach, albeit with different combinations of TF's, would be used by two groups to successfully generate iPSCs from human fibroblasts – Yamanaka and colleagues used the same four TF's as before (Takahashi K et al., 2007), while Thomson and colleagues replaced KLF4 and c-MYC in Yamanaka's combination with NANOG and LIN28 (Yu J et al., 2007). The resulting cells, as had been previously shown with mouse iPSCs, expressed pluripotency markers, had ESC-like DNA methylation patterns, and were able to produce derivates of the three germ layers *in vivo* and *in vitro*. Of particular relevance was the fact that the reprogramming process involved demethylation of the endogenous versions of the TF's being induced, while the transgene versions were, to variable extent, silenced, thus indicating that the integration or constitutive expression of the transgenes was dispensable and that the achieved state was self-sustaining (Okita K et al., 2007; Takahashi K et al., 2007; Yu J et al., 2007). These results showed not only that human somatic cells could be reverted to a stable pluripotent state, but that different combinations of TF's could be used to achieve it.

The use of retroviral transduction to induce pluripotency implicated the chromosomal integration of vectors, which represented potential risks of insertional mutations and carcinogenesis, therefore limiting the applications of iPSCs. This obstacle was overcome by using other reprogramming approaches, such as episomal vectors (Yu J et al., 2009), recombinant proteins (Zhou H et al., 2009), synthetic mRNA (Warren L et al., 2010) and microRNA (Anokye-Danso F et al., 2011), which enabled the production of hiPSCs free of vector and transgene sequences. The use of certain small molecules has also been shown to promote the reprogramming process, reducing the number of reprogramming factors and increasing efficiency (reviewed in Qin H et al., 2017).

More recently, in 2013, Mitalipov and colleagues described a method for the production of hESCs using the approach pioneered by John Gurdon of somatic cell nuclear transfer (SCNT) (Tachibana M et al., 2013). By transferring the nuclei of human fibroblasts into enucleated oocytes, they were able to produce developing blastocysts, from which nuclear transfer (NT)-ESCs were derived. When compared with iPSCs, the cells produced by this method appear to be more similar to ESCs derived from fertilized embryos in terms of gene expression and DNA methylation, which suggests a more reliable pluripotent state (Ma H et al., 2014). While retaining the nuclear genome of the donor somatic cell, they can potentially be used for autologous transplants in cell replacement therapies. Nevertheless, the production of NT-ESCs does raise some ethical concerns that do not apply to iPSCs, since it involves the

generation of human artificial embryos (albeit non-viable) and their consecutive destruction. The requirement of high-quality human oocytes (Tachibana M et al., 2013) may also be considered a substantial constraint on several levels and carry further ethical concerns (Hyun I, 2011; Bobbert M, 2006).

The reprogramming of somatic cells to pluripotency opened new doors, positively influencing the prospects of patient-specific cell replacement therapies, and contributed significantly to our understanding of the complex mechanisms underlying pluripotency maintenance and differentiation. These mechanisms will be further detailed in the following sections.

I.2.2.3. The triptych of pluripotency

Although pluripotency is a transient state *in* vivo, given the appropriate culture conditions it is virtually possible to expand hPSCs *in vitro* indefinitely, while retaining their key characteristics. This is mainly due to a balance attained by a self-sustaining network of transcription factors contributing to self-renewal. Of the six factors used in the first two papers describing the generation of hiPSCs in 2007, three have been shown to play essential roles in the circuitry regulating the maintenance of pluripotency – OCT4, SOX2, and NANOG. By either promoting or repressing the expression of myriad genes, these TF's are thought to manage a complex signaling network whose intricacies and extension are still being uncovered.

OCT4 is a homeodomain-containing TF of the POU family. It is expressed during the first stages of embryonic development in the morula and ICM of the blastocyst, being confined to primordial germ cells and suppressed in other tissues as further differentiation ensues (reviewed in Pesce M & Schöler HR, 2000, 2001). Its abrogation in mice was shown to lead to failure in ICM formation and embryo death (Nichols J et al., 1998). In mouse ESCs, while its upregulation promotes differentiation into primitive endoderm and mesoderm, its downregulation leads to dedifferentiation towards trophectoderm (Niwa H et al., 2000). SOX2 is likewise expressed during the first stages of development in the ICM and is essential in the formation of the trophoblast and embryo survival (Keramari M et al., 2010). Unlike OCT4, however, and similarly to other members of the SOX family, it is maintained during differentiation towards neuroectoderm and

throughout development in neural progenitors, playing a critical role in the formation of the nervous system and the maintenance of neural stem cells' identity [Takemoto T et al., 2011; Thomson M et al., 2011; Graham V et al., 2003]. NANOG is also a homeodomain-containing TF and was initially identified, cloned and described in mouse ESCs in 2003, being able to sustain their self-renewal in the absence of leukemia inhibitory factor (LIF) [Chambers I et al., 2003; Mitsui K et al., 2003; Wang S-H et al., 2003]. It was shown to be essential for epiblast formation and germline development in the mouse embryo and its suppression in mouse ESCs, while not immediately disrupting pluripotency, promoted spontaneous differentiation, which suggests that it may play a role in the stabilization of the pluripotent state [Chambers I et al., 2007; Mitsui K et al., 2003].

The expression of these pluripotency factors works as an autoregulatory network given that each of them promotes the transcription of their gene and those of the other two, creating stable and seemingly redundant feed-forward loops [Boyer LA et al., 2005; Rodda DJ et al., 2005]. Furthermore, they were found to bind hundreds of other genes implicated in either self-renewal or differentiation, including components of signaling pathways such as transforming growth factor (TGF)β and Wnt, as well as to genes coding for miRNA's, cell cycle regulators and chromatin modulators [Lee J et al., 2010; Zhang X et al., 2009; Boyer LA et al., 2005]. Despite the seemingly redundant action on pluripotency maintenance, it is interesting to note that instead of acting as pan-repressors of differentiation, each of the three core TF's, along with other pluripotency regulators, play varying roles in lineage determination. A study by Ivanova and colleagues systematically analyzed the phenotypes produced by overexpression or knock-down of each of core pluripotency TF's in several hESC lines and found that: 1) the result of OCT4 knock-down or overexpression is dependent on the activity of bone morphogenetic protein (BMP)4 signaling, which is a known inhibitor of neuroectoderm differentiation; specifically, OCT4 knock-down promotes a neuroectoderm fate in the absence of BMP4, but in its presence leads to trophectoderm and primitive endoderm determination; OCT4 overexpression did not cause differentiation when BMP4 was inhibited, but its presence promoted mesendoderm specification, indicated by the expression of primitive streak markers; 2) the knock-down of SOX2 did not cause the differentiation of hESCs but promoted mesendoderm fate under differentiation conditions, while its overexpression repressed mesendoderm and enhanced the differentiation towards neuroectoderm; 3) NANOG knock-down promoted neuroectoderm differentiation whereas its overexpression upregulated endoderm markers and completely repressed the neuroectoderm fate under differentiation conditions [Wang Z et al.,

2012). The fact that the overexpression of all the core TF's didn't lead to loss of pluripotency indicates that their effect on lineage determination relies primarily on the selective repression of differentiation. Therefore, it is possible to say that while OCT4 and NANOG mainly repress neuroectoderm differentiation, SOX2 represses mesendoderm phenotypes (Wang Z et al., 2012).

The core TF's have also been shown to act on the machinery regulating the cell cycle, particularly reducing the length of G_1-phase, which is consistent with rapidly dividing cells. Furthermore, G1-phase appears to be favorable to differentiation in hESCs (Singh AM et al., 2013), while S- and G2-phases were shown to promote pluripotency (Gonzales KAU et al., 2015), which indicates that cell cycle regulation is intimately related to the fate of PSCs (reviewed in Boward B et al., 2016). OCT4 has been shown to inhibit the expression of p21 and to promote cell cycle progression from G_1 to S-phase (Lee J et al., 2010) and, along with SOX2, to bind to a promoter of miR-302, a cluster of microRNA shown to inhibit cyclin D1 (Card DAG et al., 2008). NANOG was shown to promote the expression of cyclin-dependent kinase (CDK)6 and cell division cycle (CDC)25A, as well as inducing the entry in S-phase (Zhang X et al., 2009).

Other TF's have been identified to interact with the core pluripotency regulators, having a relevant role in the self-renewal of hPSCs. For example, FOXO1, which has been implicated in tissue homeostasis and autophagy, has been shown to promote the expression of both OCT4 and SOX2, playing an essential function in the regulation of hESC fate (Zhang X et al., 2011). SMAD2/3 is known to induce the expression of NANOG (Xu R-H et al., 2008) and different signaling pathways have been involved in either the self-renewal or differentiation of hPSCs. These will be detailed in the next section.

I.2.2.4. Signaling pathways for self-renewal and differentiation

Signal transduction pathways represent mechanisms through which cells interact with and respond to external stimuli, typically establishing molecular circuits between receptors on the cellular membrane and transcription factors that act on gene regulation. Functionally, although a specific pathway may play a key role in determining a specific outcome to a specific stimulus, it does not act in isolation and its result may be conditioned by concomitant factors. During embryonic development, PSCs don't remain pluripotent for long. This implies that

while the core TF's that regulate pluripotency establish a self-sustained signaling network, other signals must be involved in the decision of self-renewal *versus* differentiation.

When hESCs were first derived, they were cultured on a feeder layer of mouse embryonic fibroblasts (MEF), based on the method that had been initially established for the culture of mouse and rhesus monkey ESCs [(Thomson JA et al., 1995, 1998; Evans MJ & Kaufman MH, 1981; Martin GR, 1981)]. However, while mouse ESCs were found to retain pluripotency in feeder-free conditions when cultured in medium with serum and LIF [(Smith AG et al., 1988; Williams RL et al., 1988)], both rhesus monkey and human cells differentiated in feeder-free culture conditions, with or without LIF [(Thomson JA et al., 1995, 1998)]. It was later found that while mouse ESCs relied on the phosphorylation of Stat3 as a downstream effector of LIF and BMP-activated SMAD signaling for self-renewal [(Ying Q-L et al., 2003)], that was not the case in hESCs.

The maintenance of pluripotency in cultured hPSCs is usually reliant on the activation of two specific signaling pathways: a) TGFβ/Activin A/Nodal-activation of SMAD2/3 and b) fibroblast growth factor (FGF)2. However, the mechanisms involved in this control are still not completely clarified [(reviewed in Zhao H & Jin Y, 2017)]. TGFβ/Activin A/Nodal act through SMAD2/3, which were shown to bind to the promoter region of NANOG and directly induce its expression [(Vallier L et al., 2009; Xu R-H et al., 2008)]. However, Activin A was also shown to be involved in mesendodermal differentiation, modulated by the signaling of phosphatidylinositol 3-kinase (PI3K) [(McLean AB et al., 2007)]. Singh *et al.* proposed a model in which the levels of PI3K determine the decision of hESCs to self-renew or differentiate, by regulating the threshold of Activin A/SMAD2/3 activation [(Singh AM et al., 2012)]. According to this model, PI3K/AKT signaling is activated by FGF2, insulin-like growth factor (IGF)1 or heregulin in the culture medium and promotes the self-renewal of hES cells by 1) suppressing extracellular signal-related kinases (ERK) and Wnt differentiation signals, and 2) modulating SMAD2/3 activation to promote the expression of pluripotency-related genes. In the absence of PI3K/Akt signaling, SMAD2/3 activity is enhanced and, adjuvated by ERK and Wnt signaling, it activates genes related to mesendodermal differentiation [(Singh AM et al., 2012)]. It was later found that PI3K signaling acts on the duration of SMAD2/3 activity through activation of the mechanistic target of rapamycin complex (mTORC)2, which primes SMAD2/3 for degradation [(Yu JSL et al., 2015)]. mTORC1, likewise promoted by PI3K/Akt signaling, is likely also involved in the maintenance of pluripotency, since its inhibitor, rapamycin, was shown to induce the expression of mesendodermal marker T (homolog of Brachyury) in hESCs [(Nazareth EJP et al., 2016)]. Other than the activation of PI3K

signaling, FGF2 is also known to activate ERK signaling, which has been associated with both the maintenance of pluripotency and differentiation (Greber B et al., 2011; Na J et al., 2010; Eiselleova L et al., 2009; Li J et al., 2007). These opposing effects are not yet fully clarified but may be due to various levels of ERK activation or its modulation through other pathways.

Existing research indicates that the fate of hPSCs relies on complex crosstalk between different signaling pathways. Therefore, the same pathway may, in different molecular contexts, be involved in either self-renewal or differentiation. While Wnt/β-catenin signaling was initially associated with pluripotency maintenance in hESCs (Sato N et al., 2004), recent research indicates that it plays a rather relevant role in lineage specification (Blauwkamp TA et al., 2012; Davidson KC et al., 2012; Singh AM et al., 2012). The endogenous expression of Wnt in individual hESCs was shown to correlate with their propensity to differentiate towards specific lineages: cells expressing higher levels of Wnt differentiated preferentially to endodermal and mesodermal derivatives, while the ones expressing lower levels generated primarily neuroectodermal cells (Blauwkamp TA et al., 2012). Consistently, the inhibition of Wnt signaling by SOX2 has been reported to be determinant for neuroectodermal differentiation (Zhou C et al., 2016). Huang et al. suggested that the duration of Wnt signaling determines its outcome through a two-layer regulatory circuit involving E-cadherin (Huang T-S et al., 2015). E-cadherin, expressed from gene CDH1, is a transmembrane adhesion glycoprotein responsible for calcium-dependent cell-cell contacts (*adherens* junctions) in epithelial tissues. It is regarded as a supplementary marker of pluripotency, playing a role in the self-renewal of hESCs and its expression rapidly decreases during differentiation (Spencer H et al., 2011; Li L et al., 2009; Eastham AM et al., 2007). Huang and colleagues showed that the short-term activation of Wnt/β-catenin signaling in hESCs leads to the upregulation of E-cadherin and consequent pluripotency maintenance via PI3K/Akt activation. Furthermore, the increase in E-cadherin promotes the reduction of free cytoplasmic β-catenin, which binds to the membrane adhesion protein. Upon long-term activation of Wnt signaling, however, there is an increase in cytoplasmic β-catenin after inhibition of glycogen synthase kinase (GSK)3β, which exceeds the binding capacity of membrane E-cadherin. This leads to the translocation of β-catenin to the nucleus, where it upregulates the expression of E-cadherin inhibitor Slug, further reinforcing the accumulation of β-catenin and promoting the differentiation of hESCs to mesendoderm (Huang T-S et al., 2015).

Another signaling pathway with relevant implications in the differentiation of hPSCs is BMP4. While this growth factor was identified as promoting pluripotency in mouse ESCs (Qi X

et al., 2004), it induces the differentiation of hESCs towards mesendoderm and trophoblast cells, in a process likely mediated by FGF2/ERK and Wnt signaling (Kurek D et al., 2015; Drukker M et al., 2012; Yu P et al., 2011). Consistently, the blocking of both BMP and Activin/TGFβ signaling is known to promote neuroectodermal differentiation of hPSCs under defined conditions (Chambers SM et al., 2009).

I.2.2.5. Naïve pluripotency

One of the most striking differences between hESCs and mouse ESCs is the fact that they require significantly different conditions for *in vitro* expansion and respond differently to specific growth factors. While mouse ESCs maintain pluripotency under LIF/Stat3 and BMP4/Smad signaling or by inhibition of Erk and Gsk3, hESCs require Activin A/SMAD and FGF2 signaling (reviewed in Zhao H & Jin Y, 2017). These profound disparities raised fundamental questions, such as whether derived hESCs might be artifacts generated from *in vitro* culturing (Noggle SA et al., 2005). In 2007, two groups derived a new type of mouse ESCs from early post-implantation epiblast stage embryos, which they called epiblast-derived (Epi)SCs (Brons IGM et al., 2007; Tesar PJ et al., 2007). These cells resembled hESCs much more than mouse ESCs in terms of culture morphology and in that they similarly required Activin and FGF2 signaling to maintain self-renewal. This new evidence suggested that hESCs, as EpiSCs, are probably not so much a cell culture artifact but rather a representation of a slightly later developmental stage or primed pluripotent state, versus a naïve pluripotent state of mESCs (Nichols J & Smith AG, 2009).

Several differences have been identified between naïve and primed state pluripotent cells. Along with considerably different gene expression profiles, naïve PSCs have much lower DNA methylation and display activation of the two X chromosomes in female cells, whereas in the case of primed cells one X chromosome is inactivated, similar to what occurs during embryonic development (reviewed in Zhou X et al., 2015; Nichols J & Smith AG, 2009). This distinction between pluripotency states is relevant not only because it explained the striking differences between mESCs and hESCs, thus evidencing a further need for caution when comparing both models, but also because it raised the question of whether a naïve pluripotency state could be achieved in hESCs. Deriving naïve hPSCs could, in theory, allow more reliable comparisons with mouse ESCs, while providing a possibly better model to study early differentiation events

in the human embryo. Furthermore, while mouse ESCs tolerate single-cell dissociation, hPSCs undergo apoptosis when subjected to such a process (Ohgushi M et al., 2010; Watanabe K et al., 2007). A naïve state of hESCs consistent with the mouse counterpart could potentially be more tolerant of single-cell dissociation, thus allowing more stability and further versatility in terms of study and expansion conditions.

Different groups have published results describing the generation of hESCs exhibiting key characteristics of naïve pluripotency, either by direct isolation from human blastocysts (Guo G et al., 2016) or by reprogramming from primed state hESCs (Takashima Y et al., 2014; Theunissen TW et al., 2014). However, while the signaling pathways and transcription factors involved in their support are very similar to the ones observed in mouse ESCs, they appear to be far less stable, display considerably different epigenetic profiles and yield reduced viability upon single-cell passaging (reviewed in Bates LE & Silva JCR, 2017). Further research is needed to understand why these differences occur and, eventually, to determine the optimal conditions for the derivation and culture of naïve hESCs. This will hopefully clarify the nature of these cells and provide more sustained insights about their potential applications.

I.3. Human pluripotent stem cell culture

Generally speaking, the culture of any mammalian cell type has three main requirements that usually vary according to the nature of the cells: 1) an appropriate growth medium containing the nutrients, minerals and growth factors that allow the cells to survive and divide, 2) an extracellular matrix to provide structural support and/or extracellular signals to the cells, and 3) a set of environmental cues, such as temperature, pH and gas pressure (Chen KG et al., 2014). These key factors, along with the actual culturing procedures, are typically adjusted or engineered to meet the specific needs of the cells being grown and the ultimate purpose of the culture.

While the conditions used in the initial studies with hESCs would have been mostly focused on achieving successful derivation and expansion, the effort soon shifted towards the need to develop optimized and defined methods to enhance the reliability of these cells as research models and enable large-scale and GMP-compliant production for therapeutic purposes (Villa-Diaz LG et al., 2013). As research progressed and the knowledge base on hPSCs

widened, gradual improvements were implemented, specifically in terms of the growth media components and the support matrix/substrate used, as well as the actual culture procedures and platforms. This will be further detailed in the following sections.

I.3.1. Removing feeders

In the seminal report published by Thomson in 1998, hESCs were expanded on a feeder layer of inactivated MEF, using medium containing 20% fetal bovine serum [(Thomson JA et al., 1998)], following in part the protocol used to propagate mouse ESCs established almost twenty years earlier [(Evans MJ & Kaufman MH, 1981)]. Although it was shown to sustain the proliferation of undifferentiated hESC, this method was suboptimal and had several drawbacks in terms of consistency, safety, and scalability [(Draper J & Moore H, 2004)].

One of the first improvements was the replacement of serum. Serum provided several nutrients and vitamins necessary for cell survival and proliferation but, due to batch-to-batch variability, its propensity to induce the differentiation of cells and the risk of contamination with infectious agents, it was widely replaced by proprietary supplements with a more defined and controlled formulation [(Koivisto H et al., 2004; Amit M et al., 2000)]. As for the feeder cells, by secreting combinations of specific extracellular matrix proteins, growth factors, and cytokines, they provided the hESCs with both a suitable support substrate and the molecular cues required to proliferate and to retain pluripotency [(Abraham S et al., 2010; Prowse ABJ et al., 2007)]. Feeder cells of differing origins yielded varying degrees of efficiency, with human foreskin fibroblasts becoming frequently used to support the culture of hESCs, given their human origin and accessibility [(Hongisto H et al., 2012; Richards M et al., 2003)]. Still, their use carried significant disadvantages, such as the difficulty in achieving consistent secretion of factors, which posed reproducibility issues and possible outcome bias, as well as the risk of pathogen transmission and the laborious procedures required for cell passaging. This led to the progressive adoption of alternatives.

I.3.1.1. Substrate

Matrigel was one of the first compounds used as a substrate in feeder-free conditions, after being reported to enable, in combination with MEF-conditioned medium, the proliferation of hESCs in an undifferentiated state [(Xu C et al., 2001)]. It is an extract of mouse Englebreth-Holm-Swarm sarcomas, mainly composed of ECM basement membrane proteins such as laminin, type IV collagen, heparan sulfate proteoglycan and entactin. It was shown to be biologically active, sustaining the proliferation and differentiation of several types of cells and explants [(reviewed in Kleinman HK & Martin GR, 2005)]. While it was an improvement upon feeder-based culture for providing a more chemically defined attachment substrate and better reproducibility, Matrigel is still not fully defined, displaying lot-to-lot variability and containing undetermined growth factors and chemical compounds, which, in combination with its xenogeneic nature, make it an unsuitable matrix for the production of clinical-grade hESCs [(Chen KG et al., 2014; Hughes CS et al., 2010)]. Furthermore, not all ECM components of Matrigel are required for hESC maintenance. Of the most abundant ECM proteins present in Matrigel, laminin was found to sustain the growth of hESC, while type IV collagen led to differentiation [(Xu C et al., 2001)]. Following these findings, purified recombinant human ECM proteins have been successfully used in hPSC culture. Given the high expression of laminin-binding integrin α6β1 in hESCs, Miyazaki and colleagues tested different isoforms of recombinant laminins as substrate. They found that isoforms -111, -511 and, most efficiently, -332, to which integrin α6β1 preferentially binds, provided an effective substrate for the expansion of undifferentiated hESCs [(Miyazaki T et al., 2008)]. Vitronectin, another integrin-binding molecule, has also been shown to promote hESC attachment and self-renewal *in vitro* [(Chen G et al., 2011; Braam SR et al., 2008)]. E-cadherin, which is responsible for cell-cell adhesion in hPSCs, is another example of a recombinant attachment molecule successfully used as a substrate in feeder-free culture [(Nagaoka M et al., 2010)]. Despite some indications that recombinant adhesion molecules may yield a slower growth rate that Matrigel [(Akopian V et al., 2010; Miyazaki T et al., 2008)], they represent viable substrate options for chemically defined and xeno-free culture systems. Several synthetic compounds have also been proposed as GMP-compliant substrates for hPSC culture in both 2- and 3-dimensional systems [(Lei Y & Schaffer D V, 2013; Brafman DA et al., 2010; Villa-Diaz LG et al., 2010; Gerecht S et al., 2007)].

I.3.1.2. Medium

The role of the feeder cells in the protocol initially used to derive and expand hESCs was not limited to providing a suitable attachment substrate, but also acted as a source of soluble factors that enabled the maintenance of pluripotency. While in mESC culture the addition of LIF to the growth media was sufficient to maintain the pluripotent phenotype under feeder-free conditions, hESCs rapidly differentiated in the absence of feeder cells, with or without LIF [Reubinoff BE et al., 2000; Thomson JA et al., 1998]. The first solution to overcome this issue was to culture the cells in a medium previously conditioned by feeder cells [Xu C et al., 2001]. This methodology, when used in combination with alternative substrates, allowed the removal of feeder cells from the actual culture but not from the culturing process altogether, meaning that most of the drawbacks associated with their use, such as poor consistency and the risk of pathogen transmission, were still present [Draper J & Moore H, 2004]. A substantial effort went into determining which specific soluble factors in feeder-conditioned-media enabled pluripotency maintenance. Following a study showing that FGF2 improved the cloning efficiency of hESCs in serum-free medium [Amit M et al., 2000], Amit et al. reported that medium with serum replacement and supplemented with FGF2 and TGFβ supported the undifferentiated expansion of hESCs on fibronectin [Amit M et al., 2004]. Subsequent reports further confirmed the relevance of FGF2 for hESC self-renewal cultured in feeder-free conditions on Matrigel and laminin [Levenstein ME et al., 2006; Li Y et al., 2005; Xu C et al., 2005]. Together, these results established FGF2 as a central component in hESC culture and represented the first step towards the development of fully defined media.

Several defined media were made commercially available over the following years, although most still included bovine serum albumin (BSA) [Viswanathan P et al., 2014]. One example is mTeSR1, a widely used medium, commercialized by Stem Cell Technologies and based on a published formulation [Ludwig TE et al., 2006b, 2006a]. Adding to the xenogeneic nature and lot-to-lot variability of BSA, its role in hPSC culture was not fully understood, although its removal from mTeSR1 led to a sharp decrease in culture efficiency. Upon attempts to clarify the role of each component in mTeSR1 medium, Chen and colleagues reported the development of a defined xeno-free medium for hPSC derivation and expansion, containing only 8 essential components – insulin, selenium, transferrin, L-ascorbic acid, FGF2, and TGFβ, in basal DMEM/F-12 with sodium bicarbonate. They showed that BSA did not improve hESC survival

but rather countered the toxic effects of another component, β-mercaptoethanol, which was itself also not required [Chen G et al., 2011]. This medium, named Essential-8 (E8), in combination with the use of a defined substrate, provided what may be considered the first truly defined xeno-free approach for hPSC culture.

I.3.2. Culture systems

The establishment of defined conditions in hPSC culture is not only a pre-requisite for GMP-compliant production but also an essential factor in the actual development of robust and efficient methodologies spanning the whole production process, from cell derivation to cell banking. In general, increased control over experimental variables allows better reproducibility and reduces variance, thus leading to more reliable and comparable results that, in turn, boost scientific progress.

Initial studies with hESCs consistently reported low yields in cell cloning and frequent spontaneous differentiation [Amit M et al., 2000; Reubinoff BE et al., 2000; Thomson JA et al., 1998]. Apart from the progress made regarding media and substrate, some changes in the methods used also played a significant role in the improvement of culture efficiency. Cell passaging, for instance, is a critical step in cell expansion, often impacting its overall yield. hPSCs typically need to be passaged as clumps since single-cell dissociation leads to massive cell death by apoptosis, due to disruption of E-cadherin cell-cell adhesion and subsequent myosin-actin-dependent contractions [Chen G et al., 2010]. Different techniques have been employed such as mechanical scraping, microdissection and enzymatic digestion using collagenase or dispase, although with varying degrees of effectiveness. In this regard, Watanabe and colleagues showed that the application of a Rho-associated kinase (ROCK) chemical inhibitor – Y-27632 – to the culture medium before enzymatic cell detachment and after plating significantly improved cell survival, by suppressing the apoptotic response triggered by single-cell dissociation [Watanabe K et al., 2007]. There are, however, some indications that this molecule can affect lineage commitment [Maldonado M et al., 2016] and cellular metabolism [Vernardis SI et al., 2017]. On the other hand, cell detachment protocols using ethylenediaminetetraacetic acid (EDTA) [Beers J et al., 2012] or sodium citrate [Nie Y et al., 2014] were shown to allow high cell survival and fast recovery after

passaging, being chemically-defined, consistent and inexpensive alternatives to enzymatic methods.

The use of hPSCs in some regenerative medicine applications requires production processes that are not only GMP-compliant but also capable of generating high quantities of cells. With the increased knowledge of the biological fundamentals and the establishment of defined, xeno-free culture conditions, more efforts are being drawn towards the development of high-efficiency scalable expansion solutions (reviewed in Jenkins MJ & Farid SS, 2015; Serra M et al., 2012).

It is possible to distinguish between two main types of hPSCs expansion systems: a) planar systems, in which cells are grown on a static surface and b) three-dimensional/suspension systems. As with most mammalian cells, research laboratories typically grow hPSCs in plates, dishes or t-flasks. While these are suitable platforms when relatively low numbers of cells are required, they are very limited in terms of scalability, labor-intensive, and space consuming. Automated stacked planar bioreactors improve on regular planar platforms by reducing the workload, improving consistency and distributing the required surface area vertically, but are still more appropriate for small-scale production, such as for autologous cell therapies or personalized drug screening (Jenkins MJ & Farid SS, 2015). Three-dimensional systems, on the other hand, tend to be up-scalable, automatable, and highly optimizable. Several three-dimensional culture systems have been used to expand hPSCs, including microcarrier-based (Badenes SM et al., 2016), microencapsulation (Serra M et al., 2011), and cellular aggregates (Wang Y et al., 2013), which allow the use of spinner flasks at a smaller scale or stirred-tank bioreactors for medium- to large-scale production. The culture of cells as aggregates is likely the simplest and least laborious process, as hPSCs naturally self-aggregate when cultured in the absence of a compatible substrate (Amit M et al., 2010; Steiner D et al., 2010). The lack of control over aggregate size and homogeneity may, however, introduce bias and lead to poor nutrient diffusion and the death of innermost cells (Chen VC et al., 2012). Microcarrier-based culture may be thought of as a three-dimensional derivation of planar culture, as it relies on cellular attachment to a surface while providing a greater surface/volume ratio. It allows better control over nutrient and gas diffusion but has the downside of requiring extra material and steps for cell recovery, and the difficulty in controlling microcarrier clumping (Serra M et al., 2012). When culturing cells as aggregates or on microcarriers in stirred-suspension cultures systems, the cells are exposed to shear forces, which reduces yield. Microencapsulation of

the cells in hydrogels protects against such damage, as well as against clumping, although at the expense of much more laborious procedures and possibly lower diffusion [(Serra M et al., 2012)]. Despite the particular advantages or pitfalls of each system, accurate finetuning based on the extensive characterization and monitoring of key indicators is essential in order to improve the culture yield, retain control over quality and drive down production costs.

I.4. Cellular microenvironment

Not unlike the organisms that they compose, cells may be conceived as a product of their surroundings. From embryonic development and throughout life, the cells in the human body are tuned or conditioned to carry out determined functions, being induced to divide, differentiate, migrate, secrete soluble factors, or die. While the capacity to carry out these actions may be intrinsic, they are, to a great extent, triggered (or inhibited) by combinations of external stimuli, which compose the cellular microenvironment.

Understanding how microenvironmental cues affect hPSCs has been one of the main trends in stem cell research, as this knowledge is determinant to developing controlled and optimized protocols for expansion and differentiation, as well as more robust, unbiased *in vitro* models for toxicological assessments and drug discovery. The rise of three-dimensional culture systems and automated high-throughput technologies has provided new insights and enabled powerful novel platforms for the study of how microenvironmental properties affect stem cell fate [(Park D et al., 2015; Shao Y et al., 2015; Baker BM & Chen CS, 2012)].

I.4.1. The third dimension

Most of what is currently known regarding stem cells and, in general, eukaryotic cell biology, was assessed using homogenous cell populations cultured as monolayers on planar surfaces, even though such conditions are very far from replicating an *in vivo* environment. It is easy to understand why – simplistic models allow for much better control over the experimental setting and variables, thus reducing confounding effects and producing results with higher reproducibility and statistical significance. A potential risk, however, is that they may, as well, have a higher tendency to produce experimental artifacts, meaning that the

results obtained might not be representative of *in vivo* physiological conditions, but rather a byproduct of the conditions in which the cells are being manipulated [(Baker BM & Chen CS, 2012)]. This caveat gains particular relevance considering the great susceptibility that hPSCs display to microenvironmental changes and the subtle balance of variables controlling their fate. The unclear understanding of how hPSCs respond to changing stimuli is one of the major obstacles to the realization of their potential in regenerative medicine [(Park D et al., 2015)].

The concept of microenvironmental stimulus encompasses diverse types of chemical and physical properties, including a) soluble factors and nutrients, such as ions, glucose, amino acids, cytokines and morphogens, and their specific gradients, b) extracellular matrix composition, c) cell-cell interactions, and d) mechanical characteristics and forces [(Metallo CM et al., 2007)]. The conjugation of these factors largely contributes to the specification of cellular phenotypes and, in the case of hPSCs, to fate determination. For instance, as has been previously described, FGF2 promotes the maintenance of the pluripotent state [(Levenstein ME et al., 2006)], while BMP4 induces differentiation towards extraembryonic lineages [(Xu R-H et al., 2002)]. In combination, however, these two factors appear to promote mesendodermal differentiation through modulation of NANOG levels [(Yu P et al., 2011)]. Variations in oxygen tension have also been shown to affect the expression of pluripotency genes, with hypoxia levels contributing to the prevention of spontaneous differentiation *in vitro* [(Forristal CE et al., 2010; Ezashi T et al., 2005)]. Likewise, the extracellular matrix composition and its mechanical and geometrical properties can influence self-renewal and drive cell specification towards different lineages [(Toh Y-C et al., 2015; Pan F et al., 2013; Zhang J et al., 2012)]. It is important to note, however, that the relationship between cells and microenvironment is not necessarily unidirectional, as cells also can modulate their surroundings, to some extent.

In 2-D adherent culture systems, hPSCs typically display a flat morphology with significantly forced basal-apical polarity – while one "side" of the cell is establishing connections with the substrate via integrins, the other "side" is mostly in contact with the culture medium. This is one of the most striking differences between 2-D and 3-D culture systems [(Baker BM & Chen CS, 2012)]. When cultured as 3-D spheroids in suspension, hPSCs contact mostly with other cells, mainly via E-cadherin, while nutrient, gas, and growth factor gradients are established between the outermost cells and the cells on the inside of the aggregates [(Kinney MA et al., 2014)]. These distinct characteristics likely account for at least some of the differences that have been observed between the two systems. For instance, the 3-D culture

of hESC in microwells has been reported to result in higher expression of E-cadherin and downregulation of mesenchymal-related genes, but to yield greater mesendodermal specification upon differentiation as embryoid bodies when compared to 2-D culture [Hsiao C et al., 2014; Azarin SM et al., 2012]. Recently, Branco et al. reported that hiPSC cultured as spheroids displayed a transcriptomic profile consistent with enhanced cardiac maturation after a directed differentiation protocol versus cells cultured in 2-D [Branco MA et al., 2019]. The size of the cellular aggregates has also been shown to influence cell differentiation in embryoid bodies [Moon S-H et al., 2014; Bauwens CL et al., 2008], further evidencing that 3-dimensional systems introduce variables that may not be sufficiently represented in planar systems.

In recent years, the development of cellular organoids has gained particular relevance given their potential applications as *in vitro* models for developmental biology research and drug discovery. These are typically generated by inducing the directed differentiation of stem cells in 3-D, yielding multicellular spheroids with relatively organized structures that partly emulate tissues in the human body, such as brain [Monzel AS et al., 2017; Lancaster MA & Knoblich JA, 2014; Eiraku M & Sasai Y, 2012], gut [McCracken KW et al., 2014], liver [Takebe T et al., 2013], and kidney [Takasato M et al., 2015]. The use of such models allows a level of complexity much more resembling of physiological conditions when compared to 2-D models or homogenous 3-D models, albeit at the expense of reproducibility [reviewed in Ho BX et al., 2018; Clevers H, 2016].

I.4.2. Microscale screening technologies

The realization that stem cell fate is determined by a multitude of chemical and physical variables, along with the development of *in vitro* models with increasing complexity, poses significant challenges in terms of experimental design. One the one hand, it would be desirable to assess how the variation of particular microenvironmental cues influences the experimental outcome, both individually and in combination. On the other hand, because it is virtually impossible to fully control all variables in an experimental setting, the use of more complex models, such as three-dimensional models, with higher intrinsic variance implies that more experimental replicates are needed in order to increase the accuracy of results. These requirements are considerably difficult to meet using traditional materials and methods, such as multi-well plates and manual pipetting, due to space constraints, reagent consumption,

and the very laborious procedures involved. The rise of automation, microfabrication, and micro-handling technologies came as a valuable opportunity to face these challenges, particularly by allowing the miniaturization and parallelization of experimental conditions with high accuracy, thus reducing labor, reagent, and cellular material requirements, and greatly increasing throughput [Rothbauer M et al., 2016; Montanez-Sauri SI et al., 2015; Fernandes TG et al., 2009].

Varied microscale screening platforms for 3-dimensional cellular models have been reported over the last decades, with a particular focus on drug discovery. These include hanging-drop plates, microwell plates, microfluidic devices and cellular microarrays [reviewed in Montanez-Sauri SI et al., 2015]. While hanging-drop plates and microwell plates allow high consistency in aggregate size between replicates, they involve several technical constraints and are somewhat limited in terms of cell-ECM interaction testing [Montanez-Sauri SI et al., 2015]. Microfluidic devices are highly versatile in that they allow the testing of soluble compounds with a high degree of spatial and temporal control and concentration gradients, although they are generally limited in terms of parallelization [Chi C-W et al., 2016]. Cellular microarrays, on the other hand, allow high parallelization coupled with relatively simple production, handling, and analysis, although in most of the platforms described, the replicates share the same media formulation [Montanez-Sauri SI et al., 2015].

The development of new microscale screening platforms with high dimensionality, high parallelization capabilities, robust control over experimental conditions, and simplified handling is seen as a way of generating large and significant amounts of data, which can contribute to further the understanding of the molecular mechanisms governing stem cell self-renewal and differentiation.

I.5. Thesis outline

This thesis presents the key results and findings of research work developed at Rensselaer Polytechnic Institute, in the United States of America, and at Instituto Superior Técnico, in Lisbon. **Chapter II** describes the methods used throughout, as well as the rationale for specific implementations, protocol modifications, and analysis algorithms. The results are then presented in two main chapters: **Chapter III** focuses on the development of a three-dimensional cellular microarray chip platform for studies on hPSCs, describing the different

strategies tested, assessment of cell growth and viability on-chip and, finally, a proof-of-concept experiment that evidenced the system's advantages and limitations; **Chapter IV** focuses on the characterization of a static spheroid hPSCs culture system, and the study of how 2-D and 3-D cultured cells react differently to some of the conditions tested on the cellular microarray platform. The main conclusions and future directions are presented in **Chapter V**.

I.6. References

Abraham S, Riggs MJ, Nelson K, Lee V & Rao RR (2010). Characterization of Human Fibroblast-Derived Extracellular Matrix Components for Human Pluripotent Stem Cell Propagation. *Acta Biomaterialia* 6, 4622–4633. **DOI:** 10.1016/j.actbio.2010.07.029.

Akopian V, Andrews PW, Beil S, Benvenisty N, Brehm J, Christie M, Ford A, Fox V, Gokhale PJ, Healy L *et al.* (2010). Comparison of Defined Culture Systems for Feeder Cell-Free Propagation of Human Embryonic Stem Cells. *In Vitro Cellular & Developmental Biology - Animal* 46, 247–258. **DOI:** 10.1007/s11626-010-9297-z.

Alison M & Islam S (2009). Attributes of Adult Stem Cells. *The Journal of Pathology* 217, 144–160. **DOI:** 10.1002/path.2498.

Amit M, Carpenter MK, Inokuma MS, Chiu C-P, Harris CP, Waknitz MA, Itskovitz-Eldor J & Thomson JA (2000). Clonally Derived Human Embryonic Stem Cell Lines Maintain Pluripotency and Proliferative Potential for Prolonged Periods of Culture. *Developmental Biology* 227, 271–278. **DOI:** 10.1006/dbio.2000.9912.

Amit M, Shariki C, Margulets V & Itskovitz-Eldor J (2004). Feeder Layer- and Serum-Free Culture of Human Embryonic Stem Cells. *Biology of Reproduction* 70, 837–845. **DOI:** 10.1095/biolreprod.103.021147.

Amit M, Chebath J, Margulets V, Laevsky I, Miropolsky Y, Shariki K, Peri M, Blais I, Slutsky G, Revel M & Itskovitz-Eldor J (2010). Suspension Culture of Undifferentiated Human Embryonic and Induced Pluripotent Stem Cells. *Stem Cell Reviews and Reports* 6, 248–259. **DOI:** 10.1007/s12015-010-9149-y.

Anghileri E, Marconi S, Pignatelli A, Cifelli P, Galié M, Sbarbati A, Krampera M, Belluzzi O & Bonetti B (2008). Neuronal Differentiation Potential of Human Adipose-Derived Mesenchymal Stem Cells. *Stem Cells and Development* 17, 909–916. **DOI:** 10.1089/scd.2007.0197.

Ankrum JA, Ong JF & Karp JM (2014). Mesenchymal Stem Cells: Immune Evasive, Not Immune Privileged. *Nature Biotechnology* 32, 252–260. **DOI:** 10.1038/nbt.2816.

Anokye-Danso F, Trivedi CM, Juhr D, Gupta M, Cui Z, Tian Y, Zhang Y, Yang W, Gruber PJ, Epstein JA & Morrisey EE (2011). Highly Efficient miRNA-Mediated Reprogramming of Mouse and Human Somatic Cells to Pluripotency. *Cell Stem Cell* 8, 376–388. **DOI:** 10.1016/j.stem.2011.03.001.

Arey LB, Rogers K & Sapunar D (2017). Prenatal Development. In: *Encyclopædia Britannica*, available at https://www.britannica.com/science/prenatal-development, accessed on January 15, 2020.

Azarin SM, Lian X, Larson EA, Popelka HM, de Pablo JJ & Palecek SP (2012). Modulation of Wnt/β-Catenin Signaling in Human Embryonic Stem Cells Using a 3-D Microwell Array. *Biomaterials* 33, 2041–2049. **DOI:** 10.1016/j.biomaterials.2011.11.070.

Badenes SM, Fernandes TG, Rodrigues CAV, Diogo MM & Cabral JMS (2016). Microcarrier-Based Platforms for in Vitro Expansion and Differentiation of Human Pluripotent Stem Cells in Bioreactor Culture Systems. *Journal of Biotechnology* 234, 71–82. **DOI:** 10.1016/j.jbiotec.2016.07.023.

Baker BM & Chen CS (2012). Deconstructing the Third Dimension - How 3D Culture Microenvironments Alter Cellular Cues. *Journal of Cell Science* 125, 3015–3024. **DOI:** 10.1242/jcs.079509.

Bates LE & Silva JCR (2017). Reprogramming Human Cells to Naïve Pluripotency: How Close Are We? *Current Opinion in Genetics & Development* 46, 58–65. **DOI:** 10.1016/j.gde.2017.06.009.

Bauwens CL, Peerani R, Niebruegge S, Woodhouse KA, Kumacheva E, Husain M & Zandstra PW (2008). Control of Human Embryonic Stem Cell Colony and Aggregate Size Heterogeneity Influences Differentiation Trajectories. *Stem Cells* 26, 2300–2310. **DOI:** 10.1634/stemcells.2008-0183.

Beers J, Gulbranson DR, George N, Siniscalchi LI, Jones J, Thomson JA & Chen G (2012). Passaging and Colony Expansion of Human Pluripotent Stem Cells by Enzyme-Free Dissociation in Chemically Defined Culture Conditions. *Nature Protocols* 7, 2029–2040. **DOI:** 10.1038/nprot.2012.130.

Ben-David U & Benvenisty N (2011). The Tumorigenicity of Human Embryonic and Induced Pluripotent Stem Cells. *Nature Reviews Cancer* 11, 268–277. **DOI:** 10.1038/nrc3034.

Bianco P, Cao X, Frenette PS, Mao JJ, Robey PG, Simmons PJ & Wang C-Y (2013). The Meaning, the Sense and the Significance: Translating the Science of Mesenchymal Stem Cells into Medicine. *Nature Medicine* 19, 35–42. **DOI:** 10.1038/nm.3028.

Bianco P (2015). Stem Cells and Bone: A Historical Perspective. *Bone* 70, 2–9. **DOI:** 10.1016/j.bone.2014.08.011.

Le Blanc K, Frassoni F, Ball L, Locatelli F, Roelofs H, Lewis I, Lanino E, Sundberg B, Bernardo ME, Remberger M *et al.* (2008). Mesenchymal Stem Cells for Treatment of Steroid-Resistant, Severe, Acute Graft-versus-Host Disease: A Phase II Study. *The Lancet* 371, 1579–1586. **DOI:** 10.1016/S0140-6736(08)60690-X.

Blauwkamp TA, Nigam S, Ardehali R, Weissman IL & Nusse R (2012). Endogenous Wnt Signalling in Human Embryonic Stem Cells Generates an Equilibrium of Distinct Lineage-Specified Progenitors. *Nature Communications* 3, 1070. **DOI:** 10.1038/ncomms2064.

Bobbert M (2006). Ethical Questions Concerning Research on Human Embryos, Embryonic Stem Cells and Chimeras. *Biotechnology Journal* 1, 1352–1369. **DOI:** 10.1002/biot.200600179.

Boward B, Wu T & Dalton S (2016). Concise Review: Control of Cell Fate Through Cell Cycle and Pluripotency Networks. *Stem Cells* 34, 1427–1436. **DOI:** 10.1002/stem.2345.

Boyer LA, Lee TI, Cole MF, Johnstone SE, Levine SS, Zucker JP, Guenther MG, Kumar RM, Murray HL, Jenner RG *et al.* (2005). Core Transcriptional Regulatory Circuitry in Human Embryonic Stem Cells. *Cell* 122, 947–956. **DOI:** 10.1016/j.cell.2005.08.020.

Braam SR, Zeinstra L, Litjens S, Ward-van Oostwaard D, van den Brink S, van Laake L, Lebrin F, Kats P, Hochstenbach R, Passier R *et al.* (2008). Recombinant Vitronectin Is a Functionally Defined Substrate That Supports Human Embryonic Stem Cell Self-Renewal via AVβ5 Integrin. *Stem Cells* 26, 2257–2265. **DOI:** 10.1634/stemcells.2008-0291.

Brafman DA, Chang C-WW, Fernandez A, Willert K, Varghese S & Chien S (2010). Long-Term Human Pluripotent Stem Cell Self-Renewal on Synthetic Polymer Surfaces. *Biomaterials* 31, 9135–9144. **DOI:** 10.1016/j.biomaterials.2010.08.007.

Branco MA, Cotovio JP, Rodrigues CA V, Vaz SH, Fernandes TG, Moreira LM, Cabral JMS & Diogo MM (2019). Transcriptomic Analysis of 3D Cardiac Differentiation of Human Induced Pluripotent Stem Cells Reveals Faster Cardiomyocyte Maturation Compared to 2D Culture. *Scientific Reports* 9, 9229. **DOI:** 10.1038/s41598-019-45047-9.

Bravery CA (2015). Do Human Leukocyte Antigen-Typed Cellular Therapeutics Based on Induced Pluripotent Stem Cells Make Commercial Sense? *Stem Cells and Development* 24, 1–10. **DOI:** 10.1089/scd.2014.0136.

Breitbach M, Bostani T, Roell W, Xia Y, Dewald O, Nygren JM, Fries JWU, Tiemann K, Bohlen H, Hescheler J *et al.* (2007). Potential Risks of Bone Marrow Cell Transplantation into Infarcted Hearts. *Blood* 110, 1362–1369. **DOI:** 10.1182/blood-2006-12-063412.

Brons IGM, Smithers LE, Trotter MWB, Rugg-Gunn P, Sun B, Chuva de Sousa Lopes SM, Howlett SK, Clarkson A, Ahrlund-Richter L, Pedersen RA & Vallier L (2007). Derivation of Pluripotent Epiblast Stem Cells from Mammalian Embryos. *Nature* 448, 191–195. **DOI:** 10.1038/nature05950.

Card DAG, Hebbar PB, Li L, Trotter KW, Komatsu Y, Mishina Y & Archer TK (2008). Oct4/Sox2-Regulated MiR-302 Targets Cyclin D1 in Human Embryonic Stem Cells. *Molecular and Cellular Biology* 28, 6426–6438. **DOI:** 10.1128/MCB.00359-08.

Carlson BM (2007a). Chapter 1: An Introduction to Regeneration. In: Principles of Regenerative Biology, (Elsevier), pp. 1–29.

Carlson BM (2007b). Chapter 12: Stem Cells, Plasticity, and Regeneration. In: Principles of Regenerative Biology, (Elsevier), pp. 239–258.

Cha M-Y, Kwon Y-W, Ahn H-S, Jeong H, Lee YY, Moon M, Baik SH, Kim DK, Song H, Yi EC *et al.* (2017). Protein-Induced Pluripotent Stem Cells Ameliorate Cognitive Dysfunction and Reduce Aβ Deposition in a Mouse Model of Alzheimer's Disease. *STEM CELLS Translational Medicine* 6, 293–305. **DOI:** 10.5966/sctm.2016-0081.

Chambers I, Colby D, Robertson M, Nichols J, Lee S, Tweedie S & Smith AG (2003). Functional Expression Cloning of Nanog, a Pluripotency Sustaining Factor in Embryonic Stem Cells. *Cell* 113, 643–655. **DOI:** 10.1016/S0092-8674(03)00392-1.

Chambers I, Silva J, Colby D, Nichols J, Nijmeijer B, Robertson M, Vrana J, Jones K, Grotewold L & Smith AG (2007). Nanog Safeguards Pluripotency and Mediates Germline Development. *Nature* 450, 1230–1234. **DOI:** 10.1038/nature06403.

Chambers SM, Fasano CA, Papapetrou EP, Tomishima M, Sadelain M & Studer L (2009). Highly Efficient Neural Conversion of Human ES and IPS Cells by Dual Inhibition of SMAD Signaling. *Nature Biotechnology* 27, 275–280. **DOI:** 10.1038/nbt.1529.

Chen G, Hou Z, Gulbranson DR & Thomson JA (2010). Actin-Myosin Contractility Is Responsible for the Reduced Viability of Dissociated Human Embryonic Stem Cells. *Cell Stem Cell* 7, 240–248. **DOI:** 10.1016/j.stem.2010.06.017.

Chen G, Gulbranson DR, Hou Z, Bolin JM, Ruotti V, Probasco MD, Smuga-Otto K, Howden SE, Diol NR, Propson NE *et al.* (2011). Chemically Defined Conditions for Human IPSC Derivation and Culture. *Nature Methods* 8, 424–429. **DOI:** 10.1038/nmeth.1593.

Chen KG, Mallon BS, McKay RDG & Robey PG (2014). Human Pluripotent Stem Cell Culture: Considerations for Maintenance, Expansion, and Therapeutics. *Cell Stem Cell* 14, 13–26. **DOI:** 10.1016/j.stem.2013.12.005.

Chen VC, Couture SM, Ye J, Lin Z, Hua G, Huang H-IP, Wu J, Hsu D, Carpenter MK & Couture LA (2012). Scalable GMP Compliant Suspension Culture System for Human ES Cells. *Stem Cell Research* 8, 388–402. **DOI:** 10.1016/j.scr.2012.02.001.

Chen Z, Li Z & He Z (2014). Plasticity of Male Germline Stem Cells and Their Applications in Reproductive and Regenerative Medicine. *Asian Journal of Andrology* 17, 367–372. **DOI:** 10.4103/1008-682X.143739.

Chi C-W, Ahmed AR, Dereli-Korkut Z & Wang S (2016). Microfluidic Cell Chips for High-Throughput Drug Screening. *Bioanalysis* 8, 921–937. **DOI:** 10.4155/bio-2016-0028.

Clevers H (2016). Modeling Development and Disease with Organoids. *Cell* 165, 1586–1597. **DOI:** 10.1016/j.cell.2016.05.082.

Costamagna D, Berardi E, Ceccarelli G & Sampaolesi M (2015). Adult Stem Cells and Skeletal Muscle Regeneration. *Current Gene Therapy* 15, 348–363. **DOI:** 10.2174/1566523215666150630121024.

Cowan CA (2005). Nuclear Reprogramming of Somatic Cells After Fusion with Human Embryonic Stem Cells. *Science* 309, 1369–1373. **DOI:** 10.1126/science.1116447.

Cyranoski D (2017). Japanese man is first to receive “reprogrammed” stem cells from another person. In: *Nature*, available at https://www.nature.com/news/japanese-man-is-first-to-receive-reprogrammed-stem-cells-from-another-person-1.21730, accessed on January 15, 2020.

Davidson KC, Adams AM, Goodson JM, McDonald CE, Potter JC, Berndt JD, Biechele TL, Taylor RJ & Moon RT (2012). Wnt/β-Catenin Signaling Promotes Differentiation, Not Self-Renewal, of Human Embryonic Stem Cells and Is Repressed by Oct4. *Proceedings of the National Academy of Sciences* 109, 4485–4490. **DOI:** 10.1073/pnas.1118777109.

Dominici M, Le Blanc K, Mueller I, Slaper-Cortenbach I, Marini F., Krause DS, Deans RJ, Keating A, Prockop DJ & Horwitz EM (2006). Minimal Criteria for Defining Multipotent Mesenchymal Stromal Cells. The International Society for Cellular Therapy Position Statement. *Cytotherapy* 8, 315–317. **DOI:** 10.1080/14653240600855905.

Draper JS, Moore HD, Ruban LN, Gokhale PJ & Andrews PW (2004). Culture and Characterization of Human Embryonic Stem Cells. *Stem Cells and Development* 13, 325–336. **DOI:** 10.1089/scd.2004.13.325.

Drukker M, Tang C, Ardehali R, Rinkevich Y, Seita J, Lee AS, Mosley AR, Weissman IL & Soen Y (2012). Isolation of Primitive Endoderm, Mesoderm, Vascular Endothelial and Trophoblast Progenitors from Human Pluripotent Stem Cells. *Nature Biotechnology* 30, 531–542. **DOI:** 10.1038/nbt.2239.

Eastham AM, Spencer H, Soncin F, Ritson S, Merry CLR, Stern PL & Ward CM (2007). Epithelial-Mesenchymal Transition Events during Human Embryonic Stem Cell Differentiation. *Cancer Research* 67, 11254–11262. **DOI:** 10.1158/0008-5472.CAN-07-2253.

Eiraku M & Sasai Y (2012). Self-Formation of Layered Neural Structures in Three-Dimensional Culture of ES Cells. *Current Opinion in Neurobiology* 22, 768–777. **DOI:** 10.1016/j.conb.2012.02.005.

Eiselleova L, Matulka K, Kriz V, Kunova M, Schmidtova Z, Neradil J, Tichy B, Dvorakova D, Pospisilova S, Hampl A & Dvorak P (2009). A Complex Role for FGF-2 in Self-Renewal, Survival, and Adhesion of Human Embryonic Stem Cells. *Stem Cells* 27, 1847–1857. **DOI:** 10.1002/stem.128.

Evans MJ & Kaufman MH (1981). Establishment in Culture of Pluripotential Cells from Mouse Embryos. *Nature* 292, 154–156. **DOI:** 10.1038/292154a0.

Ezashi T, Das P & Roberts RM (2005). Low O2 Tensions and the Prevention of Differentiation of HES Cells. *Proceedings of the National Academy of Sciences* 102, 4783–4788. **DOI:** 10.1073/pnas.0501283102.

Fernandes TG, Diogo MM, Clark DS, Dordick JS & Cabral JMS (2009). High-Throughput Cellular Microarray Platforms: Applications in Drug Discovery, Toxicology and Stem Cell Research. *Trends in Biotechnology* 27, 342–349. **DOI:** 10.1016/j.tibtech.2009.02.009.

Forristal CE, Wright KL, Hanley NA, Oreffo ROC & Houghton FD (2010). Hypoxia-Inducible Factors Regulate Pluripotency and Proliferation in Human Embryonic Stem Cells Cultured at Reduced Oxygen Tensions. *REPRODUCTION* 139, 85–97. **DOI:** 10.1530/REP-09-0300.

Gao LR, Chen Y, Zhang NK, Yang XL, Liu HL, Wang ZG, Yan XY, Wang Y, Zhu ZM, Li TC *et al.* (2015). Intracoronary Infusion of Wharton's Jelly-Derived Mesenchymal Stem Cells in Acute Myocardial Infarction: Double-Blind, Randomized Controlled Trial. *BMC Medicine* 13, 162. **DOI:** 10.1186/s12916-015-0399-z.

García-Arranz M, Herreros MD, González-Gómez C, de la Quintana P, Guadalajara H, Georgiev-Hristov T, Trébol J & Garcia-Olmo D (2016). Treatment of Crohn's-Related Rectovaginal Fistula With Allogeneic Expanded-Adipose Derived Stem Cells: A Phase I-IIa Clinical Trial. *STEM CELLS Translational Medicine* 5, 1441–1446. **DOI:** 10.5966/sctm.2015-0356.

Gerecht S, Burdick JA, Ferreira LS, Townsend SA, Langer R & Vunjak-Novakovic G (2007). Hyaluronic Acid Hydrogel for Controlled Self-Renewal and Differentiation of Human Embryonic Stem Cells. *Proceedings of the National Academy of Sciences* 104, 11298–11303. **DOI:** 10.1073/pnas.0703723104.

Gonzales KAU, Liang H, Lim Y-S, Chan Y-S, Yeo J-C, Tan C-P, Gao B, Le B, Tan Z-Y, Low K-Y *et al.* (2015). Deterministic Restriction on Pluripotent State Dissolution by Cell-Cycle Pathways. *Cell* 162, 564–579. **DOI:** 10.1016/j.cell.2015.07.001.

Graham V, Khudyakov J, Ellis P & Pevny L (2003). SOX2 Functions to Maintain Neural Progenitor Identity. *Neuron* 39, 749–765. **DOI:** 10.1016/S0896-6273(03)00497-5.

Greber B, Coulon P, Zhang M, Moritz S, Frank S, Müller-Molina AJ, Araúzo-Bravo MJ, Han DW, Pape H-C & Schöler HR (2011). FGF Signalling Inhibits Neural Induction in Human Embryonic Stem Cells. *The EMBO Journal* 30, 4874–4884. **DOI:** 10.1038/emboj.2011.407.

Guo G, von Meyenn F, Santos F, Chen Y, Reik W, Bertone P, Smith A & Nichols J (2016). Naive Pluripotent Stem Cells Derived Directly from Isolated Cells of the Human Inner Cell Mass. *Stem Cell Reports* 6, 437–446. **DOI:** 10.1016/j.stemcr.2016.02.005.

Gurdon JB (1962). The Developmental Capacity of Nuclei Taken from Intestinal Epithelium Cells of Feeding Tadpoles. *Journal of Embryology and Experimental Morphology* 10, 622–640.

Gurdon JB & Byrne JA (2003). The First Half-Century of Nuclear Transplantation. *Proceedings of the National Academy of Sciences* 100, 8048–8052. **DOI:** 10.1073/pnas.1337135100.

Hayden EC (2014). Funding Windfall Rescues Abandoned Stem-Cell Trial. *Nature* 510, 18–18. **DOI:** 10.1038/510018a.

Hino K, Horigome K, Nishio M, Komura S, Nagata S, Zhao C, Jin Y, Kawakami K, Yamada Y, Ohta A *et al.* (2017). Activin-A Enhances MTOR Signaling to Promote Aberrant Chondrogenesis in Fibrodysplasia Ossificans Progressiva. *Journal of Clinical Investigation* 127, 3339–3352. **DOI:** 10.1172/JCI93521.

Ho BX, Pek NMQ & Soh BS (2018). Disease Modeling Using 3D Organoids Derived from Human Induced Pluripotent Stem Cells. *International Journal of Molecular Sciences* 19. **DOI:** 10.3390/ijms19040936.

Hongisto H, Vuoristo S, Mikhailova A, Suuronen R, Virtanen I, Otonkoski T & Skottman H (2012). Laminin-511 Expression Is Associated with the Functionality of Feeder Cells in Human Embryonic Stem Cell Culture. *Stem Cell Research* 8, 97–108. **DOI:** 10.1016/j.scr.2011.08.005.

Hossini AM, Megges M, Prigione A, Lichtner B, Toliat MR, Wruck W, Schröter F, Nuernberg P, Kroll H, Makrantonaki E *et al.* (2015). Induced Pluripotent Stem Cell-Derived Neuronal Cells from a Sporadic Alzheimer's Disease Donor as a Model for Investigating AD-Associated Gene Regulatory Networks. *BMC Genomics* 16, 84. **DOI:** 10.1186/s12864-015-1262-5.

Hsiao C, Tomai M, Glynn J & Palecek SP (2014). Effects of 3-D Microwell Culture on Initial Fate Specification in Human Embryonic Stem Cells. *AIChE Journal* 60, 1225–1235. **DOI:** 10.1002/aic.14351.

Huang T-S, Li L, Moalim-Nour L, Jia D, Bai J, Yao Z, Bennett SAL, Figeys D & Wang L (2015). A Regulatory Network Involving β-Catenin, E-cadherin, PI3k/Akt, and Slug Balances Self-Renewal and Differentiation of Human Pluripotent Stem Cells In Response to Wnt Signaling. *STEM CELLS* 33, 1419–1433. **DOI:** 10.1002/stem.1944.

Hughes CS, Postovit LM & Lajoie GA (2010). Matrigel: A Complex Protein Mixture Required for Optimal Growth of Cell Culture. *Proteomics* 10, 1886–1890. **DOI:** 10.1002/pmic.200900758.

Hyun I (2011). Moving Human SCNT Research Forward Ethically. *Cell Stem Cell* 9, 295–297. **DOI:** 10.1016/j.stem.2011.08.001.

Israel MA, Yuan SH, Bardy C, Reyna SM, Mu Y, Herrera C, Hefferan MP, Van Gorp S, Nazor KL, Boscolo FS *et al.* (2012). Probing Sporadic and Familial Alzheimer's Disease Using Induced Pluripotent Stem Cells. *Nature* 482, 216–220. **DOI:** 10.1038/nature10821.

Jaenisch R & Young R (2008). Stem Cells, the Molecular Circuitry of Pluripotency and Nuclear Reprogramming. *Cell* 132, 567–582. **DOI:** 10.1016/j.cell.2008.01.015.

Jenkins MJ & Farid SS (2015). Human Pluripotent Stem Cell-Derived Products: Advances towards Robust, Scalable and Cost-Effective Manufacturing Strategies. *Biotechnology Journal* 10, 83–95. **DOI:** 10.1002/biot.201400348.

Jiang H, Ren Y, Yuen EY, Zhong P, Ghaedi M, Hu Z, Azabdaftari G, Nakaso K, Yan Z & Feng J (2012). Parkin Controls Dopamine Utilization in Human Midbrain Dopaminergic Neurons Derived from Induced Pluripotent Stem Cells. *Nature Communications* 3, 668. **DOI:** 10.1038/ncomms1669.

Johnson W, Loskutoff N, Plante Y & Betteridge K (1995). Production of Four Identical Calves by the Separation of Blastomeres from an in Vitro Derived Four-Cell Embryo. *Veterinary Record* 137, 15–16. **DOI:** 10.1136/vr.137.1.15.

Keramari M, Razavi J, Ingman KA, Patsch C, Edenhofer F, Ward CM & Kimber SJ (2010). Sox2 Is Essential for Formation of Trophectoderm in the Preimplantation Embryo. *PLoS ONE* 5, e13952. **DOI:** 10.1371/journal.pone.0013952.

Van Keymeulen A, Rocha AS, Ousset M, Beck B, Bouvencourt G, Rock J, Sharma N, Dekoninck S & Blanpain C (2011). Distinct Stem Cells Contribute to Mammary Gland Development and Maintenance. *Nature* 479, 189–193. **DOI:** 10.1038/nature10573.

Van Keymeulen A, Fioramonti M, Centonze A, Bouvencourt G, Achouri Y & Blanpain C (2017). Lineage-Restricted Mammary Stem Cells Sustain the Development, Homeostasis, and Regeneration of the Estrogen Receptor-Positive Lineage. *Cell Reports* 20, 1525–1532. **DOI:** 10.1016/j.celrep.2017.07.066.

Kikuchi T, Morizane A, Doi D, Magotani H, Onoe H, Hayashi T, Mizuma H, Takara S, Takahashi R, Inoue H *et al.* (2017). Human IPS Cell-Derived Dopaminergic Neurons Function in a Primate Parkinson's Disease Model. *Nature* 548, 592–596. **DOI:** 10.1038/nature23664.

Kinney MA, Hookway TA, Wang Y & McDevitt TC (2014). Engineering Three-Dimensional Stem Cell Morphogenesis for the Development of Tissue Models and Scalable Regenerative Therapeutics. *Annals of Biomedical Engineering* 42, 352–367. **DOI:** 10.1007/s10439-013-0953-9.

Kleinman HK & Martin GR (2005). Matrigel: Basement Membrane Matrix with Biological Activity. *Seminars in Cancer Biology* 15, 378–386. **DOI:** 10.1016/j.semcancer.2005.05.004.

Ko K, Tapia N, Wu G, Kim JB, Bravo MJA, Sasse P, Glaser T, Ruau D, Han DW, Greber B *et al.* (2009). Induction of Pluripotency in Adult Unipotent Germline Stem Cells. *Cell Stem Cell* 5, 87–96. **DOI:** 10.1016/j.stem.2009.05.025.

Koivisto H, Hyvärinen M, Strömberg AM, Inzunza J, Matilainen E, Mikkola M, Hovatta O & Teerijoki H (2004). Cultures of Human Embryonic Stem Cells: Serum Replacement Medium or Serum-Containing Media and the Effect of Basic Fibroblast Growth Factor. *Reproductive BioMedicine Online* 9, 330–337. **DOI:** 10.1016/S1472-6483(10)62150-5.

Kuang S, Kuroda K, Le Grand F & Rudnicki MA (2007). Asymmetric Self-Renewal and Commitment of Satellite Stem Cells in Muscle. *Cell* 129, 999–1010. **DOI:** 10.1016/j.cell.2007.03.044.

Kubota H, Avarbock MR & Brinster RL (2004). Growth Factors Essential for Self-Renewal and Expansion of Mouse Spermatogonial Stem Cells. *Proceedings of the National Academy of Sciences* 101, 16489–16494. **DOI:** 10.1073/pnas.0407063101.

Kurek D, Neagu A, Tastemel M, Tüysüz N, Lehmann J, van de Werken HJG, Philipsen S, van der Linden R, Maas A, van IJcken WFJ *et al.* (2015). Endogenous Wnt Signals Mediate BMP-Induced and Spontaneous Differentiation of Epiblast Stem Cells and Human Embryonic Stem Cells. *Stem Cell Reports* 4, 114–128. **DOI:** 10.1016/j.stemcr.2014.11.007.

Lancaster MA & Knoblich JA (2014). Generation of Cerebral Organoids from Human Pluripotent Stem Cells. *Nature Protocols* 9, 2329–2340. **DOI:** 10.1038/nprot.2014.158.

Lee J, Go Y, Kang I, Han Y-M & Kim J (2010). Oct-4 Controls Cell-Cycle Progression of Embryonic Stem Cells. *Biochemical Journal* 426, 171–181. **DOI:** 10.1042/BJ20091439.

Lee K-D, Kuo TK-C, Whang-Peng J, Chung Y-F, Lin C-T, Chou S-H, Chen J-R, Chen Y-P & Lee OK-S (2004). In Vitro Hepatic Differentiation of Human Mesenchymal Stem Cells. *Hepatology* 40, 1275–1284. **DOI:** 10.1002/hep.20469.

Lee M-O, Moon SH, Jeong H-C, Yi J-Y, Lee T-H, Shim SH, Rhee Y-H, Lee S-H, Oh S-J, Lee M-Y *et al.* (2013). Inhibition of Pluripotent Stem Cell-Derived Teratoma Formation by Small Molecules. *Proceedings of the National Academy of Sciences* 110, E3281–E3290. **DOI:** 10.1073/pnas.1303669110.

Lee Y, Decker M, Lee H & Ding L (2017). Extrinsic Regulation of Hematopoietic Stem Cells in Development, Homeostasis and Diseases. *Wiley Interdisciplinary Reviews: Developmental Biology* 6, e279. **DOI:** 10.1002/wdev.279.

Lei Y & Schaffer D V (2013). A Fully Defined and Scalable 3D Culture System for Human Pluripotent Stem Cell Expansion and Differentiation. *Proceedings of the National Academy of Sciences* 110, E5039–E5048. **DOI:** 10.1073/pnas.1309408110.

Levenstein ME, Ludwig TE, Xu R-H, Llanas RA, VanDenHeuvel-Kramer K, Manning D & Thomson JA (2006). Basic Fibroblast Growth Factor Support of Human Embryonic Stem Cell Self-Renewal. *Stem Cells* 24, 568–574. **DOI:** 10.1634/stemcells.2005-0247.

Li J, Wang G, Wang C, Zhao Y, Zhang H, Tan Z, Song Z, Ding M & Deng H (2007). MEK/ERK Signaling Contributes to the Maintenance of Human Embryonic Stem Cell Self-Renewal. *Differentiation* 75, 299–307. **DOI:** 10.1111/j.1432-0436.2006.00143.x.

Li L, Wang S, Jezierski A, Moalim-Nour L, Mohib K, Parks RJ, Francesco Retta S & Wang L (2009). A Unique Interplay between Rap1 and E-cadherin in the Endocytic Pathway

Regulates Self-Renewal of Human Embryonic Stem Cells. *STEM CELLS* 28, N/A-N/A. **DOI:** 10.1002/stem.289.

Li Y, Powell S, Brunette E, Lebkowski J & Mandalam R (2005). Expansion of Human Embryonic Stem Cells in Defined Serum-free Medium Devoid of Animal-derived Products. *Biotechnology and Bioengineering* 91, 688–698. **DOI:** 10.1002/bit.20536.

Li Y, Green M, Wen Y, Wei Y, Wani P, Wang Z, Reijo Pera R & Chen B (2017). Efficacy and Safety of Immuno-Magnetically Sorted Smooth Muscle Progenitor Cells Derived from Human-Induced Pluripotent Stem Cells for Restoring Urethral Sphincter Function. *STEM CELLS Translational Medicine* 6, 1158–1167. **DOI:** 10.1002/sctm.16-0160.

Liu X, Li W, Fu X & Xu Y (2017). The Immunogenicity and Immune Tolerance of Pluripotent Stem Cell Derivatives. *Frontiers in Immunology* 8, 645. **DOI:** 10.3389/fimmu.2017.00645.

Ljujic B, Milovanovic M, Volarevic V, Murray B, Bugarski D, Przyborski S, Arsenijevic N, Lukic ML & Stojkovic M (2013). Human Mesenchymal Stem Cells Creating an Immunosuppressive Environment and Promote Breast Cancer in Mice. *Scientific Reports* 3, 2298. **DOI:** 10.1038/srep02298.

Ludwig TE, Levenstein ME, Jones JM, Berggren WT, Mitchen ER, Frane JL, Crandall LJ, Daigh C a, Conard KR, Piekarczyk MS *et al.* (2006a). Derivation of Human Embryonic Stem Cells in Defined Conditions. *Nature Biotechnology* 24, 185–187. **DOI:** 10.1038/nbt1177.

Ludwig TE, Bergendahl V, Levenstein ME, Yu J, Probasco MD & Thomson JA (2006b). Feeder-Independent Culture of Human Embryonic Stem Cells. *Nature Methods* 3, 637–646. **DOI:** 10.1038/nmeth902.

Ben M'Barek K, Habeler W, Plancheron A, Jarraya M, Regent F, Terray A, Yang Y, Chatrousse L, Domingues S, Masson Y *et al.* (2017). Human ESC–Derived Retinal Epithelial Cell Sheets Potentiate Rescue of Photoreceptor Cell Loss in Rats with Retinal Degeneration. *Science Translational Medicine* 9, eaai7471. **DOI:** 10.1126/scitranslmed.aai7471.

Ma H, Morey R, O'Neil RC, He Y, Daughtry B, Schultz MD, Hariharan M, Nery JR, Castanon R, Sabatini K *et al.* (2014). Abnormalities in Human Pluripotent Cells Due to Reprogramming Mechanisms. *Nature* 511, 177–183. **DOI:** 10.1038/nature13551.

Maldonado M, Luu RJ, Ramos MEP & Nam J (2016). ROCK Inhibitor Primes Human Induced Pluripotent Stem Cells to Selectively Differentiate towards Mesendodermal Lineage via Epithelial-Mesenchymal Transition-like Modulation. *Stem Cell Research* 17, 222–227. **DOI:** 10.1016/j.scr.2016.07.009.

Mandai M, Watanabe A, Kurimoto Y, Hirami Y, Morinaga C, Daimon T, Fujihara M, Akimaru H, Sakai N, Shibata Y *et al.* (2017). Autologous Induced Stem-Cell–Derived Retinal Cells for Macular Degeneration. *New England Journal of Medicine* 376, 1038–1046. **DOI:** 10.1056/NEJMoa1608368.

Martí M, Mulero L, Pardo C, Morera C, Carrió M, Laricchia-Robbio L, Esteban CR & Belmonte JCI (2013). Characterization of Pluripotent Stem Cells. *Nature Protocols* 8, 223–253. **DOI:** 10.1038/nprot.2012.154.

Martin GR (1981). Isolation of a Pluripotent Cell Line from Early Mouse Embryos Cultured in Medium Conditioned by Teratocarcinoma Stem Cells. *Proceedings of the National Academy of Sciences* 78, 7634–7638. **DOI:** 10.1073/pnas.78.12.7634.

Martin U (2017). Therapeutic Application of Pluripotent Stem Cells: Challenges and Risks. *Frontiers in Medicine* 4, 229. **DOI:** 10.3389/fmed.2017.00229.

McCracken KW, Catá EM, Crawford CM, Sinagoga KL, Schumacher M, Rockich BE, Tsai Y-H, Mayhew CN, Spence JR, Zavros Y & Wells JM (2014). Modelling Human Development and Disease in Pluripotent Stem-Cell-Derived Gastric Organoids. *Nature* 516, 400–404. **DOI:** 10.1038/nature13863.

McLean AB, D'Amour KA, Jones KL, Krishnamoorthy M, Kulik MJ, Reynolds DM, Sheppard AM, Liu H, Xu Y, Baetge EE & Dalton S (2007). Activin A Efficiently Specifies Definitive Endoderm from Human Embryonic Stem Cells Only When Phosphatidylinositol 3-Kinase Signaling Is Suppressed. *STEM CELLS* 25, 29–38. **DOI:** 10.1634/stemcells.2006-0219.

Metallo CM, Mohr JC, Detzel CJ, DePablo JJ, VanWie BJ & Palecek SP (2007). Engineering the Stem Cell Microenvironment. *Biotechnology Progress* 23, 18–23. **DOI:** 10.1021/bp060350a.

Mitalipov SM, Yeoman RR, Kuo H-C & Wolf DP (2002). Monozygotic Twinning in Rhesus Monkeys by Manipulation of In Vitro-Derived Embryos1. *Biology of Reproduction* 66, 1449–1455. **DOI:** 10.1095/biolreprod66.5.1449.

Mitalipov SM & Wolf D (2009). Totipotency, Pluripotency and Nuclear Reprogramming. In: Engineering of Stem Cells, (Berlin, Heidelberg: Springer Berlin Heidelberg), pp. 185–199.

Mitsui K, Tokuzawa Y, Itoh H, Segawa K, Murakami M, Takahashi K, Maruyama M, Maeda M & Yamanaka S (2003). The Homeoprotein Nanog Is Required for Maintenance of Pluripotency in Mouse Epiblast and ES Cells. *Cell* 113, 631–642. **DOI:** 10.1016/S0092-8674(03)00393-3.

Miyazaki T, Futaki S, Hasegawa K, Kawasaki M, Sanzen N, Hayashi M, Kawase E, Sekiguchi K, Nakatsuji N & Suemori H (2008). Recombinant Human Laminin Isoforms Can Support the Undifferentiated Growth of Human Embryonic Stem Cells. *Biochemical and Biophysical Research Communications* 375, 27–32. **DOI:** 10.1016/j.bbrc.2008.07.111.

Montanez-Sauri SI, Beebe DJ & Sung KE (2015). Microscale Screening Systems for 3D Cellular Microenvironments: Platforms, Advances, and Challenges. *Cellular and Molecular Life Sciences* 72, 237–249. **DOI:** 10.1007/s00018-014-1738-5.

Monzel AS, Smits LM, Hemmer K, Hachi S, Moreno EL, van Wuellen T, Jarazo J, Walter J, Brüggemann I, Boussaad I *et al.* (2017). Derivation of Human Midbrain-Specific Organoids from Neuroepithelial Stem Cells. *Stem Cell Reports* 8, 1144–1154. **DOI:** 10.1016/j.stemcr.2017.03.010.

Moon S-H, Ju J, Park S-J, Bae D, Chung H-M & Lee S-H (2014). Optimizing Human Embryonic Stem Cells Differentiation Efficiency by Screening Size-Tunable Homogenous Embryoid Bodies. *Biomaterials* 35, 5987–5997. **DOI:** 10.1016/j.biomaterials.2014.04.001.

Morrison SJ & Spradling AC (2008). Stem Cells and Niches: Mechanisms That Promote Stem Cell Maintenance throughout Life. *Cell* 132, 598–611. **DOI:** 10.1016/j.cell.2008.01.038.

Na J, Furue MK & Andrews PW (2010). Inhibition of ERK1/2 Prevents Neural and Mesendodermal Differentiation and Promotes Human Embryonic Stem Cell Self-Renewal. *Stem Cell Research* 5, 157–169. **DOI:** 10.1016/j.scr.2010.06.002.

Nagaoka M, Si-Tayeb K, Akaike T & Duncan SA (2010). Culture of Human Pluripotent Stem Cells Using Completely Defined Conditions on a Recombinant E-cadherin Substratum. *BMC Developmental Biology* 10, 60. **DOI:** 10.1186/1471-213X-10-60.

Nazareth EJP, Rahman N, Yin T & Zandstra PW (2016). A Multi-Lineage Screen Reveals MTORC1 Inhibition Enhances Human Pluripotent Stem Cell Mesendoderm and Blood Progenitor Production. *Stem Cell Reports* 6, 679–691. **DOI:** 10.1016/j.stemcr.2016.04.003.

Nichols J, Zevnik B, Anastassiadis K, Niwa H, Klewe-Nebenius D, Chambers I, Schöler H & Smith AG (1998). Formation of Pluripotent Stem Cells in the Mammalian Embryo Depends on the POU Transcription Factor Oct4. *Cell* 95, 379–391. **DOI:** 10.1016/S0092-8674(00)81769-9.

Nichols J & Smith AG (2009). Naive and Primed Pluripotent States. *Cell Stem Cell* 4, 487–492. **DOI:** 10.1016/j.stem.2009.05.015.

Nie Y, Walsh P, Clarke DL, Rowley JA & Fellner T (2014). Scalable Passaging of Adherent Human Pluripotent Stem Cells. *PLoS ONE* 9, e88012. **DOI:** 10.1371/journal.pone.0088012.

Niwa H, Miyazaki J & Smith AG (2000). Quantitative Expression of Oct-3/4 Defines Differentiation, Dedifferentiation or Self-Renewal of ES Cells. *Nature Genetics* 24, 372–376. **DOI:** 10.1038/74199.

Noggle SA, James D & Brivanlou AH (2005). A Molecular Basis for Human Embryonic Stem Cell Pluripotency. *Stem Cell Reviews* 1, 111–118. **DOI:** 10.1385/SCR:1:2:111.

Ohgushi M, Matsumura M, Eiraku M, Murakami K, Aramaki T, Nishiyama A, Muguruma K, Nakano T, Suga H, Ueno M *et al.* (2010). Molecular Pathway and Cell State Responsible for Dissociation-Induced Apoptosis in Human Pluripotent Stem Cells. *Cell Stem Cell* 7, 225–239. **DOI:** 10.1016/j.stem.2010.06.018.

Okita K, Ichisaka T & Yamanaka S (2007). Generation of Germline-Competent Induced Pluripotent Stem Cells. *Nature* 448, 313–317. **DOI:** 10.1038/nature05934.

De Paepe C, Krivega M, Cauffman G, Geens M & Van de Velde H (2014). Totipotency and Lineage Segregation in the Human Embryo. *Molecular Human Reproduction* 20, 599–618. **DOI:** 10.1093/molehr/gau027.

Pan F, Zhang M, Wu G, Lai Y, Greber B, Schöler HR & Chi L (2013). Topographic Effect on Human Induced Pluripotent Stem Cells Differentiation towards Neuronal Lineage. *Biomaterials* 34, 8131–8139. **DOI:** 10.1016/j.biomaterials.2013.07.025.

Park D, Lim J, Park JY & Lee S-H (2015). Concise Review: Stem Cell Microenvironment on a Chip: Current Technologies for Tissue Engineering and Stem Cell Biology. *STEM CELLS Translational Medicine* 4, 1352–1368. **DOI:** 10.5966/sctm.2015-0095.

Pesce M & Schöler HR (2000). Oct-4: Control of Totipotency and Germline Determination. *Molecular Reproduction and Development* 55, 452–457. **DOI:** 10.1002/(SICI)1098-2795(200004)55:4<452::AID-MRD14>3.0.CO;2-S.

Pesce M & Schöler HR (2001). Oct-4 : Gatekeeper in the Beginnings of Mammalian Development. *Stem Cells* 19, 271–278. **DOI:** 10.1634/stemcells.19-4-271.

Prowse ABJ, McQuade LR, Bryant KJ, Marcal H & Gray PP (2007). Identification of Potential Pluripotency Determinants for Human Embryonic Stem Cells Following Proteomic Analysis of Human and Mouse Fibroblast Conditioned Media. *Journal of Proteome Research* 6, 3796–3807. **DOI:** 10.1021/pr0702262.

Qi X, Li T-G, Hao J, Hu J, Wang J, Simmons H, Miura S, Mishina Y & Zhao G-Q (2004). BMP4 Supports Self-Renewal of Embryonic Stem Cells by Inhibiting Mitogen-Activated Protein Kinase Pathways. *Proceedings of the National Academy of Sciences* 101, 6027–6032. **DOI:** 10.1073/pnas.0401367101.

Qin H, Zhao A & Fu X (2017). Small Molecules for Reprogramming and Transdifferentiation. *Cellular and Molecular Life Sciences* 74, 3553–3575. **DOI:** 10.1007/s00018-017-2586-x.

Réaumur R-AF de (1712). Sur Les Diverses Reproductions Qui Se Font Dans Les Ecrevisse, Les Omars, Les Crabes, Etc. et Entr'autres Sur Celles de Leurs Jambes et de Leurs Ecailles [On the Various Reproductions Made in Crayfish, Lobsters, Crabs, Etc. and, Among Others, on Those in Their Legs and Scales]. *Mémoires de l'Académie Royale Des Sciences* 223–242.

Remak R (1855). Untersuchungen über die Entwicklung der Wirbeltiere [Studies on the development of vertebrate animals] (Berlin: G. Reimer).

Reubinoff BE, Pera MF, Fong C-Y, Trounson A & Bongso A (2000). Embryonic Stem Cell Lines from Human Blastocysts: Somatic Differentiation in Vitro. *Nature Biotechnology* 18, 399–404. **DOI:** 10.1038/74447.

Richards M, Tan S, Fong C-Y, Biswas A, Chan W-K & Bongso A (2003). Comparative Evaluation of Various Human Feeders for Prolonged Undifferentiated Growth of Human Embryonic Stem Cells. *Stem Cells* 21, 546–556. **DOI:** 10.1634/stemcells.21-5-546.

Robey PG (2000). Series Introduction: Stem Cells near the Century Mark. *Journal of Clinical Investigation* 105, 1489–1491. **DOI:** 10.1172/JCI10256.

Rodda DJ, Chew J-L, Lim L-H, Loh Y-H, Wang B, Ng H-H & Robson P (2005). Transcriptional Regulation of Nanog by OCT4 and SOX2. *Journal of Biological Chemistry* 280, 24731–24737. **DOI:** 10.1074/jbc.M502573200.

Rodrigues GMC, Matos AFS, Fernandes TG, Rodrigues CAV, Peitz M, Haupt S, Diogo MM, Brüstle O & Cabral JMS (2014). Integrated Platform for Production and Purification of Human Pluripotent Stem Cell-Derived Neural Precursors. *Stem Cell Reviews and Reports* 10, 151–161. **DOI:** 10.1007/s12015-013-9482-z.

Rojas S V, Kensah G, Rotaermel A, Baraki H, Kutschka I, Zweigerdt R, Martin U, Haverich A, Gruh I & Martens A (2017). Transplantation of Purified IPSC-Derived Cardiomyocytes

in Myocardial Infarction. *PLOS ONE* 12, e0173222. **DOI:** 10.1371/journal.pone.0173222.

Rothbauer M, Charwat V & Ertl P (2016). Cell Microarrays for Biomedical Applications. In: Microarray Technology, P.C. Li, A. Sedighi, and L. Wang, eds. (Springer New York), pp. 273–291.

Ruddy RM & Morshead CM (2018). Home Sweet Home: The Neural Stem Cell Niche throughout Development and after Injury. *Cell and Tissue Research* 371, 125–141. **DOI:** 10.1007/s00441-017-2658-0.

Samsonraj RM, Rai B, Sathiyanathan P, Puan KJ, Rötzschke O, Hui JH, Raghunath M, Stanton LW, Nurcombe V & Cool SM (2015). Establishing Criteria for Human Mesenchymal Stem Cell Potency. *STEM CELLS* 33, 1878–1891. **DOI:** 10.1002/stem.1982.

Sanchez-Ramos J, Song S, Cardozo-Pelaez F, Hazzi C, Stedeford T, Willing A, Freeman TB, Saporta S, Janssen W, Patel N *et al.* (2000). Adult Bone Marrow Stromal Cells Differentiate into Neural Cells in Vitro. *Experimental Neurology* 164, 247–256. **DOI:** 10.1006/exnr.2000.7389.

Sato N, Meijer L, Skaltsounis L, Greengard P & Brivanlou AH (2004). Maintenance of Pluripotency in Human and Mouse Embryonic Stem Cells through Activation of Wnt Signaling by a Pharmacological GSK-3-Specific Inhibitor. *Nature Medicine* 10, 55–63. **DOI:** 10.1038/nm979.

Schoenwolf GC, Bleyl SB, Brauer PR & Francis-West PH (2009a). Second Week: Becoming Bilaminar and Fully Implanting. In: Larsen's Human Embryology, (Churchill Livingstone), pp. 51–68.

Schoenwolf GC, Bleyl SB, Brauer PR & Francis-West PH (2009b). Third Week: Becoming Trilaminar and Establishing Body Axes. In: Larsen's Human Embryology, (Churchill Livingstone), pp. 69–100.

Schöndorf DC, Aureli M, McAllister FE, Hindley CJ, Mayer F, Schmid B, Sardi SP, Valsecchi M, Hoffmann S, Schwarz LK *et al.* (2014). IPSC-Derived Neurons from GBA1-Associated Parkinson's Disease Patients Show Autophagic Defects and Impaired Calcium Homeostasis. *Nature Communications* 5, 4028. **DOI:** 10.1038/ncomms5028.

Schwann T (1847). Microscopical Researches Into the Accordance in the Structure and Growth of Animals and Plants (transl. H. Smith) (London: The Sydenham Society).

Schwartz RE, Reyes M, Koodie L, Jiang Y, Blackstad M, Lund T, Lenvik T, Johnson S, Hu W-S & Verfaillie CM (2002). Multipotent Adult Progenitor Cells from Bone Marrow Differentiate into Functional Hepatocyte-like Cells. *Journal of Clinical Investigation* 109, 1291–1302. **DOI:** 10.1172/JCI15182.

Schwartz SD, Regillo CD, Lam BL, Eliott D, Rosenfeld PJ, Gregori NZ, Hubschman J-P, Davis JL, Heilwell G, Spirn M *et al.* (2015). Human Embryonic Stem Cell-Derived Retinal Pigment Epithelium in Patients with Age-Related Macular Degeneration and Stargardt's Macular Dystrophy: Follow-up of Two Open-Label Phase 1/2 Studies. *The Lancet* 385, 509–516. **DOI:** 10.1016/S0140-6736(14)61376-3.

Serra M, Correia C, Malpique R, Brito C, Jensen J, Bjorquist P, Carrondo MJT & Alves PM (2011). Microencapsulation Technology: A Powerful Tool for Integrating Expansion

and Cryopreservation of Human Embryonic Stem Cells. *PLoS ONE* 6, e23212. **DOI:** 10.1371/journal.pone.0023212.

Serra M, Brito C, Correia C & Alves PM (2012). Process Engineering of Human Pluripotent Stem Cells for Clinical Application. *Trends in Biotechnology* 30, 350–359. **DOI:** 10.1016/j.tibtech.2012.03.003.

Shao Y, Sang J & Fu J (2015). On Human Pluripotent Stem Cell Control: The Rise of 3D Bioengineering and Mechanobiology. *Biomaterials* 52, 26–43. **DOI:** 10.1016/j.biomaterials.2015.01.078.

Sharma A, Burridge PW, McKeithan WL, Serrano R, Shukla P, Sayed N, Churko JM, Kitani T, Wu H, Holmström A *et al.* (2017). High-Throughput Screening of Tyrosine Kinase Inhibitor Cardiotoxicity with Human Induced Pluripotent Stem Cells. *Science Translational Medicine* 9, eaaf2584. **DOI:** 10.1126/scitranslmed.aaf2584.

Simkin J & Seifert AW (2018). Concise Review: Translating Regenerative Biology into Clinically Relevant Therapies: Are We on the Right Path? *STEM CELLS Translational Medicine* 7, 220–231. **DOI:** 10.1002/sctm.17-0213.

Singh AM, Reynolds D, Cliff T, Ohtsuka S, Mattheyses AL, Sun Y, Menendez L, Kulik M & Dalton S (2012). Signaling Network Crosstalk in Human Pluripotent Cells: A Smad2/3-Regulated Switch That Controls the Balance between Self-Renewal and Differentiation. *Cell Stem Cell* 10, 312–326. **DOI:** 10.1016/j.stem.2012.01.014.

Singh AM, Chappell J, Trost R, Lin L, Wang T, Tang J, Wu H, Zhao S, Jin P & Dalton S (2013). Cell-Cycle Control of Developmentally Regulated Transcription Factors Accounts for Heterogeneity in Human Pluripotent Cells. *Stem Cell Reports* 1, 532–544. **DOI:** 10.1016/j.stemcr.2013.10.009.

Singh SR (2012). Stem Cell Niche in Tissue Homeostasis, Aging and Cancer. *Current Medicinal Chemistry* 19, 5965–5974. **DOI:** 10.2174/092986731120906596 5.

Smith AG, Heath JK, Donaldson DD, Wong GG, Moreau J, Stahl M & Rogers D (1988). Inhibition of Pluripotential Embryonic Stem Cell Differentiation by Purified Polypeptides. *Nature* 336, 688–690. **DOI:** 10.1038/336688a0.

Solomon S, Pitossi F & Rao MS (2015). Banking on IPSC- Is It Doable and Is It Worthwhile. *Stem Cell Reviews and Reports* 11, 1–10. **DOI:** 10.1007/s12015-014-9574-4.

Song WK, Park K-M, Kim H-J, Lee JH, Choi J, Chong SY, Shim SH, Del Priore L V. & Lanza R (2015). Treatment of Macular Degeneration Using Embryonic Stem Cell-Derived Retinal Pigment Epithelium: Preliminary Results in Asian Patients. *Stem Cell Reports* 4, 860–872. **DOI:** 10.1016/j.stemcr.2015.04.005.

Spencer H, Keramari M & Ward CM (2011). Using Cadherin Expression to Assess Spontaneous Differentiation of Embryonic Stem Cells. In: Methods in Molecular Biology (Clifton, N.J.), pp. 81–94.

Steiner D, Khaner H, Cohen M, Even-Ram S, Gil Y, Itsykson P, Turetsky T, Idelson M, Aizenman E, Ram R *et al.* (2010). Derivation, Propagation and Controlled Differentiation of Human Embryonic Stem Cells in Suspension. *Nature Biotechnology* 28, 361–364. **DOI:** 10.1038/nbt.1616.

Stevens LC (1958). Studies on Transplantable Testicular Teratomas of Strain 129 Mice. *JNCI: Journal of the National Cancer Institute* 20, 1257–1275. **DOI:** 10.1093/jnci/20.6.1257.

Stocum DL & Zupanc GKH (2008). Stretching the Limits: Stem Cells in Regeneration Science. *Developmental Dynamics* 237, 3648–3671. **DOI:** 10.1002/dvdy.21774.

Tachibana M, Amato P, Sparman M, Gutierrez NM, Tippner-Hedges R, Ma H, Kang E, Fulati A, Lee H-S, Sritanaudomchai H *et al.* (2013). Human Embryonic Stem Cells Derived by Somatic Cell Nuclear Transfer. *Cell* 153, 1228–1238. **DOI:** 10.1016/j.cell.2013.05.006.

Takahashi K, Tanabe K, Ohnuki M, Narita M, Ichisaka T, Tomoda K & Yamanaka S (2007). Induction of Pluripotent Stem Cells from Adult Human Fibroblasts by Defined Factors. *Cell* 131, 861–872. **DOI:** 10.1016/j.cell.2007.11.019.

Takahashi K & Yamanaka S (2006). Induction of Pluripotent Stem Cells from Mouse Embryonic and Adult Fibroblast Cultures by Defined Factors. *Cell* 126, 663–676. **DOI:** 10.1016/j.cell.2006.07.024.

Takasato M, Er PX, Chiu HS, Maier B, Baillie GJ, Ferguson C, Parton RG, Wolvetang EJ, Roost MS, Chuva de Sousa Lopes SM & Little MH (2015). Kidney Organoids from Human IPS Cells Contain Multiple Lineages and Model Human Nephrogenesis. *Nature* 526, 564–568. **DOI:** 10.1038/nature15695.

Takashima Y, Guo G, Loos R, Nichols J, Ficz G, Krueger F, Oxley D, Santos F, Clarke J, Mansfield W *et al.* (2014). Resetting Transcription Factor Control Circuitry toward Ground-State Pluripotency in Human. *Cell* 158, 1254–1269. **DOI:** 10.1016/j.cell.2014.08.029.

Takebe T, Sekine K, Enomura M, Koike H, Kimura M, Ogaeri T, Zhang R-R, Ueno Y, Zheng Y-W, Koike N *et al.* (2013). Vascularized and Functional Human Liver from an IPSC-Derived Organ Bud Transplant. *Nature* 499, 481–484. **DOI:** 10.1038/nature12271.

Takemoto T, Uchikawa M, Yoshida M, Bell DM, Lovell-Badge R, Papaioannou VE & Kondoh H (2011). Tbx6-Dependent Sox2 Regulation Determines Neural or Mesodermal Fate in Axial Stem Cells. *Nature* 470, 394–398. **DOI:** 10.1038/nature09729.

Tang L, Su J & Liang P (2017). Modeling Cadmium-Induced Endothelial Toxicity Using Human Pluripotent Stem Cell-Derived Endothelial Cells. *Scientific Reports* 7, 14811. **DOI:** 10.1038/s41598-017-13694-5.

Tesar PJ, Chenoweth JG, Brook FA, Davies TJ, Evans EP, Mack DL, Gardner RL & McKay RDG (2007). New Cell Lines from Mouse Epiblast Share Defining Features with Human Embryonic Stem Cells. *Nature* 448, 196–199. **DOI:** 10.1038/nature05972.

Theunissen TW, Powell BE, Wang H, Mitalipova M, Faddah DA, Reddy J, Fan ZP, Maetzel D, Ganz K, Shi L *et al.* (2014). Systematic Identification of Culture Conditions for Induction and Maintenance of Naive Human Pluripotency. *Cell Stem Cell* 15, 471–487. **DOI:** 10.1016/j.stem.2014.07.002.

Thomson JA, Kalishman J, Golos TG, Durning M, Harris CP, Becker RA & Hearn JP (1995). Isolation of a Primate Embryonic Stem Cell Line. *Proceedings of the National Academy of Sciences* 92, 7844 LP – 7848. **DOI:** 10.1073/pnas.92.17.7844.

Thomson JA, Itskovitz-Eldor J, Shapiro SS, Waknitz MA, Swiergiel JJ, Marshall VS & Jones JM (1998). Embryonic Stem Cell Lines Derived from Human Blastocysts. *Science* 282, 1145–1147. **DOI:** 10.1126/science.282.5391.1145.

Thomson M, Liu SJ, Zou L-N, Smith Z, Meissner A & Ramanathan S (2011). Pluripotency Factors in Embryonic Stem Cells Regulate Differentiation into Germ Layers. *Cell* 145, 875–889. **DOI:** 10.1016/j.cell.2011.05.017.

Till JE & McCulloch EA (1961). A Direct Measurement of the Radiation Sensitivity of Normal Mouse Bone Marrow Cells. *Radiation Research* 14, 213. **DOI:** 10.2307/3570892.

Toh Y-C, Xing J & Yu H (2015). Modulation of Integrin and E-cadherin-Mediated Adhesions to Spatially Control Heterogeneity in Human Pluripotent Stem Cell Differentiation. *Biomaterials* 50, 87–97. **DOI:** 10.1016/j.biomaterials.2015.01.019.

Vallier L, Mendjan S, Brown S, Chng Z, Teo A, Smithers LE, Trotter MWB, Cho CH-H, Martinez A, Rugg-Gunn P *et al.* (2009). Activin/Nodal Signalling Maintains Pluripotency by Controlling Nanog Expression. *Development* 136, 1339–1349. **DOI:** 10.1242/dev.033951.

Vernardis SI, Terzoudis K, Panoskaltsis N & Mantalaris A (2017). Human Embryonic and Induced Pluripotent Stem Cells Maintain Phenotype but Alter Their Metabolism after Exposure to ROCK Inhibitor. *Scientific Reports* 7, 42138. **DOI:** 10.1038/srep42138.

Villa-Diaz LG, Nandivada H, Ding J, Nogueira-de-Souza NC, Krebsbach PH, O'Shea KS, Lahann J & Smith GD (2010). Synthetic Polymer Coatings for Long-Term Growth of Human Embryonic Stem Cells. *Nature Biotechnology* 28, 581–583. **DOI:** 10.1038/nbt.1631.

Villa-Diaz LG, Ross AM, Lahann J & Krebsbach PH (2013). Concise Review: The Evolution of Human Pluripotent Stem Cell Culture: From Feeder Cells to Synthetic Coatings. *Stem Cells* 31, 1–7. **DOI:** 10.1002/stem.1260.

Viswanathan P, Gaskell T, Moens N, Culley OJ, Hansen D, Gervasio MKR, Yeap YJ & Danovi D (2014). Human Pluripotent Stem Cells on Artificial Microenvironments: A High Content Perspective. *Frontiers in Pharmacology* 5, 1–14. **DOI:** 10.3389/fphar.2014.00150.

Wabik A & Jones PH (2015). Switching Roles: The Functional Plasticity of Adult Tissue Stem Cells. *The EMBO Journal* 34, 1164–1179. **DOI:** 10.15252/embj.201490386.

Wang S-H, Tsai M-S, Chiang M-F & Li H (2003). A Novel NK-Type Homeobox Gene, ENK (Early Embryo Specific NK), Preferentially Expressed in Embryonic Stem Cells. *Gene Expression Patterns* 3, 99–103. **DOI:** 10.1016/S1567-133X(03)00005-X.

Wang Y, Chou B-K, Dowey S, He C, Gerecht S & Cheng L (2013). Scalable Expansion of Human Induced Pluripotent Stem Cells in the Defined Xeno-Free E8 Medium under Adherent and Suspension Culture Conditions. *Stem Cell Research* 11, 1103–1116. **DOI:** 10.1016/j.scr.2013.07.011.

Wang Z, Oron E, Nelson B, Razis S & Ivanova N (2012). Distinct Lineage Specification Roles for NANOG, OCT4, and SOX2 in Human Embryonic Stem Cells. *Cell Stem Cell* 10, 440–454. **DOI:** 10.1016/j.stem.2012.02.016.

Warren L, Manos PD, Ahfeldt T, Loh Y-H, Li H, Lau F, Ebina W, Mandal PK, Smith ZD, Meissner A *et al.* (2010). Highly Efficient Reprogramming to Pluripotency and

Directed Differentiation of Human Cells with Synthetic Modified mRNA. *Cell Stem Cell* 7, 618–630. **DOI:** 10.1016/j.stem.2010.08.012.

Watanabe K, Ueno M, Kamiya D, Nishiyama A, Matsumura M, Wataya T, Takahashi JB, Nishikawa S, Nishikawa S, Muguruma K & Sasai Y (2007). A ROCK Inhibitor Permits Survival of Dissociated Human Embryonic Stem Cells. *Nature Biotechnology* 25, 681–686. **DOI:** 10.1038/nbt1310.

Wernig M, Meissner A, Foreman R, Brambrink T, Ku M, Hochedlinger K, Bernstein BE & Jaenisch R (2007). In Vitro Reprogramming of Fibroblasts into a Pluripotent ES-Cell-like State. *Nature* 448, 318–324. **DOI:** 10.1038/nature05944.

Wikipedia (2017). Stem cell laws. In: *Wikipedia: The Free Encyclopedia*, available at https://en.wikipedia.org/wiki/Stem_cell_laws, accessed on June 24, 2017.

Williams RL, Hilton DJ, Pease S, Willson TA, Stewart CL, Gearing DP, Wagner EF, Metcalf D, Nicola NA & Gough NM (1988). Myeloid Leukaemia Inhibitory Factor Maintains the Developmental Potential of Embryonic Stem Cells. *Nature* 336, 684–687. **DOI:** 10.1038/336684a0.

Wilmut I, Schnieke AE, McWhir J, Kind AJ & Campbell KHS (1997). Viable Offspring Derived from Fetal and Adult Mammalian Cells. *Nature* 385, 810–813. **DOI:** 10.1038/385810a0.

Wolpert L (1995). Evolution of the Cell Theory. *Philosophical Transactions of the Royal Society B: Biological Sciences* 349, 227–233. **DOI:** 10.1098/rstb.1995.0106.

Xu C, Inokuma MS, Denham J, Golds K, Kundu P, Gold JD & Carpenter MK (2001). Feeder-Free Growth of Undifferentiated Human Embryonic Stem Cells. *Nature Biotechnology* 19, 971–974. **DOI:** 10.1038/nbt1001-971.

Xu C, Rosler E, Jiang J, Lebkowski JS, Gold JD, O'Sullivan C, Delavan-Boorsma K, Mok M, Bronstein A & Carpenter MK (2005). Basic Fibroblast Growth Factor Supports Undifferentiated Human Embryonic Stem Cell Growth Without Conditioned Medium. *Stem Cells* 23, 315–323. **DOI:** 10.1634/stemcells.2004-0211.

Xu R-H, Chen X, Li DS, Li R, Addicks GC, Glennon C, Zwaka TP & Thomson JA (2002). BMP4 Initiates Human Embryonic Stem Cell Differentiation to Trophoblast. *Nature Biotechnology* 20, 1261–1264. **DOI:** 10.1038/nbt761.

Xu R-H, Sampsell-Barron TL, Gu F, Root S, Peck RM, Pan G, Yu J, Antosiewicz-Bourget J, Tian S, Stewart R & Thomson JA (2008). NANOG Is a Direct Target of TGFβ/Activin-Mediated SMAD Signaling in Human ESCs. *Cell Stem Cell* 3, 196–206. **DOI:** 10.1016/j.stem.2008.07.001.

Ying Q-L, Nichols J, Chambers I & Smith AG (2003). BMP Induction of Id Proteins Suppresses Differentiation and Sustains Embryonic Stem Cell Self-Renewal in Collaboration with STAT3. *Cell* 115, 281–292. **DOI:** 10.1016/S0092-8674(03)00847-X.

Yoshihara M, Hayashizaki Y & Murakawa Y (2017). Genomic Instability of IPSCs: Challenges Towards Their Clinical Applications. *Stem Cell Reviews and Reports* 13, 7–16. **DOI:** 10.1007/s12015-016-9680-6.

Yu J, Vodyanik MA, Smuga-Otto K, Antosiewicz-Bourget J, Frane JL, Tian S, Nie J, Jonsdottir GA, Ruotti V, Stewart R *et al.* (2007). Induced Pluripotent Stem Cell Lines Derived from Human Somatic Cells. *Science* 318, 1917–1920. **DOI:** 10.1126/science.1151526.

Yu J, Hu K, Smuga-Otto K, Tian S, Stewart R, Slukvin II & Thomson JA (2009). Human Induced Pluripotent Stem Cells Free of Vector and Transgene Sequences. *Science* 324, 797–801. **DOI:** 10.1126/science.1172482.

Yu JSL, Ramasamy TS, Murphy N, Holt MK, Czapiewski R, Wei S-K & Cui W (2015). PI3K/MTORC2 Regulates TGF-β/Activin Signalling by Modulating Smad2/3 Activity via Linker Phosphorylation. *Nature Communications* 6, 7212. **DOI:** 10.1038/ncomms8212.

Yu P, Pan G, Yu J & Thomson JA (2011). FGF2 Sustains NANOG and Switches the Outcome of BMP4-Induced Human Embryonic Stem Cell Differentiation. *Cell Stem Cell* 8, 326–334. **DOI:** 10.1016/j.stem.2011.01.001.

Zhang J, Klos M, Wilson GF, Herman AM, Lian X, Raval KK, Barron MR, Hou L, Soerens AG, Yu J *et al.* (2012). Extracellular Matrix Promotes Highly Efficient Cardiac Differentiation of Human Pluripotent Stem Cells. *Circulation Research* 111, 1125–1136. **DOI:** 10.1161/CIRCRESAHA.112.273144.

Zhang J, Lv S, Liu X, Song B & Shi L (2018). Umbilical Cord Mesenchymal Stem Cell Treatment for Crohn's Disease: A Randomized Controlled Clinical Trial. *Gut and Liver* 12, 73–78. **DOI:** 10.5009/gnl17035.

Zhang X, Neganova I, Przyborski S, Yang C, Cooke M, Atkinson SP, Anyfantis G, Fenyk S, Keith WN, Hoare SF *et al.* (2009). A Role for NANOG in G1 to S Transition in Human Embryonic Stem Cells through Direct Binding of CDK6 and CDC25A. *The Journal of Cell Biology* 184, 67–82. **DOI:** 10.1083/jcb.200801009.

Zhang X, Yalcin S, Lee D-F, Yeh T-YJ, Lee S-M, Su J, Mungamuri SK, Rimmelé P, Kennedy M, Sellers R *et al.* (2011). FOXO1 Is an Essential Regulator of Pluripotency in Human Embryonic Stem Cells. *Nature Cell Biology* 13, 1092–1099. **DOI:** 10.1038/ncb2293.

Zhao H & Jin Y (2017). Signaling Networks in the Control of Pluripotency. *Current Opinion in Genetics and Development* 46, 141–148. **DOI:** 10.1016/j.gde.2017.07.013.

Zhou C, Yang X, Sun Y, Yu H, Zhang Y & Jin Y (2016). Comprehensive Profiling Reveals Mechanisms of SOX2-Mediated Cell Fate Specification in Human ESCs and NPCs. *Cell Research* 26, 171–189. **DOI:** 10.1038/cr.2016.15.

Zhou H, Wu S, Joo JY, Zhu S, Han DW, Lin T, Trauger S, Bien G, Yao S, Zhu Y *et al.* (2009). Generation of Induced Pluripotent Stem Cells Using Recombinant Proteins. *Cell Stem Cell* 4, 381–384. **DOI:** 10.1016/j.stem.2009.04.005.

Zhou X, Contreras-Trujillo H & Ying Q-L (2015). New Insights into the Conserved Mechanism of Pluripotency Maintenance. *Current Opinion in Genetics & Development* 34, 1–9. **DOI:** 10.1016/j.gde.2015.06.002.

II. Materials and methods

II.1. Culture of human pluripotent stem cells

The work described in this thesis is largely focused on the culture of human pluripotent stem cells (hPSC). This type of cell has very specific requirements regarding substrate, media, and passaging techniques to retain their proliferation and pluripotency capabilities. The materials and methods employed for cell culturing and expansion were based on previously established procedures and will be briefly described in this section.

II.1.1. Human pluripotent stem cell lines

Three different hPSC lines were used throughout this work:

- WA09 (H9) hESC were acquired from WiCell. This cell line was originally isolated at Dr. James Thomson's laboratory, from human blastocyst stage embryos produced by *in vitro* fertilization (Thomson JA et al., 1998).
- DF19-9-11T.H (DF19) hiPSC were also purchased from WiCell. This cell line was reprogrammed from newborn foreskin fibroblasts using six reprogramming factors – OCT4, SOX2, NANOG, LIN28, c-Myc, and KLF4 – via an integration-free approach (Yu J et al., 2009).
- Gibco cord blood-derived hiPS (CBiPS) cells were obtained from ThermoFisher Scientific. This cell line was generated by reprogramming CD34+ cord blood cells, using a non-viral and transgene-free episomal system with seven factors (SOKMNLT, SOX2, OCT4, KLF4, MYC, NANOG, LIN28, and SV40L T antigen) (Burridge PW et al., 2011).

All three cell lines have normal karyotypes and were shown to express internal and surface markers that characterize hPSC, such as OCT4, NANOG, SOX2, SSEA4, TRA-1-60, and TRA-1-81. They were also shown to produce teratomas containing cells from all the three germ lineages when injected into immunocompromised mice (Burridge PW et al., 2011; Yu J et al., 2009; Miura T et al., 2004; Thomson JA et al., 1998).

II.1.2. Maintenance and expansion of human pluripotent stem cells

The hPSC were generally cultured in 6-well polystyrene tissue culture (PS-TC) plates (Corning) or 60 mm PS-TC dishes (Corning) coated with Growth Factor Reduced Matrigel® (MG, Corning). Three media were used to maintain hPSC cultures throughout this work: mTeSR™1 (mTeSR, StemCell Technologies), TeSR™-E8™ (SCT-E8, StemCell Technologies), and Essential 8™ (TFS-E8, ThermoFisher Scientific). The culture medium was added 50 U/mL penicillin and 50 µg/mL streptomycin (Pen/Strep, ThermoFisher Scientific) and was changed daily. The cells were handled aseptically and grown at 37°C in a humidified incubator, with 5% CO_2.

The cultures were passaged when the cell colonies displayed visually dense centers and/or when the edges of separate colonies started to merge (3 to 5 days after plating). After removing the culture medium, the cells were incubated with 0.5 mM ethylenediaminetetraacetic acid (EDTA) in phosphate-buffered saline (PBS) (both from ThermoFisher Scientific) for 6 to 8 minutes, detached in fresh culture medium using a serological pipette and replated as small clumps in new MG-coated plates at a ratio of 1:6 to 1:12, depending on their initial confluency. For cryopreservation, the detached cell clumps were centrifuged and resuspended in cold culture medium containing 10% (v/v) dimethyl sulfoxide (DMSO) and frozen at -80°C overnight before being transferred into liquid nitrogen. Occasional cell differentiation was detected by visual inspection and, if significant, was marked and removed by aspiration before passaging. When the differentiation was visibly too extensive to be removed, the entire well was discarded.

II.1.3. Human pluripotent cell suspension culture as spheroids

The generation of hPSC spheroids was achieved by transferring the suspended cells to low-attachment culture plates, adapting previously described procedures [Wang Y et al., 2013; Steiner D et al., 2010]. When ready for passage, the cells were incubated with 10 µM Rho-associated coiled-coil containing protein kinase (ROCK) inhibitor Y-27632 (ROCKi, StemCell Technologies) for 1 hour in the culture medium. After removing the medium and rinsing the cell monolayer with Dulbecco's Modified Eagle Medium / F-12 (1:1) (DMEM/F-12), the cells were incubated with Accutase (ThermoFisher Scientific) for 5-7 minutes, detached and dissociated to singlets

in DMEM/F-12. The cell suspension was pelleted by centrifugation and resuspended in culture medium with 10 µM ROCKi. Cell density was determined using a hemocytometer and trypan blue (ThermoFisher Scientific) exclusion method. The suspension was transferred to Costar Ultra-Low attachment 6-well plates (Corning), 1×10^6 cells per well (1×10^6 cells/mL medium and approximately 1×10^5 cells/cm^2 well surface) in culture medium with 10 µM ROCKi. The cells were cultured at 37°C, in an incubator with a humidified atmosphere and 5% CO_2. ROCK inhibition was kept for 24 hours and approximately 80-90% of the culture medium was replaced daily.

For passage, the cell aggregates were incubated with 10 µM ROCKi for 1 hour, rinsed with DMEM/F-12, incubated with Accutase for 5-70 minutes and dissociated to singlets with a micropipette. After determining the cell density, the cells were replated in Costar Ultra-low attachment 6-well plates and cultured as described above.

II.2. Culture and expansion of human liver cancer cells

A part of the work described involved the use of human liver cancer cell line Hep G2 as a positive control for the production process of the cellular microarrays, as they had been successfully tested before [(Meli L et al., 2012)]. This cell line, acquired from ATCC, was initially derived from the liver tissue of a 15-year-old male patient with hepatocellular carcinoma and displays an epithelial morphology and abnormal karyotype [(Simon D et al., 1982; Knowles BB et al., 1980)].

Hep G2 cells were generally cultured in non-coated PS-TC T-flasks (Corning), with Eagle's Minimum Essential Medium (EMEM) supplemented with 10% fetal bovine serum (FBS) and Pen/Strep, at 37°C, 5% CO_2. The culture medium was changed twice per week. The culture was passaged when the monolayer reached approximately 80-90% confluency. Briefly, the cells were rinsed twice with PBS, incubated with 0.25% (w/v) trypsin-EDTA (ThermoFisher Scientific) for 3-5 minutes, detached in culture medium, centrifuged and resuspended in culture medium, before replating at a ratio around 1:6.

II.3. Assessment and analysis of cellular phenotype

The study of hPSCs implies a tight control over the expression of specific markers that may indicate either the maintenance of pluripotency or the differentiation into one of the three embryonic lineages, ectoderm, endoderm, or mesoderm. The culture of these cells in suspension as 3-dimensional (3-D) aggregates adds further variables that need to be evaluated to gather a wider perspective on the effects of different culture conditions. Throughout this work, different procedures were used to analyze marker expression profiles and/or morphological parameters, based on, or adapted from established laboratory protocols.

II.3.1. Estimation of cell spheroid size and number

The estimation of the diameter and shape of cellular spheroids was performed by image analysis. Briefly, monochromatic photographs of the aggregates (> 100 per condition) were taken using a Leica DMI 3000B microscope with a Nikon DXM 1220F color digital camera. The images were then processed using MATLAB (Mathworks) to determine the area, circularity, and eccentricity of the aggregates' visible sections. After the conversion of the area from pixels to μm^2, the average diameter was estimated assuming a perfect spherical shape. Aggregate size distributions were generated by kernel density estimation (see section II.6 for formulas), using a bandwidth of 12.

Two different approaches were followed to estimate the number/density of spheroids:

- During the first days after plating the cells in suspension, the aggregates are both small and abundant and, therefore, an attempt to count their total number would be impractical. The aggregates were evenly distributed on the well by agitation and visual evaluation, and 11-15 sample microphotographs were taken at similar positions in each well. The number of aggregates was assessed in each sample image using Fiji (Schindelin J et al., 2012, 2015) and the density was estimated based on the surface area of the well.
- The number of aggregates was assessed at later days in the culture. The aggregates were concentrated in the middle of the well by agitation and

sequential microphotographs were taken to capture all of them. The images were then compiled using Microsoft Office PowerPoint (Microsoft Corporation) into a single large image displaying all the aggregates, which were counted using Fiji to a total number per well.

II.3.2. Flow cytometric analysis of marker expression

The expression of pluripotency and differentiation markers was evaluated by flow cytometric analysis of immunostained cells. The cell samples were fixed using 4% (w/v) paraformaldehyde/PBS for 10 minutes at room temperature and stored in 1% (w/v) paraformaldehyde/PBS at 4°C until further processing. Before staining, the cells were washed twice in PBS to remove paraformaldehyde residues, permeabilized in a solution of 0.5% (w/v) saponin and 1.5% (v/v) normal goat serum (NGS) in PBS for 30 minutes and then blocked with 3% (v/v) NGS/PBS for 1 hour, all at room temperature. Immunobinding with the primary antibodies was done in 3% (v/v) NGS/PBS for 2 hours at room temperature, or overnight at 4°C plus 30 minutes at room temperature. The cells were washed three times with PBS and immunostained with the secondary antibody in 3% (v/v) NGS/PBS for 1 hour, at room temperature. Samples were run on a FACScalibur (Becton Dickinson) flow cytometer and the data was analyzed using FlowJo 10 (FlowJo, LLC).

II.3.3. Gene expression analysis by quantitative polymerase chain reaction

The analysis of marker expression by quantitative polymerase chain reaction (qPCR) involved several sequential steps: a) collecting the cell samples, b) ribonucleic acid (RNA) extraction and quantitation, c) complementary deoxyribonucleic acid (cDNA) synthesis by reverse transcriptase reaction, and d) quantification by real-time PCR.

II.3.3.1. Sample collection for quantitative PCR

To collect the samples, monolayer cells were incubated with 0.5 mM EDTA/PBS for 5-7 minutes and detached from the plate into DMEM/F-12 and transferred to a centrifuge tube. Cell aggregates were simply transferred with the culture medium and DMEM/F-12 into a centrifuge tube. After washing twice with cool PBS, the cells were centrifuged at 4°C, the supernatant PBS was removed, and the pellets were frozen at -80°C until further processing.

II.3.3.2. RNA extraction and quantitation

Total cellular RNA was extracted using a PureLink RNA Mini Kit (ThermoFisher Scientific), following the manufacturer's instructions. Briefly, 600 µL lysis buffer with 1% β-mercaptoethanol was added to each tube containing the pelleted cells and vortexed at high speed until the pellet dispersed completely. One volume of 70% ethanol was added to each tube and vortexed until fully homogeneous. The samples were then transferred to spin cartridges and centrifuged at 12,000 × g for 15 seconds. The RNA was bound to the cartridge and the flow-through was discarded. The samples were washed once with Wash Buffer I and twice with Wash Buffer II and the purified RNA was eluted from the cartridge in RNase-free water into a recovery tube, by centrifuging at 12,000 × g for 2 minutes. The resulting RNA samples were immediately quantitated and/or stored at -20°C.

The concentration and purity of the collected RNA were assessed by spectrophotometric analysis. The samples were loaded onto a NanoVue Plus spectrophotometer (Biochrom) and the absorbance was measured at 260 nm (for the concentration of RNA), 280 nm, 230 nm (both for estimation of purity) and 320 nm (for background correction), with RNase-free water as a reference. The RNA concentration and absorbance ratios were automatically calculated by the spectrophotometer, using a specific program. The samples were measured in duplicates or triplicates, and the average was taken as the final value.

II.3.3.3. cDNA synthesis by reverse transcriptase reaction

The synthesis of cDNA was carried out using a High Capacity cDNA Reverse Transcription Kit (ThermoFisher Scientific) according to the manufacturer's instructions. Depending on the number of samples to process, a 2× master mix was prepared containing Reverse Transcription Buffer, deoxynucleotide mix, random primers, MultiScribe™ Reverse Transcriptase, RNase inhibitor and nuclease-free water (the latter two were not part of the kit, but were also acquired from ThermoFisher Scientific), to a total of 10 µL/reaction plus excess to account for volume loss. The mix was kept on ice. Considering the quantitation in the previous step, the volume corresponding to 1 µg RNA from each sample was loaded into individual PCR tubes and topped up to 10 µL with nuclease-free water, also on ice. The master mix was distributed – 10 µL per tube – and the tubes were loaded into a BioRad T100™ Thermal Cycler (BioRad) for the reaction: 10 minutes at 25°C, 120 minutes at 37°C and 5 minutes at 85°C. The temperature was then reduced to 4°C until sample recollection and storage. The cDNA samples were stored at -20°C until the PCR step.

II.3.3.4. Quantitative PCR

qPCRs were run on an Applied Biosystems StepOne Real-Time PCR System (ThermoFisher Scientific), using MicroAmp® Fast Optical 48-Well Reaction Plates (ThermoFisher Scientific). A reaction mix for each marker was prepared, containing the 2× master mix, assay mix (primers and probes), and nuclease-free water. The mixes were loaded onto the plate and 1-2 µL of each cDNA sample was added to each corresponding well, to a total of 20 µL per well. Negative control wells were added nuclease-free water instead of cDNA. All reactions were run in duplicates and GAPDH expression was used as the endogenous control. Reaction plate design, reaction control, and analysis were done using StepOne Software v2.3 (ThermoFisher Scientific). The threshold cycle (C_T) and baseline of each marker set of samples were manually adjusted – the C_T was adjusted to the point where the differences between samples were more noticeable and the baseline was set between cycle 3 and 1-2 cycles before the start of the first amplification.

II.3.4. Immunocytochemical analysis of marker expression in cellular spheroids

The spatial distribution analysis of marker expression in cellular spheroids was achieved by immunostaining slide-mounted sections and analyzing them under a fluorescent confocal microscope.

The cell aggregates were fixed in ice-cold 4% (w/v) formaldehyde in PBS for 20 minutes, washed once in PBS and stored in PBS at 4°C. Before sectioning, the aggregates were incubated overnight in 15% (w/v) sucrose (Sigma-Aldrich), embedded in 7.5% (w/v) gelatin (Sigma-Aldrich) / 15% (w/v) sucrose in PBS, and rapidly frozen in isopentane (Sigma-Aldrich) at -80°C. 12 µm sections were obtained on a Leica CM3050S cryostat-microtome (Leica Microsystems), collected onto Superfrost™ Microscope glass slides (ThermoFisher Scientific), and stored at -20°C. For immunostaining, the sections were first de-gelatinized in PBS at 37°C for 45 minutes, and incubated in 0.1 M Glycine (Millipore) for 10 minutes to quench residual formaldehyde. Permeabilization was done with 0.1% (v/v) Triton X-100 (Sigma-Aldrich) in PBS for 10 minutes, followed by washing with PBS and blocking for 30 minutes with 10% (v/v) fetal calf serum (FCS, ThermoFisher Scientific) in 20 mM Tris-HCl pH 8.0 / 150 mM NaCl / 0.05% (v/v) Tween-20 (TBS-T, all from Sigma-Aldrich). Immunobinding to primary antibodies was done overnight at 4°C in blocking solution. The sections were then washed three times with TBS-T for 5 minutes, and incubated with the secondary antibodies at room temperature for 30 minutes in blocking solution. After washing three times with TBS-T for 5 minutes, the sections were counterstained with 1.5 µg/mL 4',6-diamidino-2-phenylindole (DAPI, Sigma-Aldrich) for 5 minutes, washed in TBS-T and covered with coverslips using Mowiol (Sigma-Aldrich). The sections were analyzed using a Leica TCS SP5 (Leica Microsystems) inverted confocal microscope.

II.4. Cellular microarray production and analysis

One of the main aims of this work was to develop a robust and efficient high-throughput 3-D cellular microarray platform for the study of hPSC. Building on previously published work, the initial strategy was to encapsulate the cells in alginate onto borosilicate glass slides (Meli L et al., 2014; Fernandes TG et al., 2010; Lee M-Y et al., 2008). The strategy had, however, to be

progressively changed due to poor cell viability and/or low microarray stability and robustness. The different approaches taken may be categorized into two main sections: 1) glass slide-based microarrays and 2) MicroPillar chip-based microarrays. The various procedures used, ranging from the preparation of the cells and printing the microarrays to the analysis of results will be further detailed.

II.4.1. Microarrayer setup and customization

The cellular microarrays were produced using a non-contact printing MicroSys 4100 XL microarrayer (Cartesian Technologies), with a single printing circuit fitted with a solenoid valve and a 0.1 mm ceramic tip, and a washing/waste circuit. The printing circuit used autoclaved ultrapure water and its flow was controlled via a piston pump and a rotary valve system, which allowed the switch between volume aspiration and dispensing. It was attached to the printing head that moved in the vertical axis to control the height of the printing tip. The washing/waste circuit used ultra-pure water and was controlled with peristaltic pumps. The printing board was composed of four main functional elements: a 96-well plate dock, the washing and waste pool, the tip drying holes and the microarray chip slots. It moved in the horizontal axis to allow a 2-D control of the printing tip position. The tip drying holes were the open end of a vacuum circuit produced by an electric air pump. The system was operated through the computer software interface AxSys MFC (Cartesian Technologies) using programmable sequences of actions. The microarrayer also contained a humidity control system: an exterior humidifier (Holmes HM486) that produced mist into the microarrayer chamber, a humidity sensor, and a fan to disperse the mist. All three elements were connected to an automatic switch that controlled the humidifier and fan based on the humidity sensor readings.

The printing of thermo-sensitive matrices required the setup of a cooling system. A copper block was attached to the printing head and connected to a cooling circuit. The terminal portion of the printing circuit (proximal to the tip) was wound around the cooling circuit tube and a probe thermometer was installed next to the printing tip to monitor the temperature. Ice cooled water was used in both the printing and washing/waste circuits.

The sequence of microarray printing generally involved six steps: 1) washing of circuit and tip; 2) aspiration of the substrate/cell suspension from the 96-well plate; 3) printing circuit pressurization and pre-dispensing; 4) washing of tip; 5) printing; and 6) washing of circuit and tip.

II.4.2. Glass slide-based cellular microarrays

A significant part of this project was directly derived from a previously published microarray chip platform developed at Rensselaer Polytechnic Institute [Meli L et al., 2014; Fernandes TG et al., 2010; Lee M-Y et al., 2008]. This platform consisted, fundamentally, of an array of alginate spots containing the cells, printed onto a glass slide coated with poly(styrene-*co*-maleic-anhydride) (PS-MA) and pre-patterned with a mixture of poly-L-lysine (PLL) and $BaCl_2$. The microarray pattern was customized according to the purpose of each experiment and/or the number of conditions to be tested, however, the same base protocol was followed consistently throughout.

The cellular microarrays were maintained in culture medium either by complete immersion of the chip in 4-well Nunc™ plates (ThermoFisher Scientific) or by attachment of Nunc™ Lab-Tek™ II slide chamber separators (ThermoFisher Scientific) with 8 wells.

Matrigel-based microarrays were also tested on this platform. In this case, the cell microarray was directly printed onto the PS-MA-coated slide without previous patterning, unless a mixture of Matrigel and alginate was being tested.

II.4.2.1. Glass slide coating and patterning for alginate microarray

Acid-cleaned borosilicate glass slides (Coresix Precision Glass, Inc.) were spin-coated with 0.1% (w/v) PS-MA dissolved in toluene (Sigma-Aldrich), for 30 seconds at 3,000 rotations per minute (rpm), allowed to dry and stored in a clean environment. In the case of alginate microarrays, at least one day before printing the cells, the slides were pre-patterned. In standard protocol, a sterile mixture of 1 part 0.1 M $BaCl_2$ (Sigma-Aldrich) to 2 parts 0.01% (w/v) PLL (Sigma-Aldrich) was prepared and printed onto the PS-MA-coated slides (typically

60 nL per spot). Different concentrations of $BaCl_2$ and $CaCl_2$ (Sigma-Aldrich) were tested. The slides were allowed to dry overnight in a clean environment.

II.4.2.2. Cell collection for microarray printing

Generally, hPS cells were collected for microarray printing at the same stage as they were passaged: around 4-5 days after plating, when presenting dense colony centers and/or merging colony edges. The cells were pre-incubated with ROCKi for 1 hour at 37°C and, after being washed twice with DMEM/F-12, they were incubated with Accutase for 5-7 minutes at 37°C and detached into DMEM/F-12. The cells were then pelleted by centrifugation and resuspended in culture medium with ROCKi. After determining the cell density using a hemocytometer, the cells were centrifuged again and resuspended in the appropriate volume of culture medium with ROCKi to achieve the target printing density.

HepG2 cells were collected for printing at around 80-90% confluency. The cells were washed twice with PBS and incubated for 5 minutes with trypsin/EDTA before being detached into DMEM with 10% FBS. After the cells were centrifuged and resuspended in fresh EMEM with 10% (v/v) FBS, the cell density was determined using a hemocytometer and adjusted for the target printing density.

II.4.2.3. Alginate-based microarray printing

Before printing the cells, the microarrayer chamber was sprayed with 70% ethanol and wiped. The printing circuit was washed with 70% (v/v) ethanol followed by ultra-pure water, to reduce the risk of contamination and the humidifier was turned on to achieve a >95% humidity level inside the chamber.

When ready to print, the cell suspension was mixed 2:1 with 3% (w/v) alginate and loaded into a 96-well plate (Corning) and onto the microarrayer plate dock. The suspension was printed onto the chips pre-patterned with $BaCl_2$/PLL or $CaCl_2$/PLL, which caused the alginate to almost immediately cross-link and encapsulate the cells. The chips were then either 1) transferred to a 4-well plate and immersed in culture medium or 2) attached to Lab-

Tek II slide chamber separators. In the latter case, the separators and the chips were pressed together for 1 minute, after which culture medium was added to the wells.

The cellular microarrays were cultured at 37°C and 5% CO_2 in a humidified incubator. hPSCs were grown in TeSR-E8 or mTeSR1 (both from Stem Cell Technologies) with Pen/Strep, with ROCKi during the first 48 hours and daily media replacement. HepG2 cells were cultured in EMEM with 10% (v/v) FBS and Pen/Strep.

II.4.2.4. Matrigel-based microarray printing

The printing of Matrigel-based cellular microarrays required the adaptation of both the microarrayer and the protocol, although the general workflow was maintained. The microarrayer was fitted with a refrigeration circuit to cool down the printing tip and circuit and the humidifier was controlled manually to reduce condensation. Both the printing and washing circuits were fed with ice-cold water and the printing sequence was accelerated to reduce the time that Matrigel was inside the circuit. The 96-well source plate was kept on ice and was only placed inside the microarrayer immediately before it was ready to aspirate the cell suspension.

After collecting the cells, the suspension was placed on ice and allowed to cool down for a few minutes before being mixed with Matrigel. The mixture ratio was determined by the lot dependent Matrigel protein concentration: a working concentration of 5 mg/mL was used, and the cell density was previously adjusted accordingly. When combinations of Matrigel and alginate were tested, the cell suspension was mixed with alginate first. The suspension was loaded on a 96-well plate and put into the microarrayer for printing. Immediately after printing, the chips were transferred into a custom humidified chamber (a 150 mm Petri dish containing water and two 35 mm Petri dish lids to hold the chip above the water) with the microarray facing down and incubated at 37°C for 20 minutes, to allow the Matrigel to completely gelate. The microarray chips were then either immersed in medium or attached to slide chamber separators, as described in Section II.4.2.3.

II.4.2.5. Cellular viability assessment on glass slide-based microarrays

The analysis of on-chip cellular viability was performed using the Live/Dead® viability/cytotoxicity kit for mammalian cells (ThermoFisher Scientific) and allowed the evaluation of cell survival and growth in different media and/or substrate formulations. The Live/Dead kit is composed of two dyes: calcein AM, which stains live/viable cells with green fluorescence, and ethidium homodimer-1 (EtHD), which stains dead/non-viable cells with red fluorescence. The adopted protocol was based on previously established procedures (Meli L et al., 2014; Fernandes TG et al., 2008, 2010).

Before staining, the microarrays were washed in DMEM/F-12 for 5 minutes, at 37°C. A control for 100% dead cells was prepared by adding 0.1% (w/v) saponin/PBS to the washing medium in this step. The cells were then incubated with the staining solution containing 1 µM Calcein AM and 2 µM EtHD for 25 minutes, at 37°C and 5% CO_2. After staining, the Lab-Tek slide chamber separator, if used, was removed and the chips were rinsed using a washing buffer (121 mM sodium chloride, 18 mM sodium bicarbonate, 1 mM calcium chloride, 4 mM potassium chloride, 0.3 mM magnesium chloride, 0.4 mM magnesium sulfate, 17.5 mM D-glucose, 17 mM HEPES, pH 7.4) three times for 10 minutes, to remove unbound dyes. An additional wash with 50 mM trehalose (Sigma-Aldrich) in PBS was performed in the case of Matrigel-based microarrays, to improve dye retention (Nierode GJ et al., 2016). The microarrays were dried using a stream of nitrogen and stored in the dark. The fluorescence was assessed by scanning the chips in a GenePix 4200A microarray scanner (Molecular Devices), using a 488 nm laser for excitation, with a blue filter for detection of green emission and a 645AF75/594 filter for detection of red. The scanner software interface GenePix Pro 6.0 was used to process the images and quantify the fluorescence intensity.

II.4.2.6. Protein expression analysis by immunofluorescence on glass slide-based microarrays

The expression of pluripotency markers was assessed on-chip by immunostaining. The adopted protocol was based on standard procedures for immunocytochemistry, using a primary antibody and a fluorophore-conjugated secondary antibody. This protocol was

performed on microarrays using the Lab-Tek II separator, which allowed differential immunostaining on the same chip.

The microarrays were rinsed with washing buffer (composition described in Section II.4.2.5) to remove the residual medium and debris, and fixed with 4% (w/v) formaldehyde (ThermoFisher Scientific) in PBS with calcium and magnesium (PBS-Ca/Mg, ThermoFisher Scientific) for 15 minutes, at room temperature. After washing twice for 5 minutes with PBS-Ca/Mg, the cells were permeabilized with 0.25% (v/v) Triton-X100 (Sigma-Aldrich) in PBS-Ca/Mg for 30 minutes and blocked with 3% (w/v) BSA (Sigma-Aldrich) in PBS-Ca/Mg for 1 hour, all at room temperature. Immunobinding with the primary antibody was done in blocking solution for 2 hours and, after washing three times 10 minutes, the cells were incubated with the secondary antibody and 1 µg/mL Hoechst 33342 (ThermoFisher Scientific), also in blocking solution, for 1 hour and 30 minutes. The microarrays were washed three times with PBS-Ca/Mg and dried with a nitrogen stream. In the case of Matrigel-based microarrays, an additional wash with 50 mM trehalose in PBS-Ca/Mg was performed before drying.

Qualitative analysis of the microarrays was performed using an Olympus IX51 inverted microscope equipped with a DP20 (Olympus) color camera.

II.4.3. MicroPillar/MicroWell chip cellular microarrays

The significant limitations related to the use of glass slide-based microarrays with hPS cells led us to gradually transition towards a different platform. The MicroPillar/MicroWell (MPMW) system (Samsung Electro-Mechanics Co) is composed of two complementary polystyrene chips with the approximate size of a standard microscope slide: a) the MicroPillar chip, with 532 (14 × 38) 0.75 mm-diameter pillars, and b) the MicroWell chip, with the same 532 respective wells of 1.2 mm diameter. In this system, the cell suspension is spotted onto the pillars while the medium is printed into the microwells. The chips are then sandwiched together with each pillar in its correspondent well, immersing the encapsulated cells in the media [Nierode GJ et al., 2016; Kwon S-J et al., 2014].

II.4.3.1. Preparation and reuse of MicroPillar and MicroWell chips

After preliminary testing with the MPMW system, a protocol was established for the initial washing and treatment of the chips, as well as a washing protocol for their reuse to reduce costs.

Initial experiments resulted in inconsistent outcomes in terms of cell viability and recurrent spot detachment from the pillars. It was also noted that some of the pillars and wells appeared to have contaminant residues that could be impacting the efficacy and robustness of the platform. A washing routine was adopted as an attempt to reduce the variability. Briefly, the MicroPillar chips were rinsed with deionized water and 70% (v/v) ethanol (aq) and blow-dried with a flow of nitrogen. A UV-treatment was performed by exposing the chips to a UV-lamp for 4 hours, as a strategy to improve spot attachment by photo-oxidation of the pillars' surface, thus reducing their hydrophobicity. The routine for the MicroWell chips was the same, but also included a sonication step in 0.1% (w/v) sodium dodecyl sulfate (SDS) (aq) for 90 minutes, between the water and ethanol washes.

The cost of the chips and the demand for large quantities due to the daily media changes required by hPSCs prompted a strategy of chip recycling. The MicroPillar chips were first incubated with trypsin/EDTA for 2 hours at 37°C to remove Matrigel and cell residues, followed by the same routine described for the first use, but with the UV-treatment/sterilization reduced to 90 minutes instead of 4 hours. The protocol for MicroWell chip recycling was also similar to the one described for the first use, but the chips were left in the SDS solution overnight after the sonication, and the UV-treatment/sterilization was reduced to 90 minutes.

II.4.3.2. Cell collection and Matrigel-based microarray production in the MicroPillar/MicroWell system

The procedure for cell collection and microarray printing using the MPMW system was, in almost its entirety, the same as described in sections II.4.2.2 and II.4.2.4, respectively. The most significant difference was the use of the MicroWell chips for incubating the cells in the culture medium, instead of using a 4-well plate or a Lab-Tek II slide chamber separator. Before collecting the cells, the media were prepared and printed into the MicroWell chips,

750 nL per well. The chips were covered with Parafilm and stored at 4°C. After printing the cell suspension, the MicroPillar chips were incubated at 37°C for 20 minutes, to allow Matrigel to gelate, as described previously. At this point, the MicroWell chips containing media were also transferred to an incubator at 37°C, to allow the media to warm up. After the incubation, the MicroPillar and the MicroWell chips were sandwiched together, with each pillar in its correspondent well, placed inside a humidity chamber (a 150 mm Petri dish with water and the lid of a 100 mm plate), pillars facing down, and incubated at 37°C and 5% CO_2. The daily media changes were carried out by replacing the MicroWell chips with new chips containing fresh media.

II.4.3.3. Staining procedure for the analysis of cellular growth, viability, and protein expression in the MicroPillar/MicroWell system

The staining for the assessment of cellular growth and viability in the MPMW system was performed similarly to what was described in section II.4.2.5, using the Live/Dead kit. The MicroPillar chips were washed and incubated with the staining solution using 4-well plates. The staining solution also contained 1 μg/mL Hoechst 33342 for controlling the total cell number per pillar.

The analysis of protein expression was performed as described previously, in section II.4.3.6, also using 4-well plates for MicroPillar chip washes and incubation steps, except in the incubations with antibodies. In this case, the antibody solutions were prepared and printed as an array onto a MicroWell chip covered with a Parafilm strip, which had been lightly pressed down to create small concave pits over each well. The hydrophobicity of Parafilm and the concave shape allowed each drop of antibody solution to remain in the position that it was printed and isolated from the rest. The MicroPillar chip was carefully placed on top of the Parafilm strip so that each pillar contacted with each respective drop. The incubation was performed inside a humidity chamber (as described in section II.4.3.2) to prevent the evaporation of the small volumes.

The MicroPillar chips were scanned in a Cellomics ArrayScan XTI (ThermoFisher Scientific) high-content platform, using a 5× objective with the following filters: 1) BGRFR 386-23 for Hoechst (blue) detection; 2) BGRFR 485-20 for green fluorescence detection and 3) BGRFR 549-15 for red fluorescence detection. Each pillar was individually scanned using the

blue channel (Hoechst) as a reference for auto-focus. The images were exported using the platform software interface, HCS Studio Cell Analysis (ThermoFisher Scientific). Automated image processing and fluorescence intensity analysis were performed using MATLAB. The quantitative data were further processed using Microsoft Office Excel 2016.

II.5. Image processing and analysis using MATLAB

The development of a high-throughput platform requires not only the capacity to efficiently test large sets of conditions but also the ability to rapidly process and analyze the readings or outcomes of those tests. Given the amount of data that is usually generated using these platforms, automated analysis is usually the most efficient approach, although it generally requires a considerable degree of optimization.

In this work, two different scanning equipment were used for microarray imaging: 1) a GenePix microarray scanner for the glass slide-based arrays and 2) a Cellomics ArrayScan high content platform for the MPMW system. While the GenePix equipment had been previously used and optimized, the Cellomics ArrayScan platform was still being optimized for this specific application at the time that the experiments were conducted. Therefore, while both systems had software interfaces with analysis capabilities, a strategy of designing and writing an analysis tool using MATLAB was adopted, to process the images gathered from the MPMW chips. Using a simple iterative computing approach, the fluorescence intensity data generated using this system allowed the indirect estimation of cellular viability. Additionally, part of the work described in this thesis involved image analysis for the measurement of cellular aggregates in suspension cultures, as referenced in section II.3.1. The methodological rationale and basic structure of each of these two MATLAB tools, as well as the algorithm for estimation of cellular viability, will be briefly detailed in the following sections.

II.5.1. Image analysis for the morphological evaluation of cellular spheroids

While different image processing software already exists for object detection and analysis, a MATLAB tool with a graphical user interface (GUI) was designed to improve the

automatization of the process of measuring cellular spheroids in images, and the compilation of results.

Monochrome microphotographs of the cell aggregates were compiled into a single folder per condition. The tool was, in part, based on a Tutorial included in the MATLAB documentation (http://www.mathworks.com/help/images/examples/detecting-a-cell-using-image-segmentation.html) and was programmed to work following a sequence of steps:

1) Load the folder containing the set of images, which lists them numerically in the background and displays the total number.
2) Load the first image, which automatically applies a series of built-in functions (including 'EDGE', 'IMDILATE', 'BWMORPH', 'IMFILL', 'IMERODE' and 'BWAREAOPEN') to process it and detect any objects/aggregates. The loaded image is displayed, and a switch allows the user to see both the original image and the identified edged aggregates.
3) If necessary, the user can adjust the detection threshold to either increase or reduce the object detection sensitivity, adjust the minimum diameter that an object needs to have to be considered and/or use an object refinement tool to interactively erase or add portions to the objects with an adjustable-diameter "brush". The refinement tool is equally useful to separate aggregates that are too close together to be automatically detected as separate objects.
4) Load the detected objects, which gathers their *area*, *perimeter*, *eccentricity*, *major axis length*, and *minor axis length*, expressed as number of pixels. The *diameter* D is automatically calculated from the *area* A, considering the conversion factor from pixels to micrometers k:

$$D = \frac{4Ak^2}{\pi} \tag{1}$$

and the dimensionless *circularity* C is calculated from both the *area* A and the *perimeter* P:

$$C = \frac{4A\pi}{P^2} \tag{2}$$

Each object/aggregate is numbered, and the calculated diameters are displayed in a table in the GUI.

5) The user can then select the aggregates and exclude any artifacts that may have been detected as objects.
6) Export the gathered properties from each aggregate to the desired file format.
7) Repeat the whole process from 2 to 6, until all the images are processed, after which the GUI displays the option to compile the data from each image into a single file.

The numerical data were processed using MATLAB for the estimation of aggregate morphological distributions. Microsoft Office Excel and R (R Core Team, 2019) were used for other statistical analyses.

II.5.2. Image processing and analysis for the assessment of fluorescence intensity in cellular microarrays

The analysis of the images gathered from the MPMW chips with the Cellomics ArrayScan would be possible with the software interface provided with the equipment. However, given the complexity of that software, the limited availability of time to use it, and the need for increased control of the processing steps and variables involved, the data was analyzed using a custom MATLAB GUI. This GUI was designed to work as a modular sequential system so that functionalities could be easily modified, or new ones could be added to the process/analysis sequence.

The data was exported using the HCS Studio Cell Analysis software. Due to some glitches in the software and the high number of images per chip, it was necessary to export the data to two different file formats: *.c01 and *.dib. The images were automatically converted to *.tif using MATLAB – c01 files were read using the Bio-Formats package (available at http://www.openmicroscopy.org/bio-formats/) (Linkert M et al., 2010) while dib files were read using the function 'READCDIB', available on Mathworks (https://www.mathworks.com/matlabcentral/fileexchange/11096-read-cellomics%C2%AE-dib-files) – and renamed using a standardized format for easier identification and downstream processing.

After converting and renaming the full set of images of each chip and gathering them into a single folder, they were processed using the GUI tool through a sequence of steps:

1) Load the folder containing the images and pre-analyze the set for the numbers of rows, columns, and color channels, along with the detection of "blank" images, by determining the fluorescence intensity maxima and standard deviation of each image.
2) Set the position for a cropping mask. Because the pillars aren't centered in all the images, twelve reference pillars are selected from the chip to set a dynamic position matrix – the user centers a round selection mask in each of the twelve reference images and the program estimates the position for every other pillar. The size of the cropping mask may be adjusted.
3) Preview the images overlaid with the cropping mask to confirm that the positioning is appropriate and, if so, trigger the cropping. The intensity of the pixels in the areas between the image angles and the round mask is set to 0.
4) If required, apply background subtraction to the selected channels. The background subtraction module determines a specific background threshold for each image and follows three main steps. Briefly:
    4.1) The intensity of each pixel in the image is iteratively exponentiated so that the relative difference between the brighter and the dimmer pixels is increased. Because the pixel values are constrained to a restrictive scale (original images are 12-bit but are processed as 16-bit), there is a maximum possible value that represents intensity saturation (*i.e.,* 65535). For each iteration, the standard deviation of pixel intensity in the whole image is calculated and, generically, the point where it reaches a maximum is considered the optimal iteration – the exponent that yields the greatest absolute difference between signal and background.
    4.2) After applying the determined exponent, a threshold is computed using "MULTITHRESH" for all non-zero pixels of the image. This function calculates a threshold using Otsu's method, which clusters the pixel values into two classes with minimal intra-class variance (Otsu N, 1979).
    4.3) A logical/binary image mask is created from the determined threshold (pixels with values below the threshold are set to 0 – "background" – and the

rest are set to 1 – “signal”) using “IMQUANTIZE”, and subsequently processed with smoothing and cleaning filters such as “BWAREAOPEN”, “BWMORPH”, and “IMFILL”, to reduce artifacts and edge roughness; the mask is applied to the original image, setting the “background” pixels to 0. The “signal” pixels are also reduced by a baseline background value – 75% of the mean intensity subtracted from the “background” pixels.

5) If required, apply peak/cell detection. The peak detection module is a basic algorithm designed to detect relatively independent spikes of fluorescence in each image, given an intensity threshold and a minimum distance between peaks; it is appropriate for an approximate count of isolated cellular nuclei or cells.
6) Export the processed chip data, namely each pillar’s total fluorescence, fluorescence average, and standard deviation; the tool also exports the total background subtracted from each image and peak counts, if those modules were used, for post-processing quality check; the cropped images are also exported, both with background and after the subtraction. The program also creates a single, full resolution image montage per channel of all the pillars, according to the original chip layout.

The exported quantitative data was analyzed using Microsoft Office Excel 2016. Image composites of the different fluorescence channels were generated with Fiji.

II.5.3. Computation of cellular viability from fluorescence intensity in microarrays

Cellular viability can usually be calculated by subtracting the number of non-viable cells from the total within a sample, thus getting the number of viable cells, and dividing that difference by the total. The use of trypan blue to discern viable from non-viable cells is standard protocol in most cell culture laboratories when dealing with cell suspensions (Strober W, 2015). In a cellular microarray, such as the MPMW chip, however, it is technically difficult to get reliable counts of total cells and/or viable cells, particularly when they are not fully discernible. To tackle this issue, a simple mathematical approach was employed to estimate the on-chip cellular viability, using the fluorescence data collected and an iterative data fitting method. The rationale for that approach will be briefly described.

The MPMW chips were stained with 1) Hoechst, which stains all the nuclei; 2) calcein AM, which stains the cytoplasm of viable cells; and 3) EtHD, which stains the nuclei of non-viable cells. It is safe to assume that:

$$F_{Hoechst} = N_T \times f_a, \qquad F_{calcein} = N_V \times f_b \times r, \qquad F_{EtHD} = N_{nV} \times f_c \tag{3}$$

where $F_{Hoescht}$, $F_{calcein}$ and F_{EtHD} are the fluorescence intensities in each pillar of Hoechst, calcein, and EtHD, respectively; N_T, N_V and N_{nV} are the numbers of total, viable and non-viable cells; f_a, f_b and f_c correspond to the mean fluorescence intensity per cell stained with Hoechst, calcein, and EtHD; and r is the mean nucleus to cytoplasm ratio. Therefore, given that the total number of cells equals the sum of viable and non-viable cells,

$$F_{Hoechst} \times \frac{1}{f_a} = F_{calcein} \times \frac{1}{f_b \times r} + F_{EtHD} \times \frac{1}{f_c} \tag{4}$$

Because the purpose of this method is not to determine the average fluorescence per cell of each dye or to calculate the nucleus to cytoplasm ratio, but rather to establish a meaningful relation between available fluorescence intensity data, it is possible to replace those variables with generic constants:

$$F_{Hoechst} = F_{calcein} \times L_a + F_{EtHD} \times L_b \tag{5}$$

For each chip, the generic constants L_a and L_b were estimated using MATLAB, by iteratively computing the minimal sum of the squared residuals $\widehat{LS}$, in the entire data set (all the pillars in the chip) with size n:

$$\widehat{LS} = \sum_{i=1}^{n} \left[F_{Hoechst_i} - \left(F_{calcein_i} \times L_a + F_{EtHD_i} \times L_b\right)\right]^2 \tag{6}$$

The viability V was then calculated:

$$V = \frac{F_{calcein} \times L_a}{F_{calcein} \times L_a + F_{EtHD} \times L_b} \tag{7}$$

II.6. Statistical analysis

The results described throughout this work are generally expressed as mean ± standard deviation (SD) or mean ± standard error of the mean (SEM), as specifically indicated. SEM corresponds the SD divided by the square root of the number of observations n:

$$SEM = \frac{SD}{\sqrt{n}} \tag{8}$$

The kernel density estimations (KDE) for the analysis of the cellular spheroid size distributions (described in section II.3.1) were calculated on MATLAB using the formula:

$$\widehat{D}(x) = \frac{1}{nh}\sum_{i=1}^{n} K\left(\frac{x - x_i}{h}\right) \tag{9}$$

where $\widehat{D}$ is the estimated density function of x (the aggregate diameter), n is the sample size, h represents the bandwidth, and K stands for the Gaussian kernel function:

$$K(u) = \frac{1}{\sqrt{2\pi}} e^{-\frac{1}{2}u^2} \tag{10}$$

A constant bandwidth of 12 was heuristically selected and used throughout the analyses of spheroid size.

For spheroid-related data, normality was assessed using the Shapiro-Wilk test. Because most data sets displayed poor correlation with the Gaussian distribution, the median and the median absolute deviation (MAD) were used as measures of central tendency and dispersion, respectively (median ± MAD), for aggregate diameter, circularity, and eccentricity. MAD was calculated using R and corresponds to:

$$MAD = k \times median(|x_i - \tilde{x}|) \tag{11}$$

with $k = 1{,}4826$.

Spearman's rank correlation coefficient (ρ) was calculated in R and used as a nonparametric measure of the correlation between initial cell densities and different metrics in aggregate culture.

II.7. References

Burridge PW, Thompson S, Millrod MA, Weinberg S, Yuan X, Peters A, Mahairaki V, Koliatsos VE, Tung L & Zambidis ET (2011). A Universal System for Highly Efficient Cardiac Differentiation of Human Induced Pluripotent Stem Cells That Eliminates Interline Variability. *PLoS ONE* 6, e18293. **DOI:** 10.1371/journal.pone.0018293.

Fernandes TG, Kwon S-J, Lee M-Y, Clark DS, Cabral JMS & Dordick JS (2008). On-Chip, Cell-Based Microarray Immunofluorescence Assay for High-Throughput Analysis of Target Proteins. *Analytical Chemistry* 80, 6633–6639. **DOI:** 10.1021/ac800848j.

Fernandes TG, Kwon S-J, Bale SS, Lee M-Y, Diogo MM, Clark DS, Cabral JMS & Dordick JS (2010). Three-Dimensional Cell Culture Microarray for High-Throughput Studies of Stem Cell Fate. *Biotechnology and Bioengineering* 106, n/a-n/a. **DOI:** 10.1002/bit.22661.

Knowles BB, Howe CC & Aden DP (1980). Human Hepatocellular Carcinoma Cell Lines Secrete the Major Plasma Proteins and Hepatitis B Surface Antigen. *Science* 209, 497–499. **DOI:** 10.1126/science.6248960.

Kwon S-J, Lee DW, Shah DA, Ku B, Jeon SY, Solanki K, Ryan JD, Clark DS, Dordick JS & Lee M (2014). High-Throughput and Combinatorial Gene Expression on a Chip for Metabolism-Induced Toxicology Screening. *Nature Communications* 5, 3739. **DOI:** 10.1038/ncomms4739.

Lee M-Y, Kumar RA, Sukumaran SM, Hogg MG, Clark DS & Dordick JS (2008). Three-Dimensional Cellular Microarray for High-Throughput Toxicology Assays. *Proceedings of the National Academy of Sciences* 105, 59–63. **DOI:** 10.1073/pnas.0708756105.

Linkert M, Rueden CT, Allan C, Burel J-M, Moore W, Patterson A, Loranger B, Moore J, Neves C, MacDonald D *et al.* (2010). Metadata Matters: Access to Image Data in the Real World. *The Journal of Cell Biology* 189, 777–782. **DOI:** 10.1083/jcb.201004104.

Meli L, Jordan ET, Clark DS, Linhardt RJ & Dordick JS (2012). Influence of a Three-Dimensional, Microarray Environment on Human Cell Culture in Drug Screening Systems. *Biomaterials* 33, 9087–9096. **DOI:** 10.1016/j.biomaterials.2012.08.065.

Meli L, Barbosa HSC, Hickey AM, Gasimli L, Nierode G, Diogo MM, Linhardt RJ, Cabral JMS & Dordick JS (2014). Three Dimensional Cellular Microarray Platform for Human Neural Stem Cell Differentiation and Toxicology. *Stem Cell Research* 13, 36–47. **DOI:** 10.1016/j.scr.2014.04.004.

Miura T, Luo Y, Khrebtukova I, Brandenberger R, Zhou D, Scott Thies R, Vasicek T, Young H, Lebkowski J, Carpenter MK & Rao MS (2004). Monitoring Early Differentiation Events in Human Embryonic Stem Cells by Massively Parallel Signature Sequencing and Expressed Sequence Tag Scan. *Stem Cells and Development* 13, 694–715. **DOI:** 10.1089/scd.2004.13.694.

Nierode GJ, Perea BC, McFarland SK, Pascoal JF, Clark DS, Schaffer D V & Dordick JS (2016). High-Throughput Toxicity and Phenotypic Screening of 3D Human Neural Progenitor Cell Cultures on a Microarray Chip Platform. *Stem Cell Reports* 7, 970–982. **DOI:** 10.1016/j.stemcr.2016.10.001.

Otsu N (1979). A Threshold Selection Method from Gray-Level Histograms. *IEEE Transactions on Systems, Man, and Cybernetics* 9, 62–66. **DOI:** 10.1109/TSMC.1979.4310076.

R Core Team (2019). R: A Language and Environment for Statistical Computing (Vienna, Austria: R Foundation for Statistical Computing).

Schindelin J, Arganda-Carreras I, Frise E, Kaynig V, Longair M, Pietzsch T, Preibisch S, Rueden C, Saalfeld S, Schmid B *et al.* (2012). Fiji: An Open-Source Platform for Biological-Image Analysis. *Nature Methods* 9, 676–682. **DOI:** 10.1038/nmeth.2019.

Schindelin J, Rueden CT, Hiner MC & Eliceiri KW (2015). The ImageJ Ecosystem: An Open Platform for Biomedical Image Analysis. *Molecular Reproduction and Development* 82, 518–529. **DOI:** 10.1002/mrd.22489.

Simon D, Aden DP & Knowles BB (1982). Chromosomes of Human Hepatoma Cell Lines. *International Journal of Cancer* 30, 27–33. **DOI:** 10.1002/ijc.2910300106.

Steiner D, Khaner H, Cohen M, Even-Ram S, Gil Y, Itsykson P, Turetsky T, Idelson M, Aizenman E, Ram R *et al.* (2010). Derivation, Propagation and Controlled Differentiation of Human Embryonic Stem Cells in Suspension. *Nature Biotechnology* 28, 361–364. **DOI:** 10.1038/nbt.1616.

Strober W (2015). Trypan Blue Exclusion Test of Cell Viability. In: Current Protocols in Immunology, (Hoboken, NJ, USA: John Wiley & Sons, Inc.), p. A3.B.1-A3.B.3.

Thomson JA, Itskovitz-Eldor J, Shapiro SS, Waknitz MA, Swiergiel JJ, Marshall VS & Jones JM (1998). Embryonic Stem Cell Lines Derived from Human Blastocysts. *Science* 282, 1145–1147. **DOI:** 10.1126/science.282.5391.1145.

Wang Y, Chou B-K, Dowey S, He C, Gerecht S & Cheng L (2013). Scalable Expansion of Human Induced Pluripotent Stem Cells in the Defined Xeno-Free E8 Medium under Adherent and Suspension Culture Conditions. *Stem Cell Research* 11, 1103–1116. **DOI:** 10.1016/j.scr.2013.07.011.

Yu J, Hu K, Smuga-Otto K, Tian S, Stewart R, Slukvin II & Thomson JA (2009). Human Induced Pluripotent Stem Cells Free of Vector and Transgene Sequences. *Science* 324, 797–801. **DOI:** 10.1126/science.1172482.

III. Development of a 3-dimensional cellular microarray for high-throughput studies on human induced pluripotent stem cells

III.1. Introduction

Human pluripotent stem cells (hPSC) are regarded as a powerful tool in the study of developmental biology, toxicology, and drug screening, and hold great potential in the development of new cellular therapies for regenerative medicine. However, comprehensive knowledge and tight control over the mechanisms and microenvironmental cues that influence self-renewal and differentiation are required for the development of reliable models and the successful realization of this potential [(Klimanskaya I et al., 2008)]. The determination of stem cell fate is conditioned by myriad variables, such as the availability of nutrients, growth factors, and the components of extracellular matrix components and its biomechanical properties [(Hazeltine LB et al., 2013)]. The testing and optimization of such microenvironmental conditions for efficient expansion and differentiation of hPSCs generally involve laborious, time-consuming, and costly protocols. Furthermore, traditional 2-dimensional culture platforms used for cell-based assays may not be suitable for an accurate representation of physiological conditions [(Baker BM & Chen CS, 2012)].

The development of microfabrication, robotic micro-handling, and liquid dispensing technologies has enabled the miniaturization of experimental platforms, thus allowing an increased throughput by testing many conditions in parallel with the use of fewer cells and reagents [(Rothbauer M et al., 2016; Fernandes TG et al., 2009)]. Cellular microarrays, in particular, have been proven useful as means of assessing the effects of variations in the cellular microenvironment and soluble compounds, through the quantification of proliferation, cytotoxicity and the expression of molecular markers [(Nierode GJ et al., 2016; Kumar N et al., 2015; Meli L et al., 2012; Fernandes TG et al., 2008)].

This chapter describes the several strategies tested for the development and optimization of a 3-dimensional high-throughput cellular microarray platform for studies with hPSCs.

III.2. Low viability of human pluripotent stem cells in alginate-based microarrays

Lee et al. previously described a 3-D microarray system in which cells are mixed with an alginate solution and spotted onto a PS-MA-coated borosilicate glass slide patterned with

PLL/$BaCl_2$. When in contact with the $BaCl_2$, the alginate crosslinks into a 3-D matrix and encapsulates the cells, while the PLL stabilizes the printed spots on the hydrophobic surface of the slide [(Lee M-Y et al., 2008)]. This system has been successfully used for studies on growth, differentiation, and toxicity screening on several human cancer cell lines, human neural stem cells, and mouse embryonic stem cells [(Meli L et al., 2012, 2014; Fernandes TG et al., 2008, 2010; Lee M-Y et al., 2008)]. The initial purpose of this work was to evaluate if this microarray system could be adapted for studies with hPSCs.

Preliminary tests using single-cell dissociated H9 human embryonic stem cells indicated an almost total loss of viability within the first 24 hours after printing, using the standard protocol (1% alginate onto 33 mM $BaCl_2$). Several different conditions were tested, using two different cell lines. To evaluate if the salt and/or the salt concentration was influencing cell viability, H9 cells were pre-incubated with 10 µM ROCK inhibitor Y-27632 (ROCKi) for 1 hour before detachment and single-cell dissociation using Accutase, and spotted in a mixture of 1% alginate (60 nL and 300 cells/spot) onto a slide patterned with PLL and either $BaCl_2$ (10 mM, 20 mM or 30 mM), $CaCl_2$ (10 mM, 20 mM, 30 mM or 50 mM), or a mixture of 10 mM $BaCl_2$ and 20 mM $CaCl_2$. The microarrays were incubated in mTeSR1 with ROCKi in 4-well plates and viability was assessed using the Live/Dead staining kit at three time-points: 3 h, 6 h, and 24 h. There were, however, no observable differences between the conditions tested. While at 3 h most of the cells stained green, indicating high viability, they progressively died and stained mostly with ethidium homodimer-1 (EtHD) at 24 h (Figure III.1 – a - c).

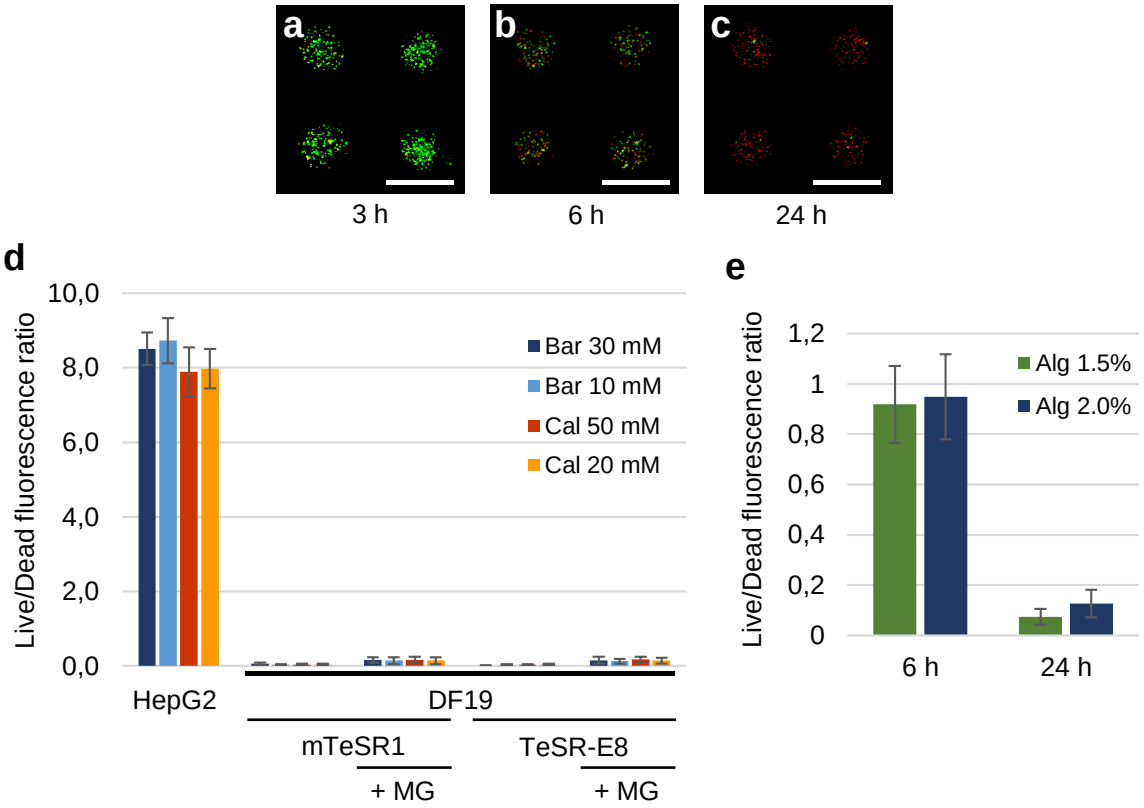

Figure III.1 – Low viability of hPS cells in alginate-based microarrays, under different conditions. **(a - c)** H9 cells printed in 1% alginate onto different concentrations of either $BaCl_2$ or $CaCl_2$ after **(a)** 3 h, **(b)** 6 h and **(c)** 24 h on-chip. Images correspondent to 50 mM $CaCl_2$ but representative of all conditions tested. Green fluorescence (calcein-AM, calcein) represents live cells and red fluorescence (Ethidium homodimer-1, EtHD) represents dead cells. Scale bar: 1 mm. **(d)** Ratio of calcein/EtHD fluorescence intensity in printed HepG2 and DF19 cells after 24 hours on-chip. HepG2 cells were used as a positive control. DF19 cells were printed onto $BaCl_2$ (Bar) or $CaCl_2$ (Cal) and incubated in either mTeSR1 or TeSR-E8 media, with or without 100 µg/mL Matrigel (MG) supplementation. Results presented as mean ± SD, ≥ 74 spots/condition. **(e)** Ratio of calcein/EtHD fluorescence intensity of DF19 cells printed in different concentrations of alginate (Alg), after 6 h and 24 h on-chip. The cells were incubated in mTeSR1 medium supplemented with 100 µg/mL Matrigel. Results presented as mean ± SD, ≥ 475 spots/condition.

To further investigate if the loss of viability could be mitigated by other factors, DF19 human induced pluripotent stem cells (hiPSC) were printed onto varying concentrations of $BaCl_2$ and $CaCl_2$, and incubated for 24 hours in either mTeSR1 or TeSR-E8 media with ROCKi. Since alginate does not provide extracellular matrix (ECM) components, it was hypothesized that supplementing the medium with Matrigel, a mixture of ECM proteins extracted from Englebreth-Holm-Swarm mice tumors, consisting mainly of laminin, collagen IV, and entactin [(Hughes CS et al., 2010)], could promote hiPSC survival. HepG2 human hepatocellular carcinoma cells were printed in parallel to serve as a positive control for the protocol, as they had been

previously studied on this system [Meli L et al., 2012]. While HepG2 cells retained high viability, most DF19 cells died after 24 hours in all the conditions tested (Figure III.1 – d). Although Matrigel supplementation appeared to increase DF19 cell viability (more than three-fold in all conditions), it was still too low to enable further studies.

Even though there were no observable differences between $BaCl_2$ and $CaCl_2$ alginate crosslinking in hiPSCs, $BaCl_2$ appeared to improve viability in HepG2 cells. Barium-crosslinked alginate is typically stiffer than calcium-crosslinked alginate [Mørch ÝA et al., 2006], so the effect of matrix stiffness on hiPSC viability was further tested by increasing the concentration of alginate. DF19 cells were mixed with alginate to either 1.5% or 2% final concentrations, printed onto $BaCl_2$ and incubated in mTeSR1 with ROCKi and 100 µg/mL Matrigel. No considerable differences were found between conditions and most of the cells died within 24 h (Figure III.1 – e). Modifications of other variables, such as cell density and spot volume, were also tested, with no significant improvement in cellular viability.

III.3. Matrigel-based matrix enhances hiPSC on-chip viability

The previous results evidenced that a simple alginate-based matrix would not sustain hPSC survival and growth on-chip but indicated that media-supplementation with Matrigel could improve viability. This was expected, considering Matrigel is known to support hPSCs attachment and self-renewal under standard culture conditions [Lam MT & Longaker MT, 2012; Xu C et al., 2001]. Matrigel is thermo-sensitive and, in concentrations over 3 mg/mL, gelates at temperatures above > 10 °C. Although the resulting gel is much softer than cross-linked alginate, it could potentially be used as an encapsulating matrix for 3-D cellular microarrays.

To test Matrigel as the encapsulating matrix in the microarray platform, a cooling block was fitted to the printing head of the arrayer to avoid clogging of the circuit. DF19 cells were mixed with Matrigel on ice to a final concentration of 5 mg/mL, printed onto PSMA-coated borosilicate glass slides, 60 nL with 300 cells/spot, in eight blocks of 4 × 5 spots, and incubated in either mTeSR1 or TeSR-E8 media with ROCKi. The matrix sustained cell survival and growth for up to seven days (Figure III.2 – a, b), but several problems were detected: 1) the spots smeared easily when the medium was added to the chips, leading to widespread spot detachment at later days; 2) the spots did not confine the cells, which tended to spread

out, thus precluding appropriate quantification (reason for the omission of day 7 in Figure III.2 – b); 3) the matrix seemed to degrade over time and, by day seven, most of the remaining cell colonies resembled a 2-dimensional morphology. The differences observed in Figures III.2 – a) and b) do not so much reflect a higher growth rate in TeSR-E8 but rather substantiate the high variability of the results.

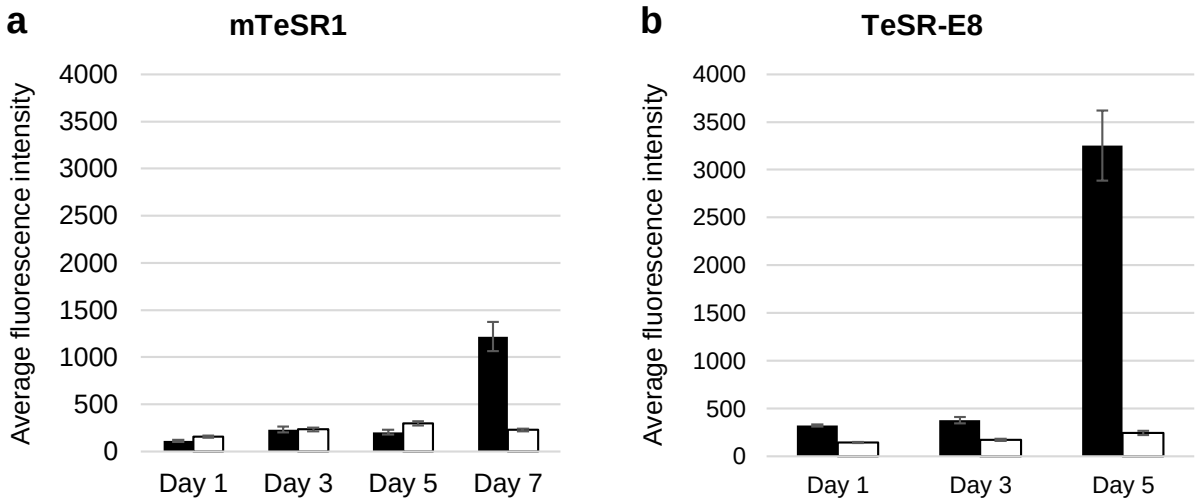

Figure III.2 – Survival and growth of DF19 in Matrigel-based microarrays. The cells were mixed with Matrigel, spotted onto glass slides, and cultured in either **(a)** mTeSR1 or **(b)** TeSR-E8. Viability was assessed by Live/Dead staining at days 1, 3, 5 and 7. Black bars represent calcein fluorescence intensity (live cells) and white bars represent EtHD fluorescence intensity (dead cells). In **(b)**, fluorescence for day 7 could not be quantified due to cells outgrowing the spots. Results presented as mean ± SEM, **(a)** ≥ 7 spots per condition, **(b)** ≥ 20 spots per condition.

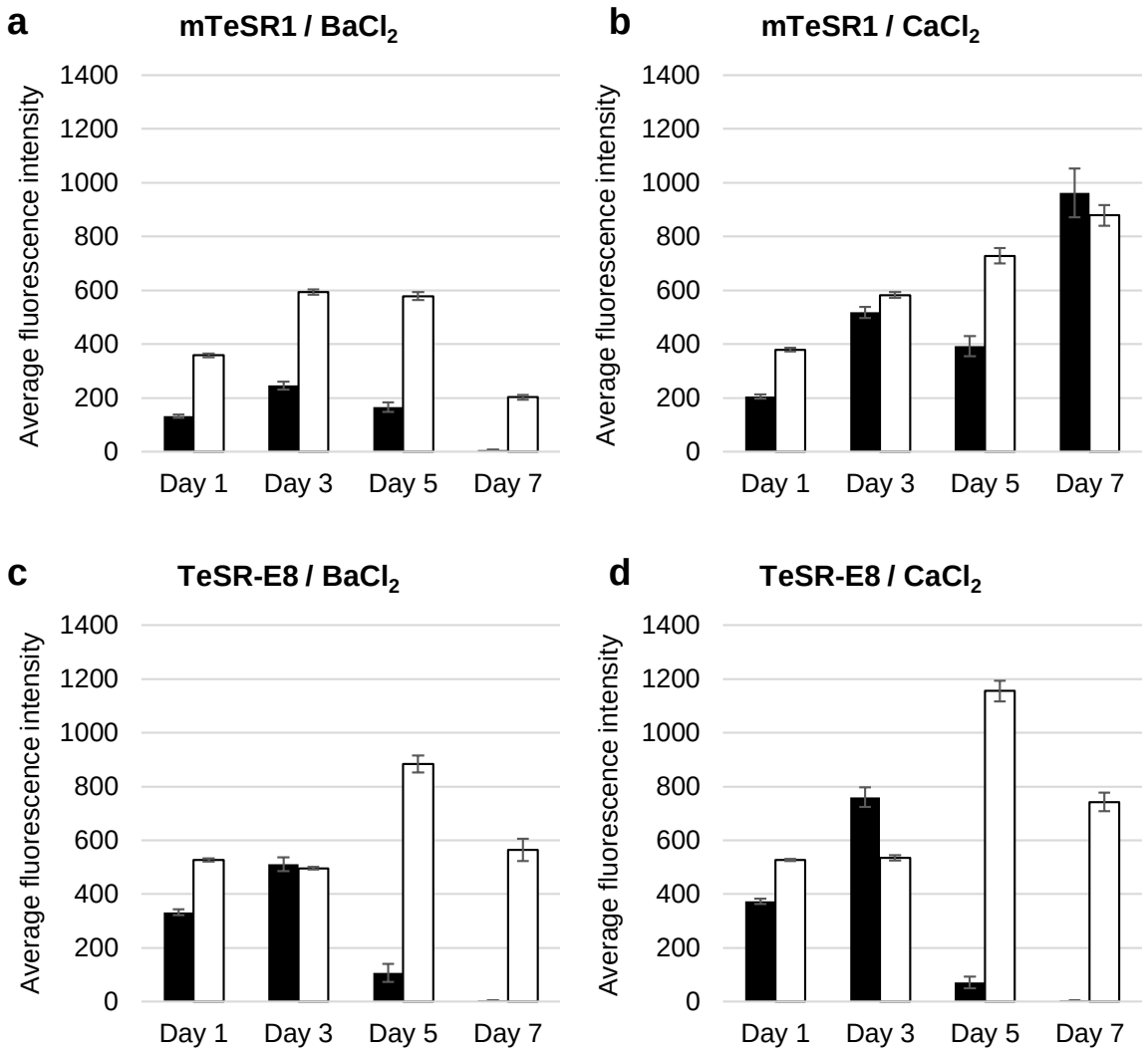

Figure III.3 – Survival and growth of DF19 cells in alginate/Matrigel-based microarrays. The cell suspension was mixed with cold Matrigel and alginate, spotted onto glass slides patterned with either 33 mM $BaCl_2$ **(a, c)** or 50 mM $CaCl_2$ **(b, d)**, and cultured in either mTeSR1 **(a, b)** or TeSR-E8 **(c, d)**, with ROCKi for 72 h. Viability was assessed by Live/Dead staining at days 1, 3, 5, and 7. Black bars represent calcein fluorescence intensity (live cells) and white bars represent EtHD fluorescence intensity (dead cells). Results presented as mean ± SEM, **(a)** 20 spots per condition, **(b)** ≥ 18 spots per condition, **(c)** ≥ 19 spots per condition, and **(d)** 20 spots per condition.

Given that alginate alone did not support hPSC survival and Matrigel alone did not provide sufficient spot stability, it was hypothesized that a mixture of the two components could provide an appropriate encapsulating matrix. DF19 cells were mixed with cold Matrigel and alginate, to final respective concentrations of 5 mg/mL and 1%, and spotted onto PS-MA coated slides pre-patterned with either 33 mM $BaCl_2$ or 50 mM $CaCl_2$. The chips were incubated in either mTeSR1 or TeSR-E8, with ROCKi during the first 72 hours. The mixture of alginate and Matrigel resulted in spots with higher stability that, unlike Matrigel alone, did

not smear or degrade as much over time. In the four conditions tested, the cells survived and proliferated during the first 3 days (Figure III.3 – a - d). After removal of ROCKi however, the viability gradually decreased in most conditions, as evidenced by a reduction in calcein staining and an increase in EtHD. Sustained survival after seven days was observed only in the cells cultured in mTeSR1 and spotted onto $CaCl_2$ (Figure III.3 – b). Overall, the cells spotted onto $CaCl_2$ appear to have had improved survival and to have grown slightly faster during the first three days. The results also suggest that the viability of the cells cultured in TeSR-E8 declined much faster between days 3 and 5, after ROCKi removal, compared to that of the cells in mTeSR1 (Figure III.5 – a). Taken together, the data indicate that calcium-cross-linked alginate may yield higher survival during the first days and that mTeSR1 may improve the survival and growth of this hiPSC line under these specific conditions, after ROCKi removal. In the condition that allowed cell survival through to day 7, it appeared that some cells were outgrowing the spots, similar to what had been observed when Matrigel alone was used as the encapsulation matrix.

It is common to assume that different cell lines may react differently to certain conditions. Given that hiPSC lines may be derived by different reprogramming methods and using different cell sources, cell line-specific parameters such as survival after single-cell dissociation and growth rate under specific conditions are likely to vary. Therefore, a different cell line of hiPSCs was used, to test if the low on-chip viability of DF19 cells was reproducible across hiPSCs. A CBiPS cell suspension was prepared in 5 mg/mL Matrigel and 1% alginate, and spotted onto PS-MA-coated borosilicate glass slides patterned with either 33 mM $BaCl_2$ or 50 mM $CaCl_2$. The chips were incubated in TeSR-E8 medium supplemented with ROCKi for the first 72 hours.

Both conditions tested yielded robust cell survival and growth (Figure III.4 – a, b). While the results suggest that $CaCl_2$ may improve cell survival through to day 3, as observed in previous experiments, by day 5 there were no considerable differences between conditions, regarding both calcein and EtHD fluorescence intensities. Nevertheless, barium-cross-linked alginate appears to have promoted faster growth between days 3 and 5, as indicated by a higher fold-increase in calcein fluorescence (Figure III.5 – b). Consistent with what had been hinted in the experiment with the DF19 cells, the alginate matrix did not prevent cellular migration and growth outside the spots. Because the survival and growth of CBiPS cells were considerably higher compared to those of DF19 cells (Figure III.5 – a, b), the

outgrowth was likewise more evident (Figure III.6 – a, b). On day 7, in both conditions, the maintenance of EtHD is indicative that the concomitant sharp decrease in calcein fluorescence does not represent cell death but rather supports the observation that the cells "escaped" the encapsulation matrix.

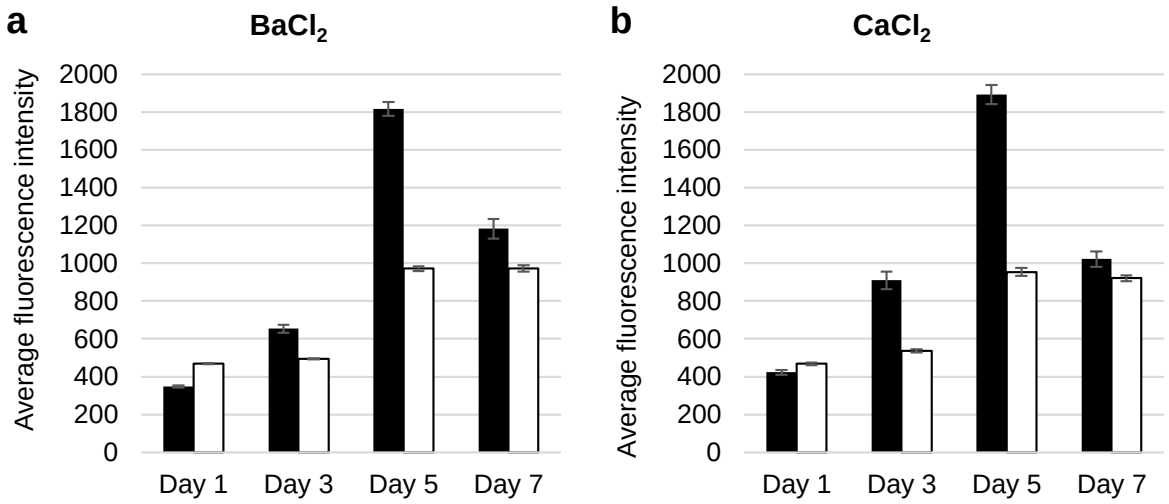

Figure III.4 – Survival and growth of CBiPS cells in alginate/Matrigel-based microarrays. The cells were mixed with Matrigel and alginate and spotted onto glass slides patterned with either **(a)** 33 mM $BaCl_2$ or **(b)** 50 mM $CaCl_2$. The chips were incubated in TeSR-E8 medium with ROCKi for 72 h and viability was assessed by Live/Dead staining at days 1, 3, 5, and 7. Black bars represent calcein fluorescence intensity (live cells) and white bars represent EtHD fluorescence intensity (dead cells). Results presented as mean ± SEM, **(a)** ≥ 41 spots per condition, **(b)** ≥ 24 spots per condition.

Overall, these results show that the use of the described glass-slide based microarray system with alginate, Matrigel, or a combination of the two as 3-D encapsulating matrices, does not allow robust survival nor controlled growth of hPSC. The poor cell viability after alginate encapsulation was enhanced by the addition of Matrigel, but the cellular outgrowth on the surface of the chip in the presence of that compound renders this system unfitting for high-throughput studies with this type of cells.

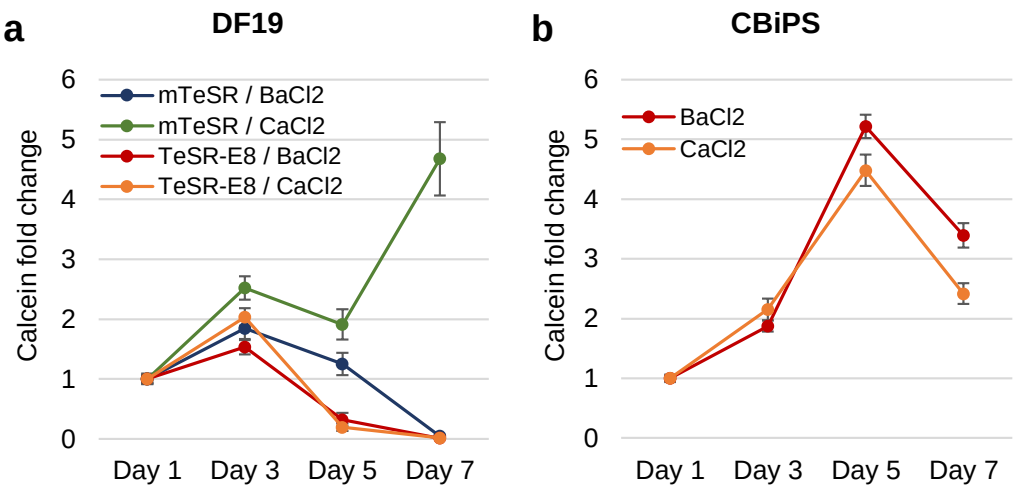

Figure III.5 – Fold-change of calcein fluorescence intensity in DF19 and CBiPS cells, in alginate/Matrigel-based microarrays. **(a)** DF19 cells were spotted onto $BaCl_2$ or $CaCl_2$ and incubated in either mTeSR1 or TeSR-E8. **(b)** CBiPS cells were spotted onto $BaCl_2$ or $CaCl_2$ and incubated in TeSR-E8. Viability was assessed by Live/Dead staining at days 1, 3, 5, and 7. Fold-change relative to day 1 of each condition. Results presented as mean ± SEM. Refer to captions of Figure III.3 and Figure III.4 for the number of replicates per condition.

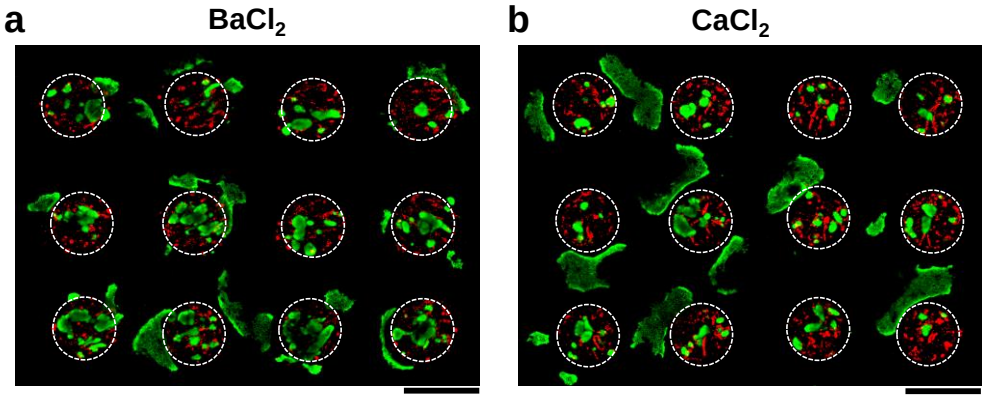

Figure III.6 – CBiPS cellular outgrowth in alginate/Matrigel-based microarrays. Representative images of cells spotted onto either **(a)** $BaCl_2$ or **(b)** $CaCl_2$, on day 7. Green fluorescence (calcein) represents live cells and red fluorescence (EtHD) represents dead cells. White dashed circles represent approximate spot positions. Scale bar = 1 mm.

III.4. Matrigel-based microarray on MicroPillar/MicroWell chips allows hiPS survival and proliferation

Experiments on glass slide microarray chips showed that Matrigel enhanced hiPSC viability and growth. However, the soft nature of the resulting gel led to spot smearing and detachment, while the apparent coating of the surrounding surface led to cellular outgrowth.

A system that allowed less disturbance of the spots and the limiting of the area around them would possibly enable the use of Matrigel as an encapsulating matrix for hPSC 3-D microarrays.

Samsung Electro-Mechanics developed a microarray chip system composed of two polystyrene chips: a MicroPillar chip with 532 (14 × 38) pillars of 0.75 mm diameter, and a complementary MicroWell chip with 532 wells of 1.2 mm diameter (Lee DW et al., 2014). The cells are printed on top of the pillars in the MicroPillar chip, while the medium is printed into the wells in the MicroWell chip. Both chips are then combined so that the encapsulated cells on each pillar are submerged in the medium inside the corresponding microwell. This system allows for a higher degree of multiplex testing than the glass slide-based microarrays, given that more conditions, such as different media, soluble factors, or drugs, can be tested in parallel in a single chip, with true, isolated replicates. Furthermore, it was recently shown to be suitable for Matrigel-based microarrays for toxicological and differentiation studies in neural stem cells (Nierode GJ et al., 2016, 2019).

Preliminary tests showed that the MicroPillar/MicroWell (MPMW) system allowed the survival and growth of hiPSC printed in Matrigel. Protocol optimizations for chip washing and UV-treatment improved the reduction of the spot detachment and sporadic cell death that were initially observed. The system also required the development of a new analysis protocol, using a Cellomics ArrayScan High-content Screening scanner and subsequent image processing for noise/background reduction and fluorescence intensity quantification.

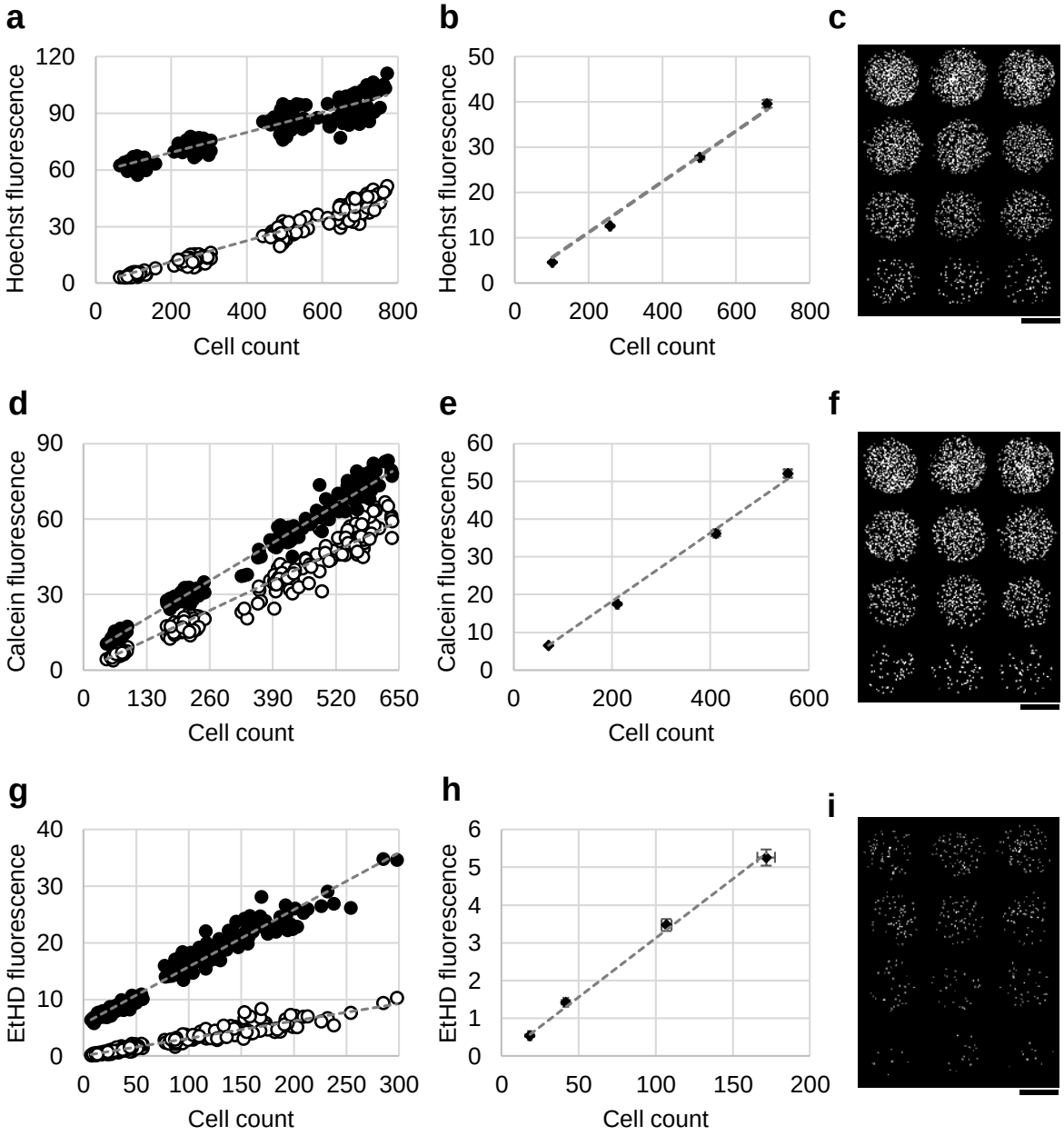

Figure III.7 – Validation of fluorescence quantification as an indicator of hiPSC number on micropillar chips. CBiPS cells were mixed with Matrigel in four different densities and spotted onto MicroPillar chips. One hour after printing, the chips were stained with **(a - c)** Hoechst, **(d - f)** calcein and **(g - i)** EtHD. The chips were scanned and the resulting images were processed for background subtraction and cell counting. **(a, d, g)** show the relation between mean fluorescence intensity and cell count, per pillar, before background subtraction (black dots) and after (white dots). **(b, e, h)** show the relation between mean fluorescence intensity after background subtraction and cell count, averaged per experimental condition, as mean ± SEM. **(c, f, i)** are representative images of each condition after background subtraction, each row corresponding to a different cell density, ordered top-down from higher to lower. Scale bar = 500 µm.

To establish a reliable quantitative method, the relation between mean fluorescence intensity and cell number was assessed. Suspensions of CBiPS cells with different densities (2.5×10^6 cells/mL or 150 cells/spot; 5×10^6 cells/mL or 300 cells/spot; 1×10^7 cells/mL or 600 cells/spot, and 1.5×10^7 cells/mL or 900 cells/spot) were prepared in 5 mg/mL Matrigel, spotted onto a MicroPillar chip and incubated in TeSR-E8 medium with ROCKi for 1 hour, followed by Live/Dead and Hoechst staining. The chip was dried and scanned, and the images processed. A simple automatic algorithm was used to determine an approximate cell number per pillar, based on fluorescence intensity peaks. The results showed that the estimated cell number and the mean fluorescence intensity of each dye were linearly correlated, both before and after background subtraction (Figure III.7 – a - i). Background subtraction allowed the reduction of replicate absolute dispersion, as indicated by the standard deviation of the fluorescence intensity of each condition, by an average of 33.9% in the case of Hoechst, 0.3% in calcein and 55.9% in EtHD (Figure III.7 – a, d, g). When the data-points were averaged per condition, the linear regressions of fluorescence intensity as a function of cell number yielded $R^2 > 0.99$ in all three fluorescence channels (Figure III.7 - b, e, h), thus validating the use of mean fluorescence intensity as an indicator of cell number. This experiment further showed that CBiPS cells retained approximately 76% viability one hour after printing, but additional experimental replicates will be required to confirm this result.

To investigate the viability and growth on-chip of hiPSC over time, CBiPS cells were printed in Matrigel, 300 cells/spot, and incubated in either mTeSR1 or TeSR-E8 media, with ROCKi for the first 48 hours. Because spot degradation at later days and inconsistent cell survival were observed in preliminary experiments, media supplementation with 100 µg/mL Matrigel, 10 ng/mL FGF, or both, were tested to evaluate the effects on spot stability and dispersion of initial survival, respectively. Staining with Live/Dead and Hoechst was performed on days 1, 3, 5, and 7, and the resulting images were processed for background subtraction and fluorescence quantification. Cellular viability was analyzed using a simple algorithm in MATLAB, by iteratively estimating two factors that yielded the least difference between the sum of the fluorescence intensities of calcein and ethidium homodimer and the intensity of Hoechst, as described in Chapter II.

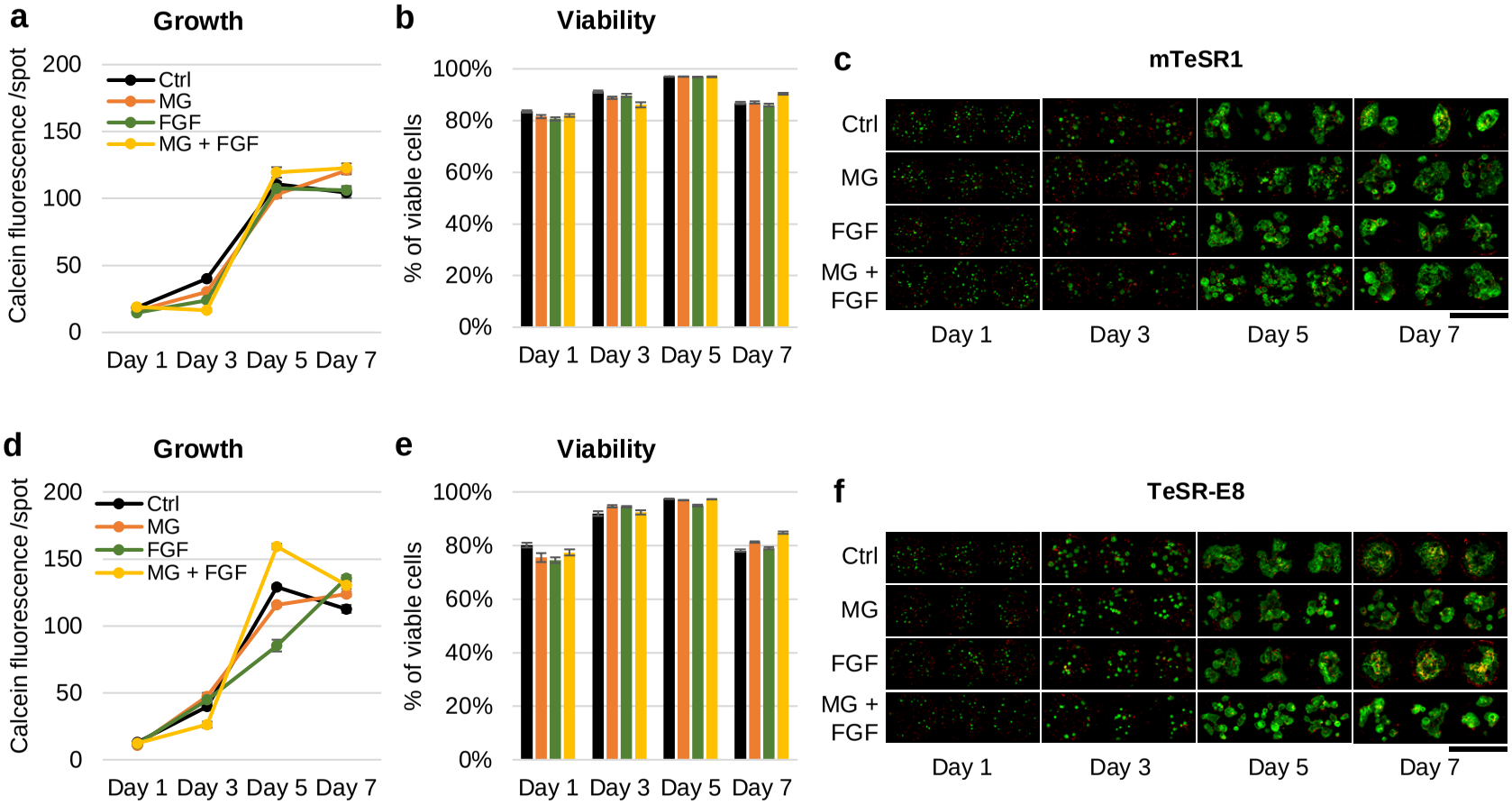

Figure III.8 - Growth and viability of CBiPS cells in Matrigel-based microarrays, on the MicroPillar/MicroWell chip system. Cells were mixed with Matrigel, spotted onto MicroPillar chips, and incubated in either **(a - c)** mTeSR1 or **(d - f)** TeSR-E8 media. Media supplementation with 100 µg/mL Matrigel (MG) and/or 10 ng/mL FGF was tested in parallel with media alone (Ctrl). Growth and viability were assessed by Live/Dead and Hoechst staining on days 1, 3, 5, and 7. **(a, d)** show the evolution of calcein staining over time, indicative of cellular proliferation in the four conditions tested. **(b, e)** show the evolution of estimated cellular viability over time. All quantitative results are presented as mean ± SEM, > 35 spots per condition. **(c, f)** are representative images of each condition on each time-point. Green fluorescence represents viable cells (calcein) and red represents dead cells (EtHD). Scale bar = 1 mm.

All the conditions tested allowed the growth of hiPSC for 7 days (Figure III.8 – a - f). In mTeSR1 medium, the cells generally displayed a lag phase of approximately two to three days, evidenced by the residual increase in calcein fluorescence (Figure III.8 – a) and estimated viability (Figure III.8 – b) between days 1 and 3, and reached a plateau at around day 5. TeSR-E8 medium, on the other hand, appears to have reduced the lag phase, with over 3-fold increases in calcein fluorescence in all conditions except in Matrigel and FGF supplementation (Figure III.8 – d), and over 10% relative increases in estimated viability in all conditions (Figure III.8 – e). All conditions appear to reach a plateau on day 5, except TeSR-E8 with FGF supplementation which, unexpectedly, displayed a more linear growth pattern. Cells grown in TeSR-E8 with Matrigel and FGF supplementation showed a steeper increase in calcein fluorescence between days 3 and 5, followed by a decrease at day 7, evidencing limited growth capacity within the 3-D matrix and increased cell death above a certain threshold. Consistent with this, the estimated viability decreased considerably between days 5 and 7. Nevertheless, on day 7, the cells cultured in mTeSR1 supplemented with Matrigel and Matrigel plus FGF displayed a higher fluorescence intensity than the conditions without Matrigel, suggesting that it may enhance the capacity of the encapsulation matrix to preserve cellular proliferation. In terms of matrix stability, Matrigel supplementation appeared to delay the degradation of the spots, as indicated by the rounder cell colonies on day 7 in the conditions containing this supplement, opposed to the flatter colonies in the conditions without it. FGF supplementation did not appear to produce any effect in terms of cell survival. Further experiments will be needed to confirm these results.

The proliferation of hiPSC on-chip does not necessarily imply self-renewal, as these cells are prone to spontaneous differentiation. To evaluate the maintenance of pluripotency on-chip, CBiPS cells were spotted onto a MicroPillar chip, incubated in TeSR-E8 and, after seven days, stained for pluripotency markers OCT4, SOX2, or SSEA4, by immunofluorescence. Although co-expression was not analyzed, all the pillars stained positive for marker expression, suggesting that pluripotency is maintained on-chip at least through to day 7 (Figure III.9 – a - c). Differentiated cells were, nevertheless, detected in some pillars by lack of marker expression, although they generally represented a small fraction of the total number of cells.

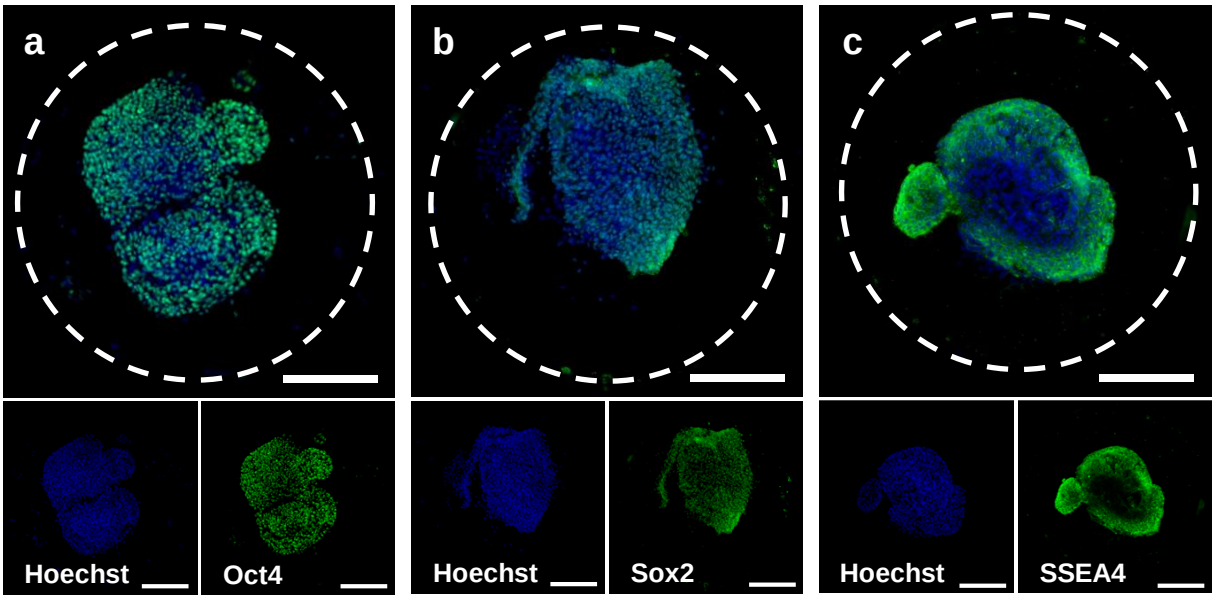

Figure III.9 – Pluripotency maintenance of CBiPS cells in Matrigel-based microarrays, on the MicroPillar/MicroWell chip system. Cells were mixed with Matrigel, spotted onto the MicroPillar chip and incubated in TeSR-E8 medium for seven days. Pluripotency was assessed by immunostaining for (a) OCT4, (b) SOX2 and (c) SSEA4, displayed in green. Cells were counterstained with Hoechst, displayed in blue. Dashed circumferences represent approximately the borders of the micropillars. Scale bar = 200 µm.

III.5. Exploratory testing of combinatorial media supplementation on pluripotency maintenance

Considering that the MicroPillar/MicroWell system was able to sustain hPSC growth and pluripotency maintenance in regular culturing conditions, its functionality as a screening platform was assessed. CBiPS cells were printed onto MicroPillar chips in Matrigel, 300 cells per spot, following the procedure adopted in previous experiments, but combinations of different soluble compounds and growth factors were added to TeSR-E8 medium, specifically a) Matrigel, 20 µg/mL, b) heparin, 10 µg/mL, c) hyaluronic acid, 20 µg/mL, d) FGF2, 10 ng/mL, and e) epidermal growth factor (EGF), 10 ng/mL. All different possible combinations were tested, along with an untreated control condition, in a total of 32 experimental conditions. The cells were cultured for seven days under these conditions, with daily media changes, after which the chip was dried and stained for OCT4 expression by immunofluorescence.

While the results did not provide any marked differences between experimental conditions, there is a suggestion that some of the combinations may have led to the loss of

pluripotency in some of the cells, with a decrease in OCT4-specific fluorescence of about 20% relative to the untreated control (Figure III.10). The combinations of hyaluronic acid with FGF or with EGF were the only that suggested an increase in OCT4 expression, although it was limited to about 5%.

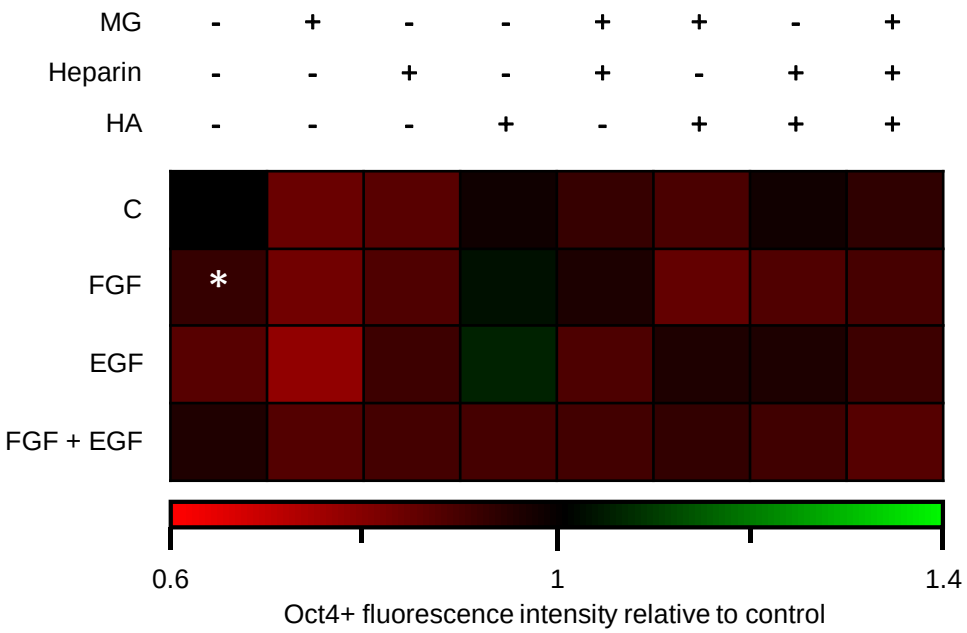

Figure III.10 – Effect of combinatorial medium supplementation on the expression of OCT4. CBiPS cells were mixed with Matrigel spotted onto MicroPillar chip and incubated in TeSR-E8 medium with combinations of Matrigel 20 µg/mL (MG), heparin 10 µg/mL, hyaluronic acid 20 µg/mL (HA), FGF2 10 ng/mL (FGF) and epidermal growth factor 10 ng/mL (EGF). Unsupplemented medium was used as control (C), and relative OCT4 expression was assessed by immunofluorescence after seven days. The heatmap represents the OCT4-specific average fluorescence intensity, normalized with Hoechst, with red indicating lower fluorescence and green indicating higher fluorescence, relative to the control. n >=3 in all conditions except the one marked with *, where n = 2.

III.6. Discussion and main conclusions

The development of a three-dimensional cellular microarray platform capable of performing screening tests on hPSCs would, in theory, allow the high-throughput generation of quantitative data regarding cell proliferation, viability, and differentiation upon different combinations of stimuli. This study describes several of the strategies employed to develop such a platform and the subsequent tests performed to validate its usefulness.

The first strategy consisted of a glass-based microarray with the encapsulation of cells in alginate. This platform had been previously shown to allow the growth and differentiation of mouse embryonic stem cells [(Fernandes TG et al., 2010)]. The tests carried out using hESC line H9 and hiPSC line DF19, however, were not successful as it was not possible to retain cell viability past the initial 24 hours. Human and mouse embryonic stem cells, although sharing the same designation, require different conditions in culture and it is now fairly established that each represents a different stage of pluripotency [(Zhao H & Jin Y, 2017; Nichols J & Smith AG, 2009)]. One striking difference is that mESCs tolerate single-cell dissociation, while this process promotes apoptosis in hESCs. As the microarraying protocol used required single-cell dissociation, a ROCK inhibitor was added to the culture medium as an attempt to mitigate the apoptotic effect [(Watanabe K et al., 2007)]. However, all the conditions tested resulted in massive cell death. It is possible that alginate, being a relatively inert matrix, does not allow the single cells to establish any connections, either with any extracellular matrix components or with other cells, thus promoting cell death. Although alginate has been previously described as an effective encapsulation matrix for hPSCs, the cells were then encapsulated as aggregates [(Serra M et al., 2011; Siti-Ismail N et al., 2008)]. This limitation is further supported by the fact that the addition of dilute Matrigel to the culture media improved, although only slightly, the cell viability after 24 hours.

The second strategy tested involved the use of Matrigel as an encapsulating matrix. Matrigel has been extensively shown to support the attachment and self-renewal of hPSCs in traditional culture platforms [(Chen KG et al., 2014)] and, consistent with this, it allowed cell survival and proliferation of encapsulated DF19 cells on the microarray. However, due to its softer and labile nature, other limitations were identified, such as spot degradation and detachment, and evasion of cells from the spots and onto the surrounding glass surface. These issues impact both the robustness and accuracy of the microarray as a screening platform due to the loss of replicates and the lack of confinement of the cells. Furthermore, the fast degradation of the matrix resulted in a cell phenotype much more resembling of a 2-dimensional culture by day 7.

In an attempt to surpass these limitations, a mixture of alginate and Matrigel was tested, using different growth media and salts for alginate cross-linking. The use of mTeSR1 medium with calcium-cross-linked alginate was the only of the tested conditions that enabled the survival of DF19 cells on day 7, with an approximate 5-fold expansion, while both calcium-

and barium-cross-linked alginate with TeSR-E8 allowed the expansion of CBiPS cells. The use of calcium-cross-linked alginate appeared to outperform barium in both media during the initial 5 days, suggesting that the cells may favor the softer nature of the calcium-generated matrix and/or that the barium might have a residual toxic effect. It is also interesting to note that, although TeSR-E8 medium did not support DF19 cell survival after the removal of ROCK inhibitor, it appeared to yield higher initial viability after printing. While the issue of cell survival was solved, this strategy did not prevent cell evasion from the spots. One of the strongest arguments in favor of using cellular microarrays is the possibility to test many independent replicates in parallel. The lack of cell containment compromises the independence and integrity of each replicate and is, therefore, a highly detrimental limitation.

The final strategy tested was a MicroPillar/MicroWell chip system composed of two complementary chips. This system improved on the previous two by allowing complete independence between replicates as well as higher throughput in terms of parallel conditions, since each replicate is in its independent well. Using Matrigel as the encapsulating matrix, this system enabled robust cell survival and expansion to about 5-fold after the first 5 days. From day 5 to day 7, the results suggest that the cells stopped expanding, although another possible explanation is that Matrigel degradation may have led to poor cell retainment. Despite slight timepoint differences, both mTeSR1 and TeSR-E8 media yielded similar results in terms of cell expansion and cell viability. Immunostaining for pluripotency markers revealed that CBiPS cells retained the expression of OCT4 and SSEA-4 after seven days on the microarray in TeSR-E8 medium, thus suggesting pluripotency maintenance. For further evidence, this expression should be quantified in future experiments, as well as the co-expression of several markers, since the presence of differentiated cells was also detected.

The functionality of the system as a screening platform was evaluated by testing OCT4 expression after incubation with different combinations of growth factors and extracellular matrix compounds. The tested compounds included FGF2, EGF, Matrigel, heparin, and hyaluronic acid. FGF2 is one of the main components of hPSC culture media and has been shown to promote pluripotency maintenance (Levenstein ME et al., 2006). On the other hand, data on the effect that EGF might have on pluripotency maintenance is very scarce. Both heparin (Furue MK et al., 2008) and hyaluronic acid (Gerecht S et al., 2007) have also been associated with pluripotency maintenance, although heparin has recently been reported to enhance cardiac specification under differentiation conditions (Lin Y et al., 2017). Although the results obtained were generally

inconclusive, there were some indications that the addition of Matrigel and EGF to the growth medium might lead to reduced expression of OCT4, whereas the supplementation with hyaluronic acid may enhance it. The inconsistent results are indicative that further optimization is required, particularly on the immunostaining protocol. Additional experiments will be necessary to validate the outcomes.

Overall, this study described the testing of several platforms and strategies, and the development of a functional high-throughput cellular microarray system for studies on human pluripotent stem cells, with Matrigel as an encapsulating matrix. While the system is not completely optimized, these results provide a solid base for future studies.

III.7. References

Baker BM & Chen CS (2012). Deconstructing the Third Dimension - How 3D Culture Microenvironments Alter Cellular Cues. *Journal of Cell Science* 125, 3015–3024. **DOI:** 10.1242/jcs.079509.

Chen KG, Mallon BS, McKay RDG & Robey PG (2014). Human Pluripotent Stem Cell Culture: Considerations for Maintenance, Expansion, and Therapeutics. *Cell Stem Cell* 14, 13–26. **DOI:** 10.1016/j.stem.2013.12.005.

Fernandes TG, Kwon S-J, Lee M-Y, Clark DS, Cabral JMS & Dordick JS (2008). On-Chip, Cell-Based Microarray Immunofluorescence Assay for High-Throughput Analysis of Target Proteins. *Analytical Chemistry* 80, 6633–6639. **DOI:** 10.1021/ac800848j.

Fernandes TG, Diogo MM, Clark DS, Dordick JS & Cabral JMS (2009). High-Throughput Cellular Microarray Platforms: Applications in Drug Discovery, Toxicology and Stem Cell Research. *Trends in Biotechnology* 27, 342–349. **DOI:** 10.1016/j.tibtech.2009.02.009.

Fernandes TG, Kwon S-J, Bale SS, Lee M-Y, Diogo MM, Clark DS, Cabral JMS & Dordick JS (2010). Three-Dimensional Cell Culture Microarray for High-Throughput Studies of Stem Cell Fate. *Biotechnology and Bioengineering* 106, n/a-n/a. **DOI:** 10.1002/bit.22661.

Furue MK, Na J, Jackson JP, Okamoto T, Jones M, Baker D, Hata R-I, Moore HD, Sato JD & Andrews PW (2008). Heparin Promotes the Growth of Human Embryonic Stem Cells in a Defined Serum-Free Medium. *Proceedings of the National Academy of Sciences* 105, 13409–13414. **DOI:** 10.1073/pnas.0806136105.

Gerecht S, Burdick JA, Ferreira LS, Townsend SA, Langer R & Vunjak-Novakovic G (2007). Hyaluronic Acid Hydrogel for Controlled Self-Renewal and Differentiation of Human Embryonic Stem Cells. *Proceedings of the National Academy of Sciences* 104, 11298–11303. **DOI:** 10.1073/pnas.0703723104.

Hazeltine LB, Selekman JA & Palecek SP (2013). Engineering the Human Pluripotent Stem Cell Microenvironment to Direct Cell Fate. *Biotechnology Advances* 31, 1002–1019. **DOI:** 10.1016/j.biotechadv.2013.03.002.

Hughes CS, Postovit LM & Lajoie GA (2010). Matrigel: A Complex Protein Mixture Required for Optimal Growth of Cell Culture. *Proteomics* 10, 1886–1890. **DOI:** 10.1002/pmic.200900758.

Klimanskaya I, Rosenthal N & Lanza R (2008). Derive and Conquer: Sourcing and Differentiating Stem Cells for Therapeutic Applications. *Nature Reviews Drug Discovery* 7, 131–142. **DOI:** 10.1038/nrd2403.

Kumar N, Richter J, Cutts J, Bush KT, Trujillo C, Nigam SK, Gaasterland T, Brafman D & Willert K (2015). Generation of an Expandable Intermediate Mesoderm Restricted Progenitor Cell Line from Human Pluripotent Stem Cells. *ELife* 4. **DOI:** 10.7554/eLife.08413.

Lam MT & Longaker MT (2012). Comparison of Several Attachment Methods for Human IPS, Embryonic and Adipose-Derived Stem Cells for Tissue Engineering. *Journal of Tissue Engineering and Regenerative Medicine* 6, s80–s86. **DOI:** 10.1002/term.1499.

Lee DW, Choi Y, Seo YJ, Lee M, Jeon SY, Ku B, Kim S, Yi SH & Nam D (2014). High-Throughput Screening (HTS) of Anticancer Drug Efficacy on a Micropillar/Microwell Chip Platform. *Analytical Chemistry* 86, 535–542. **DOI:** 10.1021/ac402546b.

Lee M-Y, Kumar RA, Sukumaran SM, Hogg MG, Clark DS & Dordick JS (2008). Three-Dimensional Cellular Microarray for High-Throughput Toxicology Assays. *Proceedings of the National Academy of Sciences* 105, 59–63. **DOI:** 10.1073/pnas.0708756105.

Levenstein ME, Ludwig TE, Xu R-H, Llanas RA, VanDenHeuvel-Kramer K, Manning D & Thomson JA (2006). Basic Fibroblast Growth Factor Support of Human Embryonic Stem Cell Self-Renewal. *Stem Cells* 24, 568–574. **DOI:** 10.1634/stemcells.2005-0247.

Lin Y, Linask KL, Mallon B, Johnson K, Klein M, Beers J, Xie W, Du Y, Liu C, Lai Y *et al.* (2017). Heparin Promotes Cardiac Differentiation of Human Pluripotent Stem Cells in Chemically Defined Albumin-Free Medium, Enabling Consistent Manufacture of Cardiomyocytes. *STEM CELLS Translational Medicine* 6, 527–538. **DOI:** 10.5966/sctm.2015-0428.

Meli L, Jordan ET, Clark DS, Linhardt RJ & Dordick JS (2012). Influence of a Three-Dimensional, Microarray Environment on Human Cell Culture in Drug Screening Systems. *Biomaterials* 33, 9087–9096. **DOI:** 10.1016/j.biomaterials.2012.08.065.

Meli L, Barbosa HSC, Hickey AM, Gasimli L, Nierode G, Diogo MM, Linhardt RJ, Cabral JMS & Dordick JS (2014). Three Dimensional Cellular Microarray Platform for Human Neural Stem Cell Differentiation and Toxicology. *Stem Cell Research* 13, 36–47. **DOI:** 10.1016/j.scr.2014.04.004.

Mørch ÝA, Donati I & Strand BL (2006). Effect of Ca^{2+}, Ba^{2+}, and Sr^{2+} on Alginate Microbeads. *Biomacromolecules* 7, 1471–1480. **DOI:** 10.1021/bm060010d.

Nichols J & Smith AG (2009). Naive and Primed Pluripotent States. *Cell Stem Cell* 4, 487–492. **DOI:** 10.1016/j.stem.2009.05.015.

Nierode GJ, Perea BC, McFarland SK, Pascoal JF, Clark DS, Schaffer D V & Dordick JS (2016). High-Throughput Toxicity and Phenotypic Screening of 3D Human Neural Progenitor Cell Cultures on a Microarray Chip Platform. *Stem Cell Reports* 7, 970–982. **DOI:** 10.1016/j.stemcr.2016.10.001.

Nierode GJ, Gopal S, Kwon P, Clark DS, Schaffer DV & Dordick JS (2019). High-Throughput Identification of Factors Promoting Neuronal Differentiation of Human Neural Progenitor Cells in Microscale 3D Cell Culture. *Biotechnology and Bioengineering* 116, 168–180. **DOI:** 10.1002/bit.26839.

Rothbauer M, Charwat V & Ertl P (2016). Cell Microarrays for Biomedical Applications. In: Microarray Technology, P.C. Li, A. Sedighi, and L. Wang, eds. (Springer New York), pp. 273–291.

Serra M, Correia C, Malpique R, Brito C, Jensen J, Bjorquist P, Carrondo MJT & Alves PM (2011). Microencapsulation Technology: A Powerful Tool for Integrating Expansion and Cryopreservation of Human Embryonic Stem Cells. *PLoS ONE* 6, e23212. **DOI:** 10.1371/journal.pone.0023212.

Siti-Ismail N, Bishop AE, Polak JM & Mantalaris A (2008). The Benefit of Human Embryonic Stem Cell Encapsulation for Prolonged Feeder-Free Maintenance. *Biomaterials* 29, 3946–3952. **DOI:** 10.1016/j.biomaterials.2008.04.027.

Watanabe K, Ueno M, Kamiya D, Nishiyama A, Matsumura M, Wataya T, Takahashi JB, Nishikawa S, Nishikawa S, Muguruma K & Sasai Y (2007). A ROCK Inhibitor Permits Survival of Dissociated Human Embryonic Stem Cells. *Nature Biotechnology* 25, 681–686. **DOI:** 10.1038/nbt1310.

Xu C, Inokuma MS, Denham J, Golds K, Kundu P, Gold JD & Carpenter MK (2001). Feeder-Free Growth of Undifferentiated Human Embryonic Stem Cells. *Nature Biotechnology* 19, 971–974. **DOI:** 10.1038/nbt1001-971.

Zhao H & Jin Y (2017). Signaling Networks in the Control of Pluripotency. *Current Opinion in Genetics and Development* 46, 141–148. **DOI:** 10.1016/j.gde.2017.07.013.

IV. Characterization of human pluripotent stem cell spheroids cultured in static suspension

IV.1. Introduction

Over the last 20 years, the great majority of the studies performed on human pluripotent stem cells relied on 2-dimensional culture platforms. While these provide a simplistic model with better control of variables and less confounding effects, they may not be fully suited to recapitulate the 3-dimensional physiological environment, particularly regarding cell-cell contacts, soluble factor gradients and biomechanical cues [(Baker BM & Chen CS, 2012)].

In 2000, Itskovitz-Eldor et al. reported that hESCs were able to aggregate when cultured in suspension and to generate progeny from all three germ layers as embryoid bodies [(Itskovitz-Eldor J et al., 2000)]. Ten years later, Steiner et al. described a method for the culture of hPSCs as spheroids in suspension, with the maintenance of pluripotency [(Steiner D et al., 2010)]. Culture of hPSCs as spheroids has since been extensively reported as a 3-dimensional alternative to adherent models, as well as an efficient scalable method for expansion [(Lei Y & Schaffer D V, 2013; Wang Y et al., 2013; Chen VC et al., 2012)]. However, not many studies focused on the actual characterization of hiPSC cultured as aggregates nor on how these cells respond to external stimuli in comparison with cells cultured in 2-dimensions. The specification and optimization of culture and differentiation conditions is a critical step towards the use of pluripotent stem cells in clinical applications. Consequently, the extensive characterization of *in vitro* models is essential to ensure their robustness and significance.

In this chapter, hiPSC spheroids were characterized in terms of morphology and gene expression over time. Furthermore, the effect of different pre-detachment cell densities was assessed in terms of spheroid number and morphology. Finally, the effect of some of the conditions tested on the microarray platform described in Chapter III was evaluated in both 2-D and 3-D cultured cells.

IV.2. Characterization of hiPSC spheroids growth under static defined conditions

In order to characterize the growth of hPSCs spheroids in terms of cell number, CBiPS cells were incubated with ROCK inhibitor Y-27632 (ROCKi) for 1 hour before detachment and single-cell dissociation using Accutase, resuspended in Essential 8™ (E8) medium containing

ROCKi and plated on Ultra-Low attachment plates, 1×10^6 cells per well, or on Matrigel-coated tissue culture-treated plates, 2×10^5 cells per well. The number of cells was assessed daily. While some cell death was observed on day 1 in cells cultured on Matrigel, these cells had recovered by day 2 and displayed exponential growth until day 4, plateauing on day 6 (see Figure IV.1 – a, orange dataset). On the other, the death of cells cultured in suspension was much more pronounced during the first two days, with the exponential phase appearing to start only by day 4.

The size and morphology of hiPSC spheroids were evaluated by image analysis. Microphotographs of the cellular aggregates were taken between days two and seven, processed using MATLAB and the diameter was calculated based on the section area. In terms of size, the spheroids displayed an approximately linear increase in diameter between days 2 and 6, with an apparent plateauing at day 7, with a median of 183 µm ± 21 µm (Figure IV.1 – b). The kernel density estimation of the diameter distributions corroborated the consistent growth with clearly defined peaks, although suggesting an increase in size dispersion between days 2 and 5, followed by concentration until day 7 when 90% of the estimated density was between 139 µm and 236 µm (Figure IV.1 – c - f). In terms of morphology, the spheroids' cross-sections displayed a consistent circularity throughout the experiment, which correlates with edge smoothness. The pronounced spike on day 3 may be best explained by sampling error (Figure IV.1 – g). As for eccentricity, which refers to the difference between major and minor axes of the spheroids' cross-sections, there was a median decrease of 42.3% between days 2 and 7, suggesting that the aggregates became more spherical as days progressed (Figure IV.1 – h).

IV.3. Expression of pluripotency and differentiation markers in hiPSC spheroids

Several studies have previously shown that hiPSCs cultured as spheroids under appropriate conditions retain the expression of pluripotency markers, as well as the ability to differentiate into all three embryonic lineages (Li X et al., 2018; Chen VC et al., 2012; Zweigerdt R et al., 2011; Steiner D et al., 2010). However, there is a limited number of reports focusing on the actual impact that

this culture method may have on the expression of genetic markers versus traditional monolayer culture.

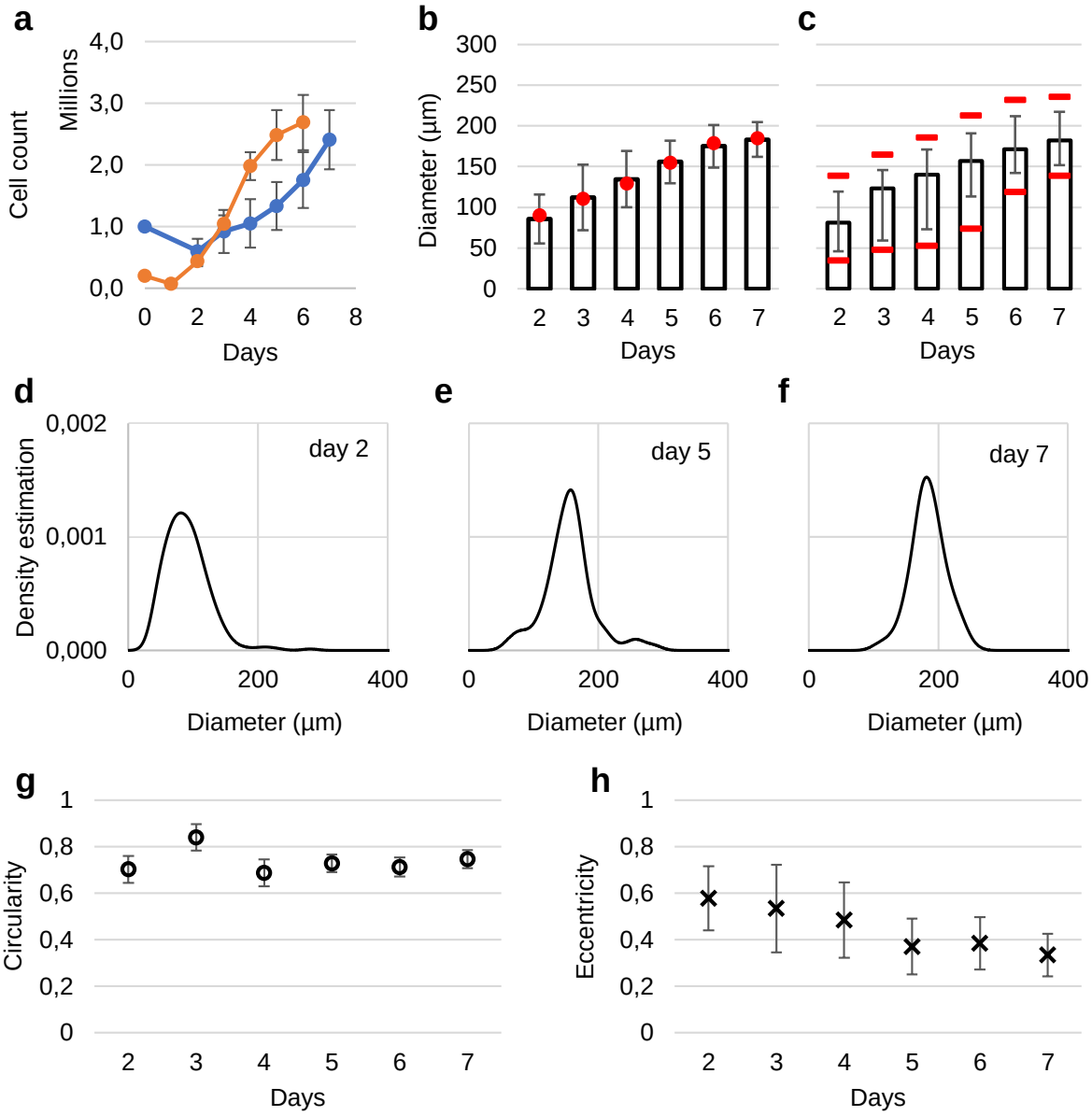

Figure IV.1 – Characterization of hPSC growth as spheroids in suspension. **(a)** Daily cell count of CBiPS cells cultured on either Matrigel-coated tissue culture plates (orange) or low-attachment plates (blue). Results presented as mean ± SD, n ≥ 3 except datapoint for day 1 of cells cultured on Matrigel, where n = 1. **(b – h)** Variation of CBiPS spheroid diameter distribution and morphology over time. Basic statistical estimators are presented in **(b)**, where the bars represent the median, the red dots represent the mean and the error bars represent the median absolute deviation (MAD). The key features of kernel density estimation (KDE) are presented in **(c)** where the bars represent the diameter at the density peak, error bars represent the minimum diameter range that contains 75% of density, and red bars represent the minimum diameter range that contains 90% of density. Representation of kernel density estimation (KDE) of CBiPS diameter distribution on **(d)** day 2, **(e)** day 5, and **(f)** day 7. KDE with Gaussian kernel, bandwidth = 12. **(g)** presents the circularity of spheroids, median ± MAD. **(h)** presents the eccentricity of spheroids, median ± MAD. ≥144 cellular aggregates per data point.

To evaluate the impact of 3-D culture on the expression of key genetic markers, CBiPS cells were incubated with ROCKi for 1 hour, detached and dissociated to single cells using Accutase, and replated on Ultra-Low attachment culture plates. The cells were cultured in E8 medium with ROCKi during the first 24 hours, with partial medium exchange daily. Samples were collected on days 0, 1, 3, 5, and 7, and the expression of genetic markers on spheroids was quantified using quantitative PCR (qPCR).

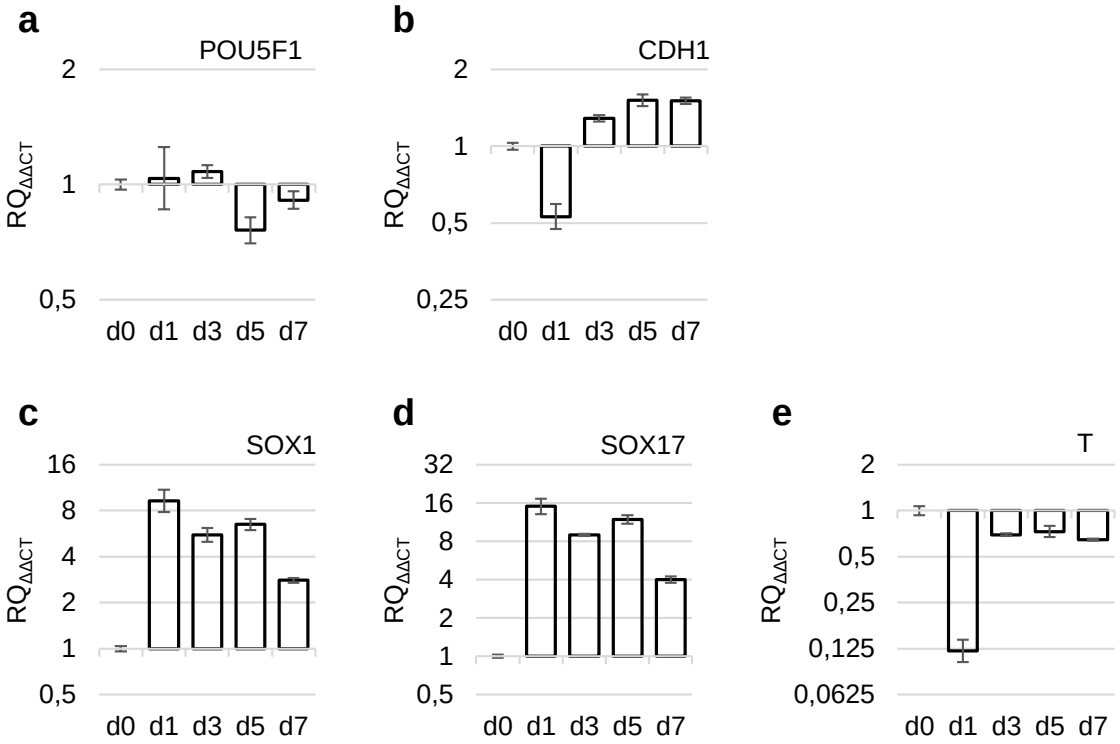

Figure IV.2 – Expression of pluripotency and differentiation genetic markers in hiPSC cultured as spheroids. CBiPS cells were plated as single cells on low-attachment plates and cultured in E8 medium with ROCKi during the first 24 hours. Quantitative PCR analysis was run on samples from days 0, 1, 3, 5, and 7, using GAPDH as the internal control, to evaluate the relative expression of **(a)** POU5F1 (OCT4), **(b)** CDH1 (E-cadherin), **(c)** SOX1, **(d)** SOX17, and **(e)** T (Brachyury). The expression on day 0 was used as the experimental control. Results presented as the relative quantification (RQ) of base 2 of the ΔΔCT between day 0 and days 1-7 ± SE. Experimental replicates ≥ 2 per condition.

The results suggest that the expression of POU5F1, the gene for OCT4, was not very much affected by the culture method, with ΔΔCT variations of less than 25% relative to day 0 (Figure IV.2 – a). As for CDH1, which codes for E-cadherin, there was a sharp 47% decrease on day 1, followed by an increase and plateauing on day 7, with an expression about 50% higher more than at day 0 (Figure IV.2 – b). Although the differences in the expression of the

pluripotency markers tested were not very pronounced, there were considerable changes in terms of the expression of differentiation markers. The expression of SOX1, an early marker of ectodermal differentiation, was over eight times higher on day 1 than on day 0. Throughout the experiment, the expression decreased to about 280% of the control by day 7 (Figure IV.2 – c). SOX17, a genetic marker for definitive endoderm precursors, had an expression pattern very similar to SOX1, although higher – on day 1 it was overexpressed by 15-fold relative to day 0, followed by a gradual decrease down to 4-fold by day 7 (Figure IV – d). As for the expression of mesendodermal differentiation marker T, the results indicated a sharp decrease on day 1, at 12% of the control, followed by an increase to about 65% on day 7 (Figure IV.2 – e).

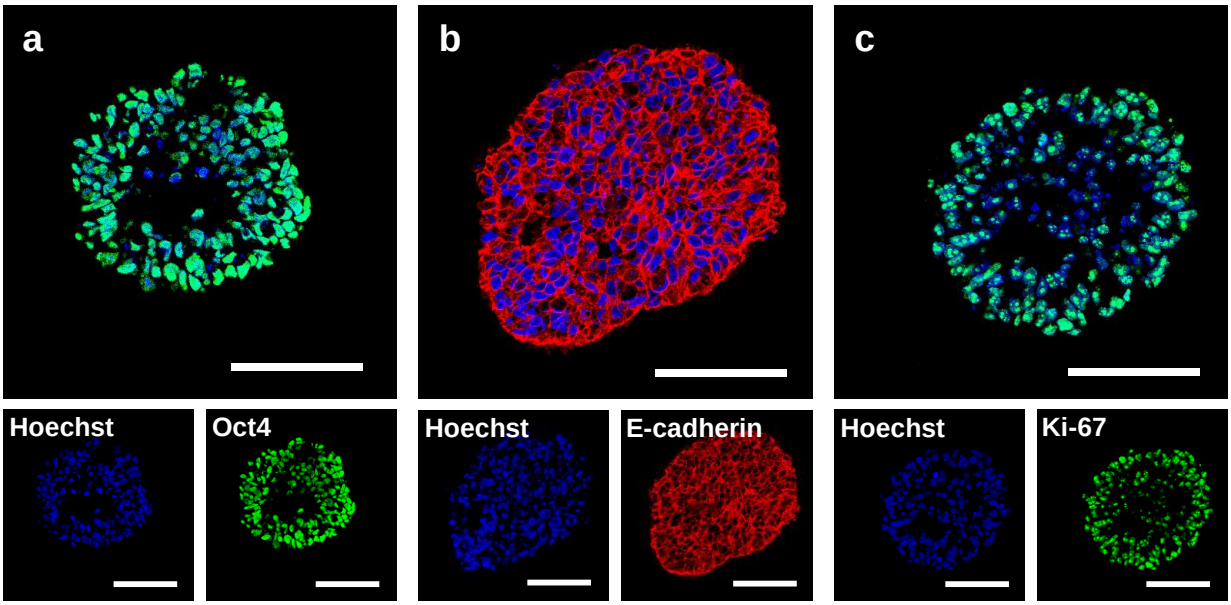

Figure IV.3 – Expression of pluripotency and cell proliferation markers in hiPSC cultured as spheroids. CBiPS were plated on low-attachment plates and cultured as aggregates in E8 medium for 7 days. Aggregate sections were immunostained for **(a)** OCT4 (green), **(b)** E-cadherin (red) or **(c)** Ki-67 (green), counterstained with Hoechst (blue), and analyzed by confocal microscopy. Scale bar = 100 µm.

To further evaluate the expression of pluripotency markers, sections of 7-day CBiPS aggregates were immunostained and analyzed using confocal microscopy. OCT4 and E-cadherin were expressed across the entire sections, indicating the maintenance of pluripotency (Figure IV.3 – a and b, respectively). The expression of proliferation marker Ki-

67 was also assessed, with cells on the outside staining more brightly than cells on the inside, thus suggesting higher proliferation on the outside (Figure IV.3 – c).

IV.4. Effect of pre-seeding cell density on the efficiency of hiPSC spheroid production

A significant initial challenge in the generation of hPSC aggregates was related to the poor viability of these cells when dissociated to single cells. This limitation was largely overcome by the use of ROCKi, which counters dissociation-induced apoptosis (Steiner D et al., 2010; Watanabe K et al., 2007). Nevertheless, considerable inconsistency was observed among experiments in terms of cell survival and spheroid production after plating in non-adherent conditions.

One of the variables that were not being particularly controlled in previous experiments was the cellular density at the time of cell detachment, before plating in suspension. To test if this variable was influencing the yield of spheroid production, CBiPS cells were plated as clumps at different densities on Matrigel-coated plates and cultured for four days in E8 medium. The cells were then incubated with ROCKi for 1 hour, detached and dissociated to single cells using Accutase and replated on Ultra-Low attachment culture plates for aggregation. The number of aggregates was estimated by sampling on day 1 and directly assessed on day 7, along with the estimation of cell number. While it was not possible to establish a clear correlation by regression analysis, Spearman's rank correlation test returned a coefficient of 0.66 with a p-value < 0.05 between pre-seeding cell density and the aggregate number on day 1, suggesting that higher pre-seeding cell densities promote increased aggregate generation (Figure IV.4 – a). Conversely, the opposite trend was observed in terms of aggregate number and cell number on day 7, with negative coefficient values under -0.6 indicating an inverse correlation (Figure IV.4 – b and c, respectively). A coefficient of 0.47 between pre-seeding cell density and the number of cells per aggregate was also observed, hinting that higher pre-seeding densities may lead to larger aggregates. However, the p-value of 0.15 indicates low statistical significance (Figure IV.4 – d). A higher number of data points should clarify these results.

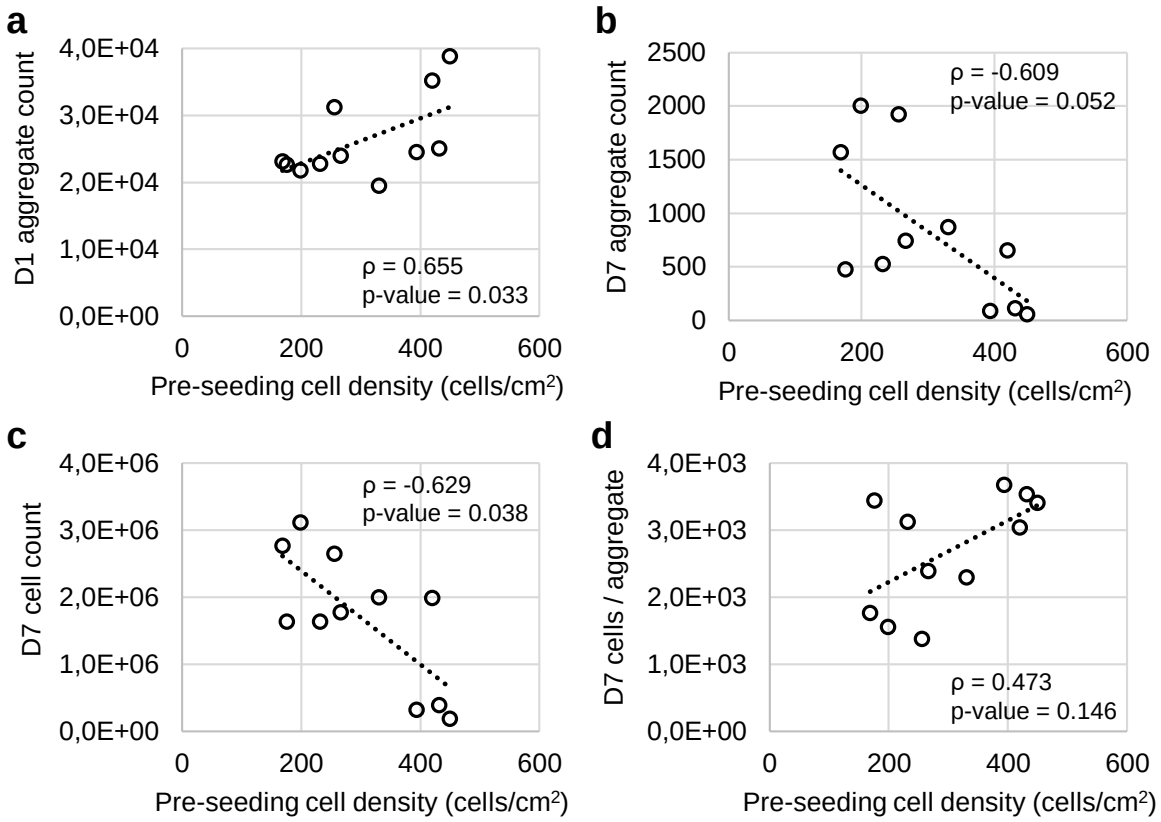

Figure IV.4 – Effect of pre-seeding cell density on hiPSC spheroid yield. CBiPS cells were plated on Matrigel-coated plates at different densities. Four days later, the cells were detached, dissociated and replated on low-attachment plates and cultured for seven days in E8 medium. The number of aggregates was assessed on **(a)** day 1 and **(b)** day 7. **(c - d)** The cell number was assessed on day 7, both in **(c)** absolute terms and **(d)** relative to the number of aggregates. The pre-seeding cell density corresponds to the cellular density before detachment and replating in suspension. Results of Spearman's rank correlation test displayed in terms of coefficient (ρ) and p-value. Dotted lines represent the result of linear regression.

The effect of pre-seeding cell density was further characterized in terms of spheroid size and morphology on day 7. The aggregate diameter appears to be correlated with the density, with a coefficient of 0.52, however, the p-value of 0.11 does not grant the test statistical significance (Figure IV.5 – a). To understand if the dispersion of the diameter distribution was being affected, the correlation between pre-seeding density and the median absolute deviation of the spheroid diameter was also evaluated. Surprisingly, the test returned a strong correlation coefficient of 0.83, with a p-value < 0.005, thus indicating that higher densities promote increased dispersion of aggregate size (Figure IV.5 – b). In terms of morphology, lower pre-seeding cell densities appear to promote slightly more spherical-

shaped aggregates, with a moderate inverse correlation between density and circularity and a moderate correlation between density and eccentricity (Figure IV.5 – c and d, respectively).

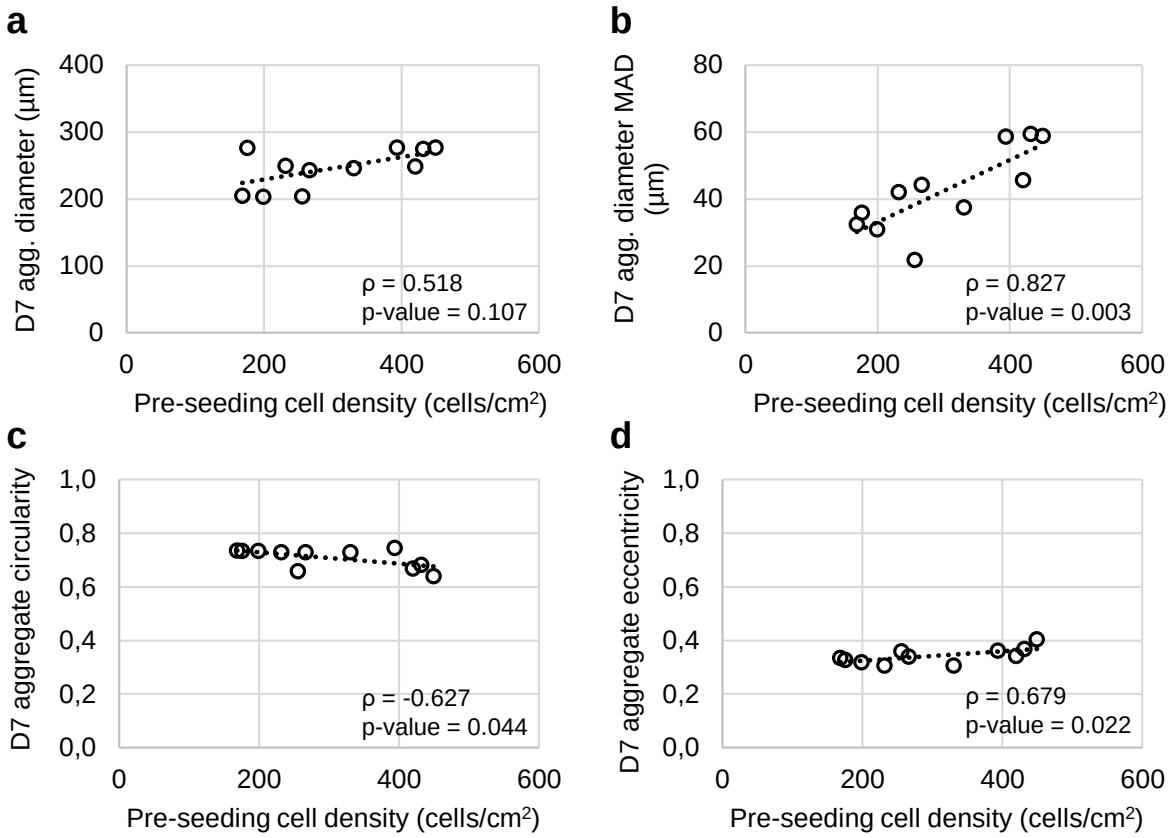

Figure IV.5 – Effect of pre-seeding cell density on the size and morphology of hiPSC spheroids. CBiPS cells were plated on Matrigel-coated plates at different densities. Four days later, the cells were detached, dissociated and replated on low-attachment plates and cultured for seven days in E8 medium. On day 7, the aggregates were evaluated in terms of (a) median diameter, (b) median absolute deviation of diameter, (c) median circularity, and (d) median eccentricity. The pre-seeding cell density corresponds to the cellular density before detachment and replating in suspension. Results of Spearman's rank correlation test displayed in terms of coefficient (ρ) and p-value. Dotted lines represent the result of linear regression.

IV.5. Characterization of hiPSC spheroid culture with combinatorial medium supplementation

The extensive characterization of a cellular model should not only focus on basal growth and phenotype but also the cellular response to specific stimuli. In Chapter III, a 3-D cellular microarray platform was used to screen different combinations of medium supplements, evaluating their effect on the maintenance of OCT4 expression. Part of the

tested conditions was replicated on hiPSC spheroid culture to determine their effect on spheroid size and morphology.

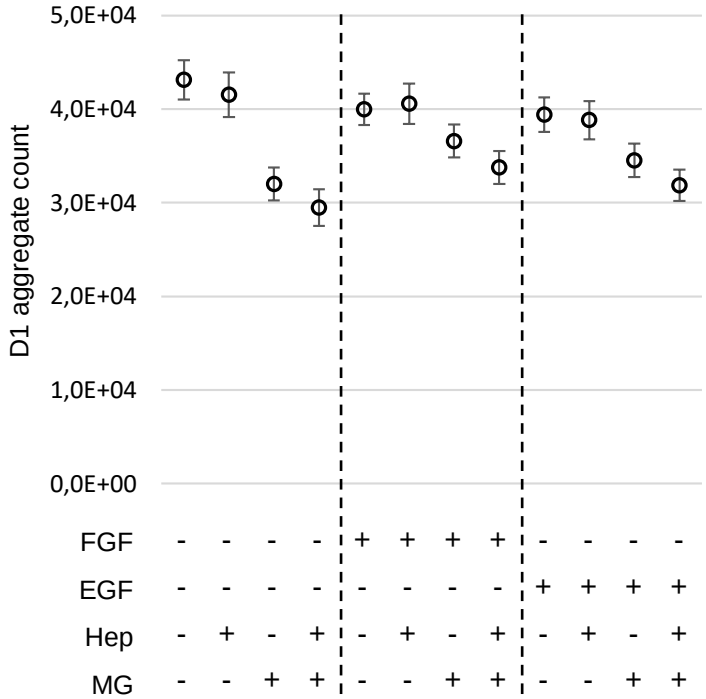

Figure IV.6 – Effect of combinatorial medium supplementation on the number of hiPSC aggregates. CBiPS were plated on low-attachment plates and cultured as aggregates in E8 medium for seven days, supplemented with combinations of FGF2 10 ng/mL (FGF), EGF 10 ng/mL (EGF), heparin 10 µg/mL (Hep) and Matrigel 20 µg/mL (MG). Results correspond to the estimated total number of aggregates on day 1, based on the average of 30 microphotographs per condition. Error bars correspond to SEM.

CBiPS cells were plated on Ultra-Low attachment plates and cultured in suspension in E8 medium with ROCKi during the first 24 hours, and with different combinations of basic fibroblast growth factor 10 ng/mL (FGF2), epidermal growth factor 10 ng/mL (EGF), Matrigel 20 µg/mL (MG) and heparin 10 µg/mL (Hep). To evaluate how the different conditions affected the initial cell survival and aggregate formation, the number of aggregates was estimated on day 1. None of the conditions resulted in a higher aggregate number than the control. However, of all the compounds tested, the only that appears to have caused a significant impact on the initial number of aggregates was Matrigel, as all combinations including it yielded a considerably lower number of aggregates relative to the control (Figure IV.6). Heparin, when added on its own, with FGF, or with EGF, had very little effect when compared to the control, FGF, or EGF, respectively. FGF and EGF had a very similar effect

overall, although with slightly lower aggregate numbers than the control. It is interesting to note that these growth factors, in particular FGF, appear to mitigate the effect of Matrigel, since FGF/MG and FGF/MG/Hep yielded a considerably higher number of aggregates than MG and MG/Hep, respectively.

The effects of the different combinations of compounds on the size and morphology of the spheroids were also assessed. Figure IV.7 displays the kernel density analysis of the diameter distributions, with relatively clear peaks in all conditions tested, although the position of the peak and the curve width/dispersion and skewness vary considerably. The control resulted in the peak at the higher diameter value, 181 µm (Figure IV.7 – a). This is consistent with the sample median diameter of 187 µm ± 31 µm (Figure IV.8 – a). FGF resulted in a peak at a lower diameter value (147 µm) but with higher density, indicating that the distribution was less disperse (Figure IV.7 – b). On the other hand, EGF yielded a distribution peaking at a slightly lower diameter than the control but also with a lower density (Figure IV.7 – c). All the other conditions tested yielded wider curves, indicating that the addition of heparin and Matrigel to the culture medium led to higher heterogeneity in diameter size. Matrigel, in particular, appeared to sharply increase the heterogeneity, as suggested by the wider and more irregular curves (Figure IV.7 – g - i) and by the larger minimum diameter span for 90% of the density (Figure IV.8 – b). However, it is also suggested that the combination of Matrigel and heparin partially mitigated this effect, with more defined peaks and with higher densities (Figure IV.7 – j - l).

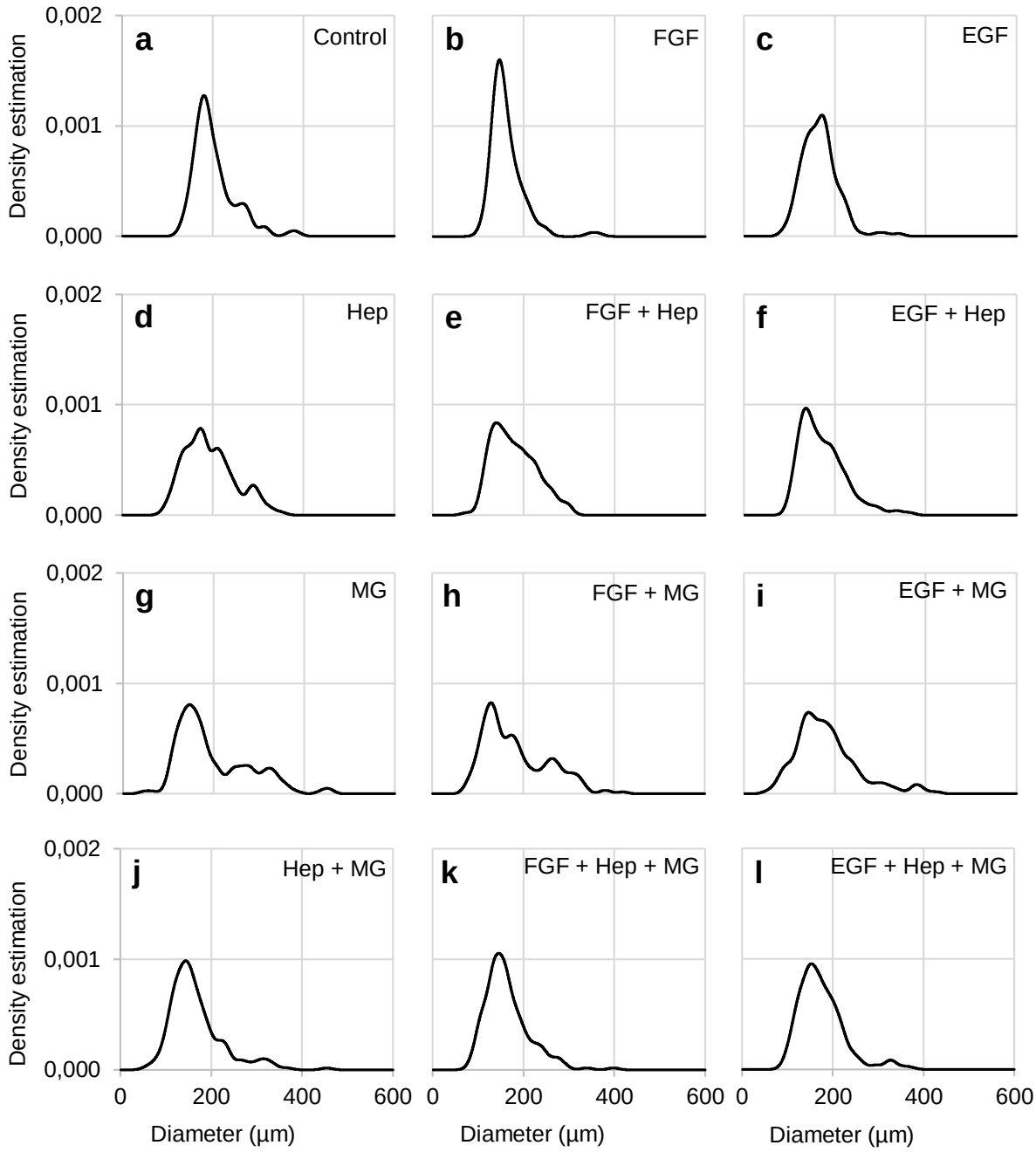

Figure IV.7 – Kernel density estimation of the diameter of hiPSC spheroids with combinatorial medium supplementation. **(a – l)** CBiPS were plated on low-attachment plates and cultured as aggregates in E8 medium for seven days, supplemented with combinations of FGF2 10 ng/mL (FGF), EGF 10 ng/mL (EGF), heparin 10 µg/mL (Hep) and Matrigel 20 µg/mL (MG). Unsupplemented medium was used as control. KDE with Gaussian kernel, bandwidth = 12. Results representative of ≥ 112 cellular aggregates per condition.

In terms of morphology, the different combinations do not appear to have significantly affected the circularity of the cellular aggregates, with all the median values ranging between 0.69 and 0.73 (Figure IV.8 – c). This is not the case for eccentricity, though, with the control

condition yielding the lowest median value (0.34 ± 0.10) and heparin appearing to generally promote higher values (Figure IV.8 – d).

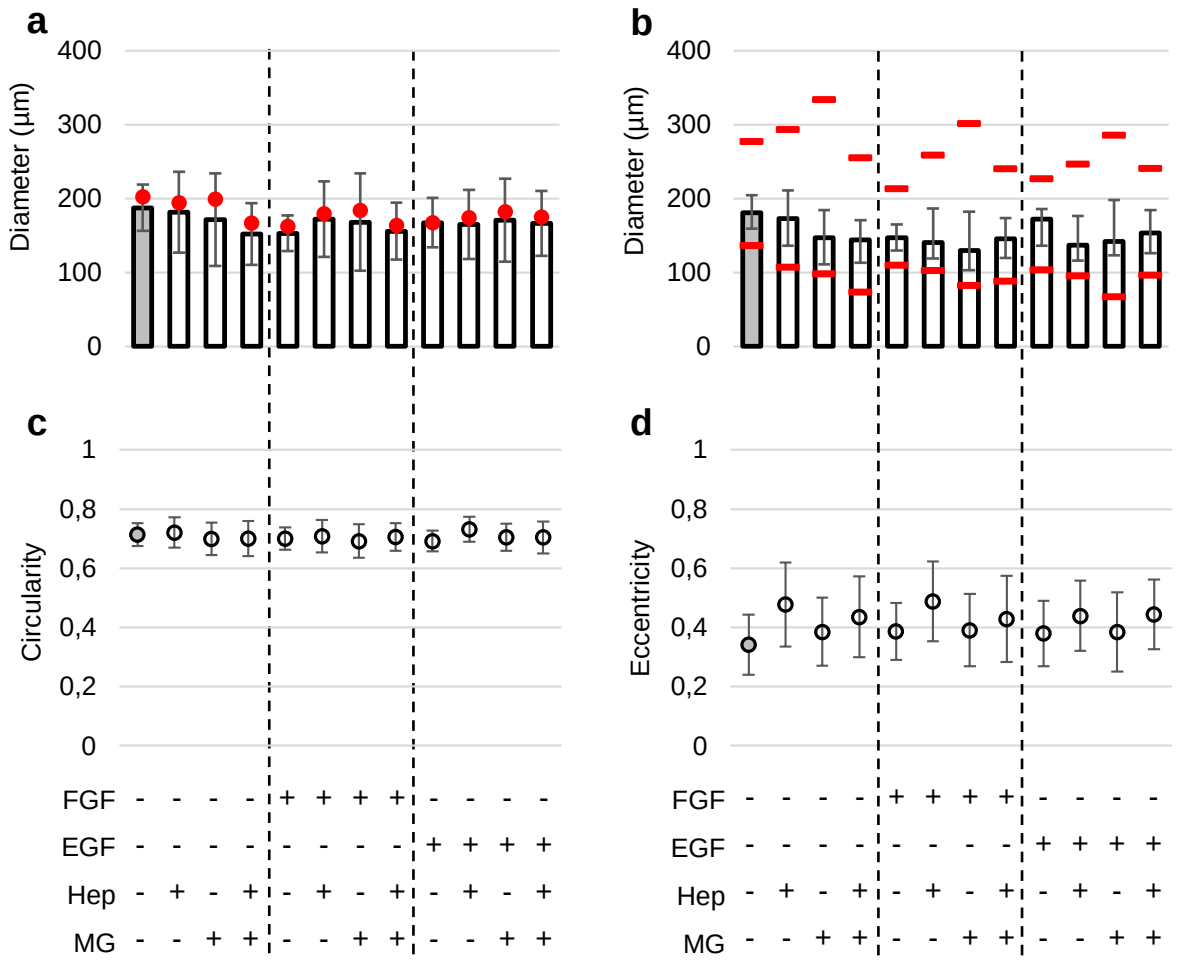

Figure IV.8 – Characterization of hiPSC spheroids regarding size and morphology after culture with combinatorial medium supplementation. **(a - b)** Statistical analysis of spheroid diameter distribution. Basic statistical estimators from samples are presented in **(a)**, where the bars represent the median, the red dots represent the mean and the error bars represent the median absolute deviation (MAD). The key features of kernel density estimation (KDE) are presented in **(b)** where the bars represent the diameter at the density peak, error bars represent the minimum diameter range that contains 50% of density, and red bars represent the minimum diameter range that contains 90% of density. Gray bars correspond to the unsupplemented control condition. **(c – d)** The morphology of the spheroids was analyzed in terms of **(c)** circularity and **(d)** eccentricity. Results expressed as median ± MAD. ≥ 112 cellular aggregates per condition.

IV.6. Study of the effect of combinatorial medium supplementation on the expression of pluripotency and differentiation markers in 2- and 3-D culture systems

While the results obtained from the combinatorial medium supplementation experiment on the microarray platform in the previous chapter were not conclusive, there were indications that some of the conditions tested led to decreased expression of OCT4, which could be indicative of loss of pluripotency. The results previously described suggest that these conditions favor alterations in terms of spheroid size and morphology. In order to further understand how the cells respond to these stimuli in regard to pluripotency and differentiation marker expression, the same conditions were tested on standard-scaled monolayer or spheroid culture systems.

CBiPS cells were plated on either Matrigel-coated culture plates or Ultra-Low attachment plates as spheroids, and cultured in E8 medium supplemented with the same combinations tested in the previous section. After seven days, the cells were detached and/or dissociated and processed for flow cytometry to assess the expression of OCT4. In 2-D culture, despite small variations, the fraction of OCT4-positive cells remained very close to the control in almost all conditions, with some of the conditions with heparin leading to a decrease close to 10% (Figure IV.9 – a). The effect of heparin becomes much more evident when the average fluorescence intensity is considered. Figure IV.9 – b shows that all the conditions with heparin led to a considerable decrease in the average fluorescence intensity relative to the control, of up to 29% in EGF/Hep/MG. Heparin alone led to a decrease of 23%. These results also suggest an increase of the average fluoresce in conditions with Matrigel and/or FGF, without heparin. In spheroid culture, all the conditions with heparin led to a significant decrease in the fraction of OCT4-positive cells relative to the control, with heparin alone causing a 44% reduction (Figure IV.9 – c). While the fraction of OCT4-positive cells did not seem to be affected in combinations without heparin, the average fluorescence intensity was lower in all the test conditions, relative to the unsupplemented control (Figure IV.9 – d). When taken together, these results suggest a considerably different response to the same conditions between cells cultured in 2-D and 3-D, particularly regarding the effect of heparin.

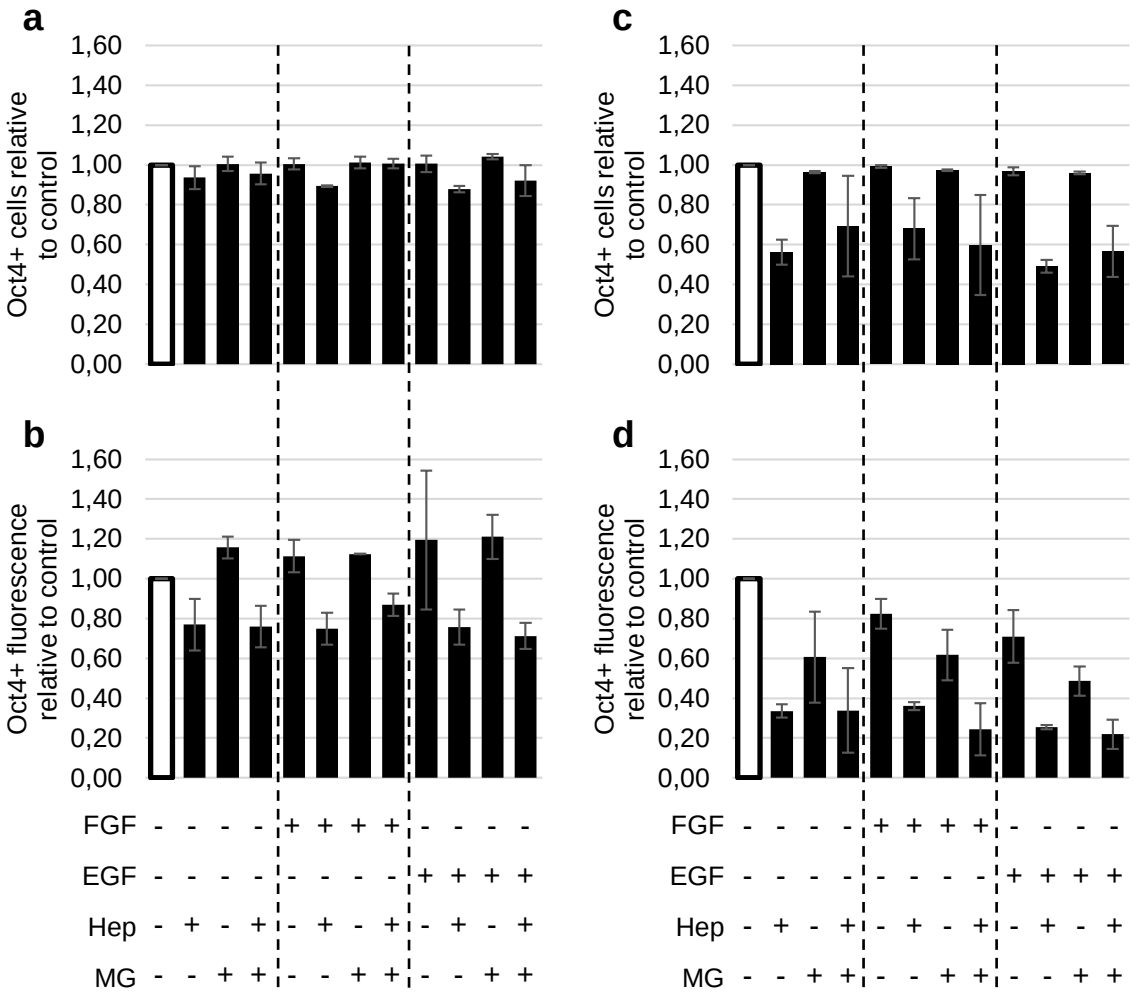

Figure IV.9 – Flow cytometric analysis of OCT4 expression in hiPSC after culture with combinatorial medium supplementation, in 2-D and 3-D systems. CBiPS cells were cultured either **(a – b)** attached on Matrigel-coated plates or **(c – d)** as spheroids in suspension, in E8 medium supplemented with combinations of FGF2 (FGF), EGF, heparin (Hep), and Matrigel (MG). Results displayed in terms of **(a, c)** the fraction of OCT4-positive particles relative to the control and **(b, d)** the average fluorescence intensity relative to the control. White bars correspond to the control condition. Error bars refer to standard deviation. Number of events ≥ 10000 per condition, n = 2.

To further understand how the different combinations of compounds affect hiPSC spheroids in term of pluripotency and differentiation, the expression of genetic markers was assessed by qPCR, again at day 7. Consistent with the flow cytometry results, all the condition containing heparin led to a marked decrease in the expression of POU5F1, with heparin alone resulting in a 69% reduction relative to the untreated control. As for the other compounds tested, the results were very similar to the untreated control, with the most significant effect being a 19% reduction in the condition with FGF alone (Figure IV.10 – a). Similar results were

observed regarding NANOG expression, with all Hep+ conditions leading to a sharp decrease while MG+/Hep- conditions resulted in a slight increase (Figure IV.10 – b). In terms of differentiation, three genetic markers were assessed. The expression of SOX1 was lower by 30% and 29% in the cells cultured with Heparin alone and Matrigel alone, respectively, while the combination of both compounds resulted in an expression closer to the untreated control, with only a 13% decrease. The addition of FGF appeared to mitigate these effects, with the expression of SOX1 in all FGF+ conditions being close to the control, except FGF+/Hep+/MG+, where the expression increased by 43%. The most evident effect on SOX1 expression was caused by the combinations containing EGF and heparin, with over two-fold the expression in the control, suggesting some bias towards ectodermal commitment (Figure IV.10 – c). As for SOX17, similarly to SOX1, its expression was slightly decreased in the conditions with heparin alone and Matrigel alone. However, the combination of the two compounds led to a considerable increase to over 2-fold the expression in the control, in conditions both with and without the growth factors (Figure IV.10 – d). T was overexpressed in all Hep+ conditions, suggesting that the compound may promote or introduce a bias towards mesendodermal differentiation. Also, while it did not appear to affect the other two differentiation markers, FGF seemed to have slightly inhibited the expression of T, with a decrease of 34%.

Taken together, these results strongly suggest that the addition of heparin to the culture medium has different effects on cells cultured in 2-D and 3-D, with a considerably more likely loss of pluripotency in cells cultured as spheroids when compared to cells cultured in monolayer. Furthermore, the increase in the expression of T gene in Hep+ conditions is suggestive of epithelial-mesenchymal transition, which is typically accompanied by a strong reduction in CDH1/E-cadherin expression. To assess the difference between the response of the two culture systems, clarify the cellular phenotype regarding pluripotency, and to gain some insight into the potential role of E-cadherin in this effect, a direct 2-D *versus* 3-D comparison was carried out.

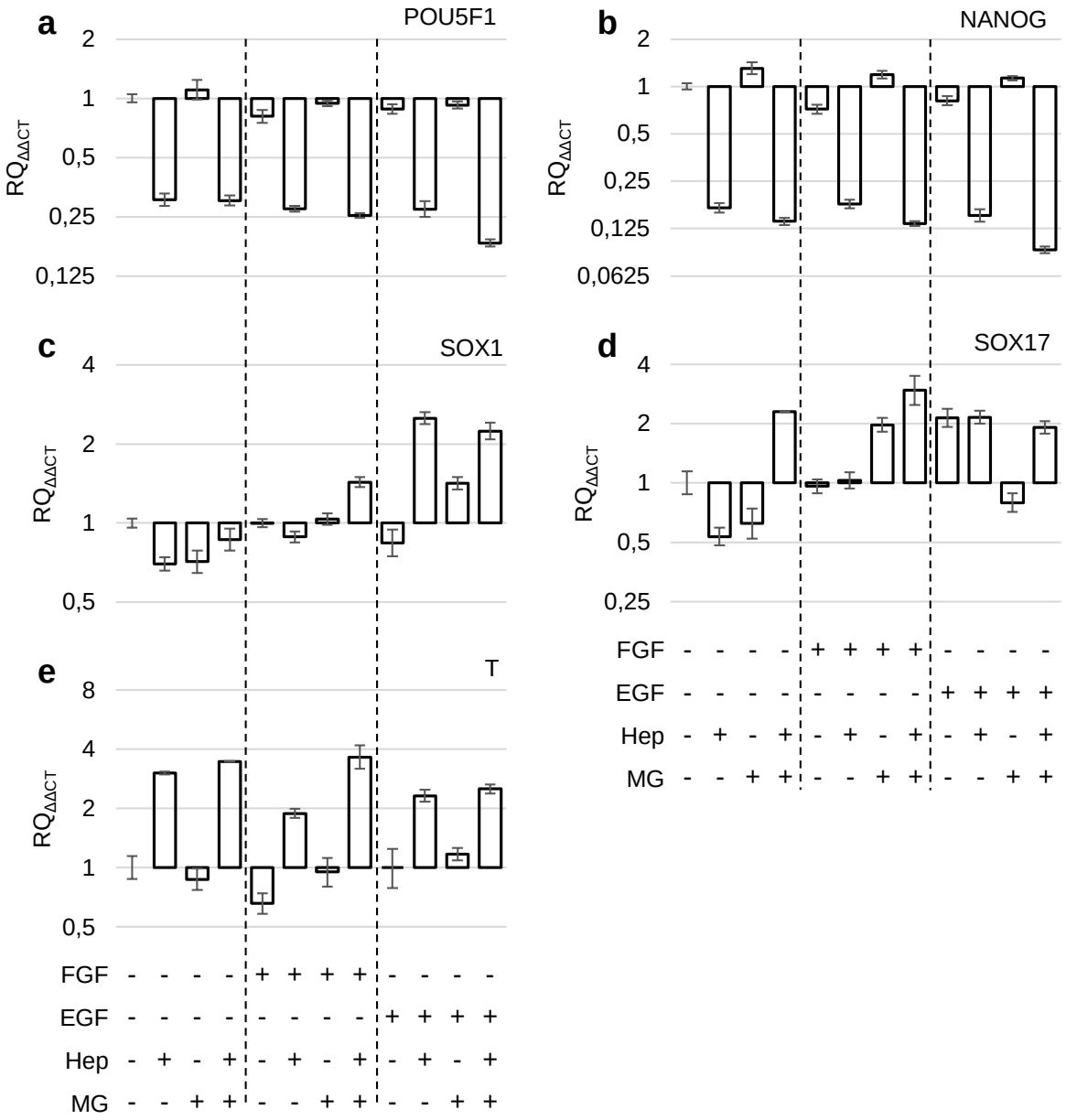

Figure IV.10 – Expression of pluripotency and differentiation genetic markers in hiPSC spheroids after combinatorial medium supplementation. CBiPS cells were cultured as spheroids in suspension for seven days, in E8 supplemented with combinations of FGF2 (FGF), EGF, heparin (Hep), and Matrigel (MG). Quantitative PCR analysis was run, using GAPDH as the internal control, to evaluate the relative expression of **(a)** POU5F1 (OCT4), **(b)** NANOG, **(c)** SOX1, **(d)** SOX17, and **(e)** T (Brachyury). Expression in sample cultured in the unsupplemented medium was used as the experimental control. Results presented as the relative quantification (RQ) of base 2 of the ΔΔCT between control and test conditions ± SE. Experimental replicates ≥ 2 per condition.

CBiPS cells were dissociated to single-cells and plated on either Matrigel-coated plates for monolayer culture or Ultra-low attachment plates for spheroid culture. Two seeding

densities were tested in monolayer culture to control the effect of cell density. The cells were cultured for seven days in E8 medium with or without heparin, after which they were processed for qPCR to evaluate the expression of POU5F1 and CDH1. Consistent with the previous results, the expression of POU5F1 decreased in all conditions containing heparin, although, this decrease was particularly stronger in cells cultured as spheroids, with a 64% reduction from the expression on day 0. There was also a considerable difference between the two seeding densities in monolayer-cultured cells, suggesting that cell density may play a role in the observed effect (Figure IV.11 – a). As for the expression of CDH1, there was a striking difference between the two culture systems – while heparin did not appear to have any significant effect in cells cultured in monolayer, in spheroids it led to a 71% decrease in CDH1 expression (Figure IV.11 – b).

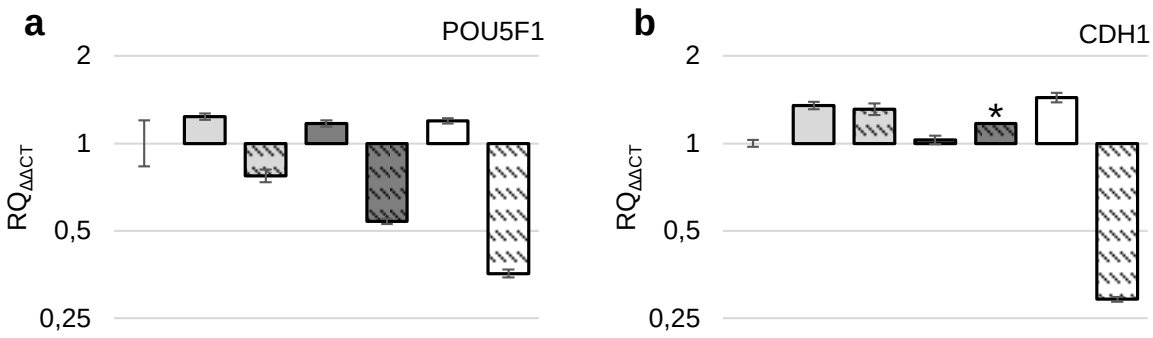

Figure IV.11 – Effect of heparin on the expression of POU5F1 and CDH1 in cells cultured in 2- and 3-D. CBiPS cells were plated as single cells on Matrigel-coated plates, at 5.0 × 10^3 cells/cm^2 (light gray bars) or at 2.0 × 10^4 cells/cm^2 (dark gray bars), or on low attachment plates at 1.0 × 10^5 cells/cm^2 (white bars), and cultured for seven days in E8 medium (clear bars) or E8 with heparin 10 µg/mL (dashed bars). Quantitative PCR analysis was run using GAPDH as the internal control, to evaluate the relative expression of **(a)** POU5F1 (OCT4) and **(b)** CDH1 (E-cadherin). Expression before plating, at day 0, was used as the experimental control. Results presented as the relative quantification (RQ) of base 2 of the ΔΔCT between the experimental control and the test conditions ± SE. Experimental replicates ≥ 2 per condition except where marked with *, where a single measurement was taken.

IV.7. Discussion and main conclusions

The growing knowledge of the immense complexity and span of the microenvironmental variables that influence cell behavior, and of how the implicit nature of *in vitro* research models determines their biological and clinical significance has prompted the

development and adoption of new techniques and analytical technologies in the field of stem cell biology. The use of three-dimensional culture models, in particular, has gained increasing relevance, as it is generally accepted that they mimic aspects of the cellular environment in living organisms that are largely non-existent or compromised in traditional two-dimensional models [Cimetta E & Vunjak-Novakovic G, 2014; Baker BM & Chen CS, 2012; Metallo CM et al., 2007]. With a higher level of complexity, the use of three-dimensional culture systems as research models also entails the need for a much broader control over different variables and for extensive characterization.

In this chapter, different methods were employed to characterize hiPSCs cultured as spheroids in short-term static suspension with xeno-free chemically defined medium E8, in terms of growth and aggregate size and morphology. These cells were also compared with cells cultured in monolayer regarding the expression of pluripotency and differentiation markers, and their response to medium additives.

CBiPS cells cultured in static suspension in E8 medium displayed a considerably lower yield when compared with cells cultured in monolayer, mainly due to increased initial cell death and likely a longer lag phase. The increased cell death after single-cell dissociation during passaging has been reported in previous studies as one of the main limitations of this culture system [Larijani MR et al., 2011; Steiner D et al., 2010]. This effect is thought to be related to the disruption of E-cadherin during enzymatic dissociation, an adhesion protein responsible for cell-cell connections and having a critical role in hPSC survival [Ohgushi M et al., 2010; Xu Y et al., 2010]. Recently, Nath *et al*. have suggested the use of Botulinum hemagglutinin as a viable alternative to enzymatic dissociation for the passaging of hPSC aggregates cultured in suspension [Nath SC et al., 2018]. This compound selectively binds to E-cadherin, disrupting the cell-cell interactions and causing partial disaggregation of cellular spheroids, but appears to allow a faster recovery and to improve post-passaging cell survival compared to enzymatic methods.

Consistent with the increase in cell number between days 2 and 7, the diameter of the spheroids increased steadily, with a relatively stable dispersion. After one week in culture, the spheroids displayed a median diameter of 183 µm with a coefficient of variation of 11.8%, which is lower than previously reported in static suspension culture systems [Larijani MR et al., 2011; Amit M et al., 2010]. In terms of morphology, two metrics were considered: a) circularity, which is essentially a ratio between the expected perimeter of the section based on its area and the measured perimeter, and provides an indicator of edge smoothness or regularity; and b)

eccentricity, which is calculated based on the difference between the major and minor axes and, therefore, constitutes an indicator of how spherical the aggregates are. The results showed that circularity was not significantly changed throughout the experiment, while eccentricity tended to decrease with time, thus suggesting that the aggregates became more spherical. While these indicators may provide useful insights, they are based on single 2-D projections of each aggregate and, therefore, the extrapolation of the resulting data should be cautious.

Immunocytochemical analysis of day 7 CBiPS spheroid sections showed differential expression of Ki-67 between innermost and outermost cells, indicating higher proliferative activity on the outside of the aggregates and corroborating previous reports [(Abecasis B et al., 2017; Nath SC et al., 2017)]. Expression of pluripotency marker POU5F1 in cells after seven days in suspension was shown to be similar to that in cells cultured in monolayer, and is consistent with the expression of OCT4 as observed by immunocytochemical analysis on spheroid sections, thus strongly indicating the overall maintenance of pluripotency. As for CDH1, there was a considerably decreased expression on day 1, followed by a moderate increase relative to cells cultured in monolayer. The initial decrease may be related to the use of ROCK inhibitor Y-27632 during the first day in suspension, as this molecule has been previously described to reduce the expression of E-cadherin in hiPSC and promote mesendodermal differentiation [(Maldonado M et al., 2016)]. While this effect may also explain the increase in the expression of definitive endoderm marker SOX17, the hypothesis of a ROCKi-induced EMT bias is countered by the increase in SOX1 and the sharp decrease in T expression on day 1, thus suggesting that other effectors should be considered. As for the mild increase in CDH1 after ROCKi removal, it is consistent with a report from Azarin *et al*. where the expression of E-cadherin increased in hESCs cultured in 3-D microwells [(Azarin SM et al., 2012)]. It is important to note that despite the considerable variations quantified in the expression of differentiation markers, the overall late amplification curves obtained in qPCR for these markers indicate a relatively low amount of target sequences. Further experiments will be required to validate these results.

In an attempt to understand the variables at play in the overall efficiency of aggregate formation and growth, different pre-seeding cell densities were tested. The results presented suggest that higher pre-seeding cell densities promote a higher aggregate count on day 1, but a lower efficiency after one week, as indicated by lower aggregate count and cell count on day 7. The higher aggregate count on day 1 in higher cell densities may be due to incomplete

dissociation of the cells before seeding on low-attachment plates, or to faster reaggregation, based on the assumption that the enzymatic dissociation is not as effective and/or aggressive on high-density cultures compared to low-density cultures. Whether the lower efficiency was due to higher cell death after ROCKi removal or to lower growth rate was not investigated. It has been previously described that high-density hPSC cultures have a lower proliferation rate and a higher propensity for spontaneous differentiation [(Wu J et al., 2015)]. In addition, Nath *et al*. have reported that small hiPSC spheroids formed by forced aggregation tend to grow slower [(Nath SC et al., 2017)]. Although the size of cell aggregates was not assessed on day 1, higher pre-seeding densities might produce higher aggregate count but smaller aggregates, which could result in less viability and proliferative ability after ROCKi removal. In this scenario, only the larger aggregates would proliferate, which would be consistent with the suggestion of a higher median diameter in higher pre-seeding densities. The higher diameter dispersion and aggregate irregularity in higher densities would be consistent with increased spontaneous differentiation, but this hypothesis should be confirmed with additional experiments.

Finally, CBiPS cell aggregates were characterized and compared to cells cultured in monolayer in response to the addition of compounds to the culture medium, replicating some of the conditions tested on the microarray platform and described in the previous chapter. The addition of Matrigel to E8 was shown to promote a decrease in the initial aggregate number on day 1 in suspension culture. Although the cell number was not assessed, this effect may be due to an increased cellular aggregation in the presence of extracellular matrix components in the culture medium. This hypothesis is supported by the considerably higher diameter dispersion on day 7 in the presence of Matrigel, which resulted, at least in part, from increased initial clustering of aggregates. On the other hand, FGF2, which plays a complex role in the survival and self-renewal of hPSC [(Chen G et al., 2011, 2012; Eiselleova L et al., 2009; Levenstein ME et al., 2006)] appears to produce compacter aggregates with a lower dispersion relative to the control, thus suggesting that it might affect clustering. Previous reports have linked FGF2 to the phosphorylation of GSK-3β, with consequent cytoplasmic accumulation and nuclear translocation of β-catenin and expression of EMT-promoting transcription factors in hPSC [(Kinehara M et al., 2013, 2014; Ding VMY et al., 2010)]. Considering this effect, the increase of FGF2 concentration in the culture medium might be modulating the expression of E-cadherin expression leading to decreased cell-cell adhesion, which would be consistent with the decreased aggregation.

When compared with cells cultured in monolayer, CBiPS cultured in suspension were seemingly more reactive to the addition of heparin to the culture medium, as indicated by a considerable decrease of OCT4 positive cells and average fluorescence intensity, evaluated by flow cytometry. This effect was further supported by the striking decrease in the expression of pluripotency marker genes POU5F1 and NANOG in cells cultured in suspension with heparin. Interestingly, the morphology of the spheroids also appeared to be affected, with a generally increased eccentricity in the conditions containing heparin, thus suggesting that differentiating aggregates are less spherical. Analysis of the expression of differentiation markers supported the hypothesis of heparin-induced differentiation, with overexpression of mesendodermal marker T, suggestive of EMT, although the effect was not as clear regarding the expression of SOX17. Conversely, the addition of heparin also appeared to promote overexpression of SOX1 in the presence of EGF, which suggests interactions with different signaling pathways. In the presence of heparin, cells cultured in suspension displayed a sharp decrease in the expression of CDH1 with the addition of heparin, while its expression in monolayer cells did not seem to be affected. Heparin has been previously reported to promote hESC self-renewal in cells cultured in monolayer, in serum-free medium (Furue MK et al., 2008). More recently, however, it has been found to promote the cardiac differentiation of hPSCs through modulation of Wnt signaling, though the exact mechanism is yet not known (Lin Y et al., 2017). Heparin is a known inhibitor of protein kinase 2 (CK2), a serine/threonine protein kinase involved in the regulation of gene expression and protein synthesis (O'Farrell F et al., 1999). Although the role of CK2 in hPSC has not been described and its activity is not fully clarified, it has been reported to contribute to E-cadherin stabilization in the cell membrane (Lickert H et al., 2000; Serres M et al., 2000), to act synergistically with GSK-3β in the degradation of cytoplasmic β-catenin (Bek S, 2002) and to suppress EMT (Golden D & Cantley LG, 2015; Deshiere A et al., 2013). Assuming that this activity of CK2 is maintained in hPSCs, it could, hypothetically, play a role in the observed effect of heparin.

It is yet relevant to note that because the heparin used is not synthetic but isolated from porcine intestinal mucosa, there is a possibility that the observed effects are not caused by heparin itself but rather by a contaminant. Therefore, additional experiments should be carried out to validate the hypothesis that heparin, in fact, contributes to mesendodermal differentiation of hPSC in suspension and to explore its putative mechanism of action.

In summary, different methodologies were used to analyze and characterize hiPSCs cultured for a short period in suspension in chemically-defined conditions, regarding spheroid size and morphology, and the expression of pluripotency and differentiation markers. Results indicated that lower pre-seeding cell densities resulted in a higher yield of aggregate formation, along with higher uniformity in terms of size and shape after seven days in culture. Additionally, consistent evidence is presented pointing to a different response to the addition of heparin to the culture medium between cells cultured in monolayer and as aggregates in static suspension. Overall, this study corroborates the notion that 2-D and 3-D culture systems of hiPSCs may lead to significantly different results and highlights the importance of performing extensive characterization of *in vitro* models as means to better understand the different variables at stake and hold greater control over experimental settings.

IV.8. References

Abecasis B, Aguiar T, Arnault É, Costa R, Gomes-Alves P, Aspegren A, Serra M & Alves PM (2017). Expansion of 3D Human Induced Pluripotent Stem Cell Aggregates in Bioreactors: Bioprocess Intensification and Scaling-up Approaches. *Journal of Biotechnology* 246, 81–93. **DOI:** 10.1016/j.jbiotec.2017.01.004.

Amit M, Chebath J, Margulets V, Laevsky I, Miropolsky Y, Shariki K, Peri M, Blais I, Slutsky G, Revel M & Itskovitz-Eldor J (2010). Suspension Culture of Undifferentiated Human Embryonic and Induced Pluripotent Stem Cells. *Stem Cell Reviews and Reports* 6, 248–259. **DOI:** 10.1007/s12015-010-9149-y.

Azarin SM, Lian X, Larson EA, Popelka HM, de Pablo JJ & Palecek SP (2012). Modulation of Wnt/β-Catenin Signaling in Human Embryonic Stem Cells Using a 3-D Microwell Array. *Biomaterials* 33, 2041–2049. **DOI:** 10.1016/j.biomaterials.2011.11.070.

Baker BM & Chen CS (2012). Deconstructing the Third Dimension - How 3D Culture Microenvironments Alter Cellular Cues. *Journal of Cell Science* 125, 3015–3024. **DOI:** 10.1242/jcs.079509.

Bek S (2002). Protein Kinase CKII Regulates the Interaction of Beta-Catenin with Alpha-Catenin and Its Protein Stability. *Journal of Cell Science* 115, 4743–4753. **DOI:** 10.1242/jcs.00154.

Chen G, Gulbranson DR, Hou Z, Bolin JM, Ruotti V, Probasco MD, Smuga-Otto K, Howden SE, Diol NR, Propson NE *et al.* (2011). Chemically Defined Conditions for Human IPSC Derivation and Culture. *Nature Methods* 8, 424–429. **DOI:** 10.1038/nmeth.1593.

Chen G, Gulbranson DR, Yu P, Hou Z & Thomson JA (2012). Thermal Stability of Fibroblast Growth Factor Protein Is a Determinant Factor in Regulating Self-Renewal, Differentiation, and Reprogramming in Human Pluripotent Stem Cells. *Stem Cells* 30, 623–630. **DOI:** 10.1002/stem.1021.

Chen VC, Couture SM, Ye J, Lin Z, Hua G, Huang H-IP, Wu J, Hsu D, Carpenter MK & Couture LA (2012). Scalable GMP Compliant Suspension Culture System for Human ES Cells. *Stem Cell Research* 8, 388–402. **DOI:** 10.1016/j.scr.2012.02.001.

Cimetta E & Vunjak-Novakovic G (2014). Microscale Technologies for Regulating Human Stem Cell Differentiation. *Experimental Biology and Medicine* 239, 1255–1263. **DOI:** 10.1177/1535370214530369.

Deshiere A, Duchemin-Pelletier E, Spreux E, Ciais D, Combes F, Vandenbrouck Y, Couté Y, Mikaelian I, Giusiano S, Charpin C *et al.* (2013). Unbalanced Expression of CK2 Kinase Subunits Is Sufficient to Drive Epithelial-to-Mesenchymal Transition by Snail1 Induction. *Oncogene* 32, 1373–1383. **DOI:** 10.1038/onc.2012.165.

Ding VMY, Ling L, Natarajan S, Yap MGS, Cool SM & Choo ABH (2010). FGF-2 Modulates Wnt Signaling in Undifferentiated HESC and IPS Cells through Activated PI3-K/GSK3β Signaling. *Journal of Cellular Physiology* 225, 417–428. **DOI:** 10.1002/jcp.22214.

Eiselleova L, Matulka K, Kriz V, Kunova M, Schmidtova Z, Neradil J, Tichy B, Dvorakova D, Pospisilova S, Hampl A & Dvorak P (2009). A Complex Role for FGF-2 in Self-Renewal, Survival, and Adhesion of Human Embryonic Stem Cells. *Stem Cells* 27, 1847–1857. **DOI:** 10.1002/stem.128.

Furue MK, Na J, Jackson JP, Okamoto T, Jones M, Baker D, Hata R-I, Moore HD, Sato JD & Andrews PW (2008). Heparin Promotes the Growth of Human Embryonic Stem Cells in a Defined Serum-Free Medium. *Proceedings of the National Academy of Sciences* 105, 13409–13414. **DOI:** 10.1073/pnas.0806136105.

Golden D & Cantley LG (2015). Casein Kinase 2 Prevents Mesenchymal Transformation by Maintaining Foxc2 in the Cytoplasm. *Oncogene* 34, 4702–4712. **DOI:** 10.1038/onc.2014.395.

Itskovitz-Eldor J, Schuldiner M, Karsenti D, Eden A, Yanuka O, Amit M, Soreq H & Benvenisty N (2000). Differentiation of Human Embryonic Stem Cells into Embryoid Bodies Comprising the Three Embryonic Germ Layers. *Molecular Medicine* 6, 88–95. **DOI:** 10.1007/BF03401776.

Kinehara M, Kawamura S, Tateyama D, Suga M, Matsumura H, Mimura S, Hirayama N, Hirata M, Uchio-Yamada K, Kohara A *et al.* (2013). Protein Kinase C Regulates Human Pluripotent Stem Cell Self-Renewal. *PLoS ONE* 8, e54122. **DOI:** 10.1371/journal.pone.0054122.

Kinehara M, Kawamura S, Mimura S, Suga M, Hamada A, Wakabayashi M, Nikawa H & Furue MK (2014). Protein Kinase C-Induced Early Growth Response Protein-1 Binding to SNAIL Promoter in Epithelial-Mesenchymal Transition of Human Embryonic Stem Cells. *Stem Cells and Development* 23, 2180–2189. **DOI:** 10.1089/scd.2013.0424.

Larijani MR, Seifinejad A, Pournasr B, Hajihoseini V, Hassani S-N, Totonchi M, Yousefi M, Shamsi F, Salekdeh GH & Baharvand H (2011). Long-Term Maintenance of Undifferentiated Human Embryonic and Induced Pluripotent Stem Cells in Suspension. *Stem Cells and Development* 20, 1911–1923. **DOI:** 10.1089/scd.2010.0517.

Lei Y & Schaffer D V (2013). A Fully Defined and Scalable 3D Culture System for Human Pluripotent Stem Cell Expansion and Differentiation. *Proceedings of the National Academy of Sciences* 110, E5039–E5048. **DOI:** 10.1073/pnas.1309408110.

Levenstein ME, Ludwig TE, Xu R-H, Llanas RA, VanDenHeuvel-Kramer K, Manning D & Thomson JA (2006). Basic Fibroblast Growth Factor Support of Human Embryonic Stem Cell Self-Renewal. *Stem Cells* 24, 568–574. **DOI:** 10.1634/stemcells.2005-0247.

Li X, Ma R, Gu Q, Liang L, Wang LL, Zhang Y, Wang X, Liu X, Li Z, Fang J *et al.* (2018). A Fully Defined Static Suspension Culture System for Large-Scale Human Embryonic Stem Cell Production. *Cell Death & Disease* 9, 892. **DOI:** 10.1038/s41419-018-0863-8.

Lickert H, Bauer A, Kemler R & Stappert J (2000). Casein Kinase II Phosphorylation of E-cadherin Increases E-cadherin/β-Catenin Interaction and Strengthens Cell-Cell Adhesion. *Journal of Biological Chemistry* 275, 5090–5095. **DOI:** 10.1074/jbc.275.7.5090.

Lin Y, Linask KL, Mallon B, Johnson K, Klein M, Beers J, Xie W, Du Y, Liu C, Lai Y *et al.* (2017). Heparin Promotes Cardiac Differentiation of Human Pluripotent Stem Cells in Chemically Defined Albumin-Free Medium, Enabling Consistent Manufacture of Cardiomyocytes. *STEM CELLS Translational Medicine* 6, 527–538. **DOI:** 10.5966/sctm.2015-0428.

Maldonado M, Luu RJ, Ramos MEP & Nam J (2016). ROCK Inhibitor Primes Human Induced Pluripotent Stem Cells to Selectively Differentiate towards Mesendodermal Lineage via Epithelial-Mesenchymal Transition-like Modulation. *Stem Cell Research* 17, 222–227. **DOI:** 10.1016/j.scr.2016.07.009.

Metallo CM, Mohr JC, Detzel CJ, DePablo JJ, van Wie BJ & Palecek SP (2007). Engineering the Stem Cell Microenvironment. *Biotechnology Progress* 23, 18–23. **DOI:** 10.1021/bp060350a.

Nath SC, Horie M, Nagamori E & Kino-Oka M (2017). Size- and Time-Dependent Growth Properties of Human Induced Pluripotent Stem Cells in the Culture of Single Aggregate. *Journal of Bioscience and Bioengineering* 124, 469–475. **DOI:** 10.1016/j.jbiosc.2017.05.006.

Nath SC, Tokura T, Kim MH & Kino-Oka M (2018). Botulinum Hemagglutinin-Mediated in Situ Break-up of Human Induced Pluripotent Stem Cell Aggregates for High-Density Suspension Culture. *Biotechnology and Bioengineering* 115, 910–920. **DOI:** 10.1002/bit.26526.

O'Farrell F, Loog M, Janson IM & Ek P (1999). Kinetic Study of the Inhibition of CK2 by Heparin Fragments of Different Length. *Biochimica et Biophysica Acta (BBA) - Protein Structure and Molecular Enzymology* 1433, 68–75. **DOI:** 10.1016/S0167-4838(99)00147-8.

Ohgushi M, Matsumura M, Eiraku M, Murakami K, Aramaki T, Nishiyama A, Muguruma K, Nakano T, Suga H, Ueno M *et al.* (2010). Molecular Pathway and Cell State Responsible for Dissociation-Induced Apoptosis in Human Pluripotent Stem Cells. *Cell Stem Cell* 7, 225–239. **DOI:** 10.1016/j.stem.2010.06.018.

Serres M, Filhol O, Lickert H, Grangeasse C, Chambaz EM, Stappert J, Vincent C & Schmitt D (2000). The Disruption of Adherens Junctions Is Associated with a Decrease of E-cadherin Phosphorylation by Protein Kinase CK2. *Experimental Cell Research* 257, 255–264. **DOI:** 10.1006/excr.2000.4895.

Steiner D, Khaner H, Cohen M, Even-Ram S, Gil Y, Itsykson P, Turetsky T, Idelson M, Aizenman E, Ram R *et al.* (2010). Derivation, Propagation and Controlled Differentiation of Human Embryonic Stem Cells in Suspension. *Nature Biotechnology* 28, 361–364. **DOI:** 10.1038/nbt.1616.

Wang Y, Chou B-K, Dowey S, He C, Gerecht S & Cheng L (2013). Scalable Expansion of Human Induced Pluripotent Stem Cells in the Defined Xeno-Free E8 Medium under Adherent and Suspension Culture Conditions. *Stem Cell Research* 11, 1103–1116. **DOI:** 10.1016/j.scr.2013.07.011.

Watanabe K, Ueno M, Kamiya D, Nishiyama A, Matsumura M, Wataya T, Takahashi JB, Nishikawa S, Nishikawa S, Muguruma K & Sasai Y (2007). A ROCK Inhibitor Permits Survival of Dissociated Human Embryonic Stem Cells. *Nature Biotechnology* 25, 681–686. **DOI:** 10.1038/nbt1310.

Wu J, Fan Y & Tzanakakis ES (2015). Increased Culture Density Is Linked to Decelerated Proliferation, Prolonged G 1 Phase, and Enhanced Propensity for Differentiation of Self-Renewing Human Pluripotent Stem Cells. *Stem Cells and Development* 24, 892–903. **DOI:** 10.1089/scd.2014.0384.

Xu Y, Zhu X, Hahm HS, Wei W, Hao E, Hayek A & Ding S (2010). Revealing a Core Signaling Regulatory Mechanism for Pluripotent Stem Cell Survival and Self-Renewal by Small Molecules. *Proceedings of the National Academy of Sciences* 107, 8129–8134. **DOI:** 10.1073/pnas.1002024107.

Zweigerdt R, Olmer R, Singh H, Haverich A & Martin U (2011). Scalable Expansion of Human Pluripotent Stem Cells in Suspension Culture. *Nature Protocols* 6, 689–700. **DOI:** 10.1038/nprot.2011.318.

v. General discussion and conclusion

V.1. General discussion and concluding remarks

Fueled by the expectation that stem cells will contribute significantly to the development of new clinical therapies, the last two decades have seen considerable progress in the areas of stem cell biology and engineering. Pluripotent stem cells have gathered much of that attention due to their capacity to self-renew and to produce any cell of the adult body, thus potentially allowing the regeneration of tissues with limited regenerative ability, or even the reconstruction of entire organs. However, the translation of this potential to clinical applications is largely dependent on the tight control of the conditions leading to self-renewal and differentiation, which requires a deep knowledge of the molecular pathways and mechanisms involved. For this, it is essential to develop and implement robust research models that are not only efficient from a technical point of view but also biologically relevant in that they are able to resemble the cellular environment in live organisms. This thesis focused on the development and characterization of two three-dimensional culture systems of human pluripotent stem cells, highlighting their main characteristics and challenges.

In the first part of this work, different strategies were tested to develop a three-dimensional cellular microarray platform with human pluripotent stem cells, using cellular encapsulation. Following previous studies, a glass slide-based microarray platform using alginate as the encapsulation matrix was tested [(Meli L et al., 2014; Fernandes TG et al., 2010)]. However, the use of alginate was shown to produce low cellular viability. This was likely due to the cells being printed as single cells, in addition to the fact that alginate does not provide a functional matrix to which the cells can attach. The use of Matrigel, on the other hand, supported cell survival and proliferation but did not provide enough spot stability nor did it successfully retain the cells inside the printed spots. Similar unsuccessful results were observed using a combination of Matrigel and alginate, with poor cell survival or poor cell retainment in the spots, using different culture media. A different microarray platform was tested based on a two-chip system composed of a MicroPillar chip and a MicroWell chip. The nature of this system enables the complete isolation between replicates and, therefore, the screening of many different soluble formulations at the same time, which is a common limitation in other cellular microarray platforms [(Montanez-Sauri SI et al., 2015)]. With the use of Matrigel as the encapsulation matrix, this system allowed cell survival and proliferation in two culture media, with evidence of pluripotency maintenance. Additionally, an automated image analysis tool

was developed to assess on-chip fluorescence, thus allowing a fast and consistent result quantification solution. Also, a new method to estimate the percentage of viable cells on-chip using Live/Dead and Hoechst staining is proposed. As a proof of concept experiment, different combinations of medium additives were tested on the microarray platform and the expression of OCT4 was assessed after seven days. While the results were generally not conclusive, there were indications that some combination caused changes in the expression of this pluripotency marker.

Although promising results were obtained using the MicroWell/MicroPillar chip system, further optimization is required, particularly in terms of spot stability over longer periods, and the immunocytochemistry protocol to evaluate the expression of marker proteins. Notably, Nierode et al. have recently reported the pre-coating of the MicroPillar chip with polydopamine, which improved spot stability by enabling covalent attachment to the Matrigel [(Nierode GJ et al., 2019; Lee H et al., 2009)]. Furthermore, it is also critical to perform a more comprehensive characterization of this platform in regard to how the cellular phenotype and the differentiation potential are affected, to better grasp its usefulness and robustness as a screening platform for studies with human pluripotent stem cells.

The second part of this work focused on the characterization of static suspension culture of human pluripotent stem cells. The purpose of this section was not so much to evaluate this culture system in terms of proliferation potential, but rather to assess how different morphological parameters may be affected under different conditions, to gain insights on the effect that the culture system has on the expression of pluripotency and differentiation markers in comparison with monolayer cells, and to replicate some of the conditions tested on the microarray platform. Initial results evidenced cell proliferation and pluripotency maintenance in static suspension using xeno-free chemically-defined Essential-8 medium, which was consistent with previous reports [(Li X et al., 2018; Wang Y et al., 2013)]. Image analysis was used to assess the spheroid apparent diameter, circularity, and eccentricity. The effect of pre-seeding cell density was evaluated as to the generation of spheroids, indicating that higher pre-seeding densities lead to an increased number of aggregates on the first day, but a lower total cell count and higher diameter dispersion after seven days.

Some of the medium additive combinations tested on the microarray platform were replicated both in monolayer cells and in cellular aggregates. The modest results observed in the microarray platform were also observed in monolayer cells, in terms of OCT4-positive cells

and average of OCT4-specific fluorescence intensity. However, in cells cultured as spheroids, heparin appeared to cause a considerable decrease in the expression of OCT4. This effect did not correlate with the results obtained in the microarray. On the one hand, this may be further evidence that the microarray platform and the immunostaining protocol require optimization. On the other hand, the results may point to the hypothesis that, when compared with the cells cultured in suspension, the cells cultured on the microarray respond differently to the same stimuli. This would not be a far-fetched assumption, considering the fact that cells encapsulated in Matrigel in a miniaturized culture system are subjected to microenvironmental conditions quite different from the ones that cells cultured as spheroids in suspension are subjected to. Regarding the effect of the different combinations of medium additives on the cells cultured as spheroids, the results suggested that heparin may promote mesendodermal differentiation, as supported by an increase in the expression of T, concomitant with a decrease of POU5F1, NANOG, and, particularly, CDH1, which was not affected in monolayer cells.

Overall, the systems, techniques, and results discussed in this thesis constitute an interesting and relevant base for future work aiming at the exploration of the role of microenvironmental variables in the cellular phenotype and the development of robust *in vitro* cellular models for the study of human pluripotent stem cells.

V.2. Future trends

The increasing complexity of what is known about stem cells will likely be accompanied by a growing complexity of the models used to study them, with the introduction of new variables. For instance, the advantage of using three-dimensional culture models does not lie directly on the dimensionality variable, but rather on the membrane interactions, cytoskeletal tensions, soluble factor gradients, and other finer characteristics that become more relevant and/or pronounced in a three-dimensional context [(Baker BM & Chen CS, 2012)]. With this in mind, it is not enough to simply use more complex models – their potential rises from the possibility to actively control, engineer or finetune the variables that were previously not being considered, spanning across the control of cell aggregation and

aggregate size, the modulation of the biophysical properties of encapsulation matrices, and the temporal and spatial regulation of exposure to morphogens (Kinney MA et al., 2014).

As relevant as the level of complexity tested *in vitro*, is the capacity to retrieve and analyze data from that testing. The use of high-content screening platforms, in combination with robust image analysis algorithms, improved automation, and machine learning, will likely boost the generation of data from high-throughput screening platforms and contribute to further the understanding of the mechanisms regulating stem cells (Nierode G et al., 2016; Li L et al., 2015; Shariff A et al., 2010).

V.3. References

Baker BM & Chen CS (2012). Deconstructing the Third Dimension - How 3D Culture Microenvironments Alter Cellular Cues. *Journal of Cell Science* 125, 3015–3024. **DOI:** 10.1242/jcs.079509.

Fernandes TG, Kwon S-J, Bale SS, Lee M-Y, Diogo MM, Clark DS, Cabral JMS & Dordick JS (2010). Three-Dimensional Cell Culture Microarray for High-Throughput Studies of Stem Cell Fate. *Biotechnology and Bioengineering* 106, n/a-n/a. **DOI:** 10.1002/bit.22661.

Kinney MA, Hookway TA, Wang Y & McDevitt TC (2014). Engineering Three-Dimensional Stem Cell Morphogenesis for the Development of Tissue Models and Scalable Regenerative Therapeutics. *Annals of Biomedical Engineering* 42, 352–367. **DOI:** 10.1007/s10439-013-0953-9.

Lee H, Rho J & Messersmith PB (2009). Facile Conjugation of Biomolecules onto Surfaces via Mussel Adhesive Protein Inspired Coatings. *Advanced Materials* 21, 431–434. **DOI:** 10.1002/adma.200801222.

Li L, Zhou Q, Voss TC, Quick KL & LaBarbera DV (2015). High-Throughput Imaging: Focusing in on Drug Discovery in 3D. *Methods* 96, 97–102. **DOI:** 10.1016/j.ymeth.2015.11.013.

Li X, Ma R, Gu Q, Liang L, Wang LL, Zhang Y, Wang X, Liu X, Li Z, Fang J *et al.* (2018). A Fully Defined Static Suspension Culture System for Large-Scale Human Embryonic Stem Cell Production. *Cell Death & Disease* 9, 892. **DOI:** 10.1038/s41419-018-0863-8.

Meli L, Barbosa HSC, Hickey AM, Gasimli L, Nierode GJ, Diogo MM, Linhardt RJ, Cabral JMS & Dordick JS (2014). Three Dimensional Cellular Microarray Platform for Human Neural Stem Cell Differentiation and Toxicology. *Stem Cell Research* 13, 36–47. **DOI:** 10.1016/j.scr.2014.04.004.

Montanez-Sauri SI, Beebe DJ & Sung KE (2015). Microscale Screening Systems for 3D Cellular Microenvironments: Platforms, Advances, and Challenges. *Cellular and Molecular Life Sciences* 72, 237–249. **DOI:** 10.1007/s00018-014-1738-5.

Nierode GJ, Kwon PS, Dordick JS & Kwon S-J (2016). Cell-Based Assay Design for High-Content Screening of Drug Candidates. *Journal of Microbiology and Biotechnology* 26, 213–225. **DOI:** 10.4014/jmb.1508.08007.

Nierode GJ, Gopal S, Kwon P, Clark DS, Schaffer DV & Dordick JS (2019). High-Throughput Identification of Factors Promoting Neuronal Differentiation of Human Neural Progenitor Cells in Microscale 3D Cell Culture. *Biotechnology and Bioengineering* 116, 168–180. **DOI:** 10.1002/bit.26839.

Shariff A, Kangas J, Coelho LP, Quinn S & Murphy RF (2010). Automated Image Analysis for High-Content Screening and Analysis. *Journal of Biomolecular Screening* 15, 726–734. **DOI:** 10.1177/1087057110370894.

Wang Y, Chou B-K, Dowey S, He C, Gerecht S & Cheng L (2013). Scalable Expansion of Human Induced Pluripotent Stem Cells in the Defined Xeno-Free E8 Medium under Adherent and Suspension Culture Conditions. *Stem Cell Research* 11, 1103–1116. **DOI:** 10.1016/j.scr.2013.07.011.